

Ōhau Channel diversion wall: 7-year review Water quality review and modelling



ERI REPORT NUMBER 169

by

Matthew J. Prentice and Deniz Özkundakci

A client report prepared for
Bay of Plenty Regional Council

2024

Email: matthew.prentice@waikato.ac.nz

Te Tumu Whakaora Taiao - Environmental Research Institute
Division of Health, Engineering, Computing & Science,
University of Waikato, Private Bag 3105,
Hamilton 3240, New Zealand



Cite report as:

Prentice M.J., Özkundakci D. 2024. Ōhau Channel diversion wall: 7-year review — Water quality review and modelling. ERI Report 169, a client report prepared for Bay of Plenty Regional Council. Environmental Research Institute – Te Tumu Whakaora Taiao, Division of Health, Engineering, Computing & Science, University of Waikato, Hamilton, New Zealand. 90 pp. DOI: 10.15663/ERI.Report.169 ISSN 2463-6029 (Print) & ISSN 2350-3432 (Online)

Cover picture:

Ōhau Channel diversion wall in Lake Rotoiti

Reviewed by:



Whitney Woelmer
Senior Research Officer
University of Waikato

Approved for release by:



Charles Lee
Academic Co-Director
Environmental Research Institute

EXECUTIVE SUMMARY

Lake Rotoiti experienced significant degradation in water quality from the 1960s to the early 2000s due to nutrient-laden waters flowing from Lake Rotorua via the Ōhau Channel. To address this, an in-lake diversion wall was constructed in 2007/2008 to block the influx of these nutrient-rich waters. However, during this period, water quality in Lake Rotorua also improved due to enhanced catchment management practices and alum dosing. Consequently, there is now a question of whether and to what extent the diversion wall is still necessary to prevent water quality deterioration in Lake Rotoiti, at its current Trophic Level Index (TLI) and target TLI of 3.5.

This report presents the findings and implications of a comprehensive study commissioned by the Bay of Plenty Regional Council to evaluate the impact of the Ōhau Channel diversion wall on the water quality of Lake Rotoiti, New Zealand. The study, guided by specific research questions outlined in the “Terms of Reference: Ōhau wall: 7-year review”, aimed to assess the effectiveness of the wall in improving water quality, its influence on achieving TLI targets, and its impact on the quality of the Kaituna River. Additionally, the study investigated the potential consequences of removing the diversion wall, considering the altered water residence time and its effects on bottom water dissolved oxygen (DO) levels. An assessment of the holes in the diversion wall was also carried out to understand the amount of water leaking through the wall into Lake Rotoiti.

To address the above research questions, this study consisted of three main components: 1) analysis of observed changes in water quality, 2) lake system modelling, and 3) assessment of holes in the diversion wall. Data analysis involved statistical analyses to determine differences in water quality pre- and post-wall construction. Lake system modelling included configuring a 3-D hydrodynamic-only model to assess for variation in hydrodynamics, and a coupled hydrodynamic-ecological model to assess for variation TLI with and without the wall using scenario simulations over a prolonged period (i.e., 19 years for the hydrodynamic model; 8 years for the hydrodynamic-ecological model). Assessment of wall holes involved data analysis and hydrodynamic model scenario testing to evaluate their impact on Lake Rotoiti.

The data analysis of existing water quality data for Lake Rotoiti, employing a three-step approach (in increasing levels of complexity and inference), revealed nuanced insights into the impacts of the Ōhau Channel diversion wall. While descriptive statistics (i.e., approach 1) indicated overall improvement in water quality post-wall construction in Lake Rotoiti, correlation analysis (i.e., approach 2) between water quality in Lake Rotorua and Rotoiti suggests limited statistical significance in observed differences, except for Secchi depth, indicating altered connectivity between Lake Rotorua and Rotoiti. An intervention analysis (i.e., approach 3), employing interrupted time series analysis, detected significant step changes in total nitrogen (TN), Secchi depth, and TLI post-wall construction, suggesting immediate positive effects on lake water quality persisting throughout the study period. The estimated improvements due to the diversion wall were a decrease in TN by 203 mg m⁻³, an increase in Secchi depth by 2.5 m, and a decrease in TLI by 0.59 units. The data analysis supports the long-held observations of the Lake Rotoiti community, who have noticed a visible improvement in water quality immediately following the construction of the diversion wall. The data analysis revealed that the diversion wall has had no significant impact on bottom water DO demand in Lake Rotoiti, as measured by volumetric hypolimnetic oxygen demand, which remained largely unchanged. Any year-to-year variations are likely attributed to changes in prevailing in-lake and meteorological conditions.

Hydrodynamic model simulations revealed that the wall was effective in reducing the accumulation of Ōhau Channel inflow in the system, increasing the fraction of Ōhau Channel inflow short-circuited down the Kaituna River and, consequently, increasing the residence time of Lake Rotoiti. In terms of accumulation of Ōhau Channel-derived water in Lake Rotoiti, the wall resulted in a substantial reduction as evidenced by an annual cumulative contribution of Ōhau Channel water to Lake Rotoiti of 22.0% without a wall in place, but 0.3% with a wall in place. Concerning the fraction of Ōhau Channel-derived water short-circuited down the Kaituna River, the wall resulted in a substantial increase, as evidenced by the proportion of Ōhau Channel water being diverted down the Kaituna River being 55.2% without a wall in place, but 99.3% with a wall in place. Regarding the residence time in Lake Rotoiti, the wall resulted in a substantial increase, i.e., a factor of 3.3, as evidenced by a residence time of 8.2 years without a wall in place, but 26.9 years with a wall in place.

Coupled hydrodynamic-ecological model simulations revealed the removal of the wall lead to a small deterioration of water quality in Lake Rotoiti, which could be mitigated with improved water quality in the Ōhau Channel inflow. The various scenario testing revealed that removal of the wall alongside a maximum TLI in Lake Rotorua of ~4.3 would likely be required to maintain the current TLI in Lake Rotoiti; however, removal of the wall alongside a maximum TLI in Lake Rotorua of ~4.0 would be required to maintain the current TLI and each of Trophic Level nitrogen, Trophic Level phosphorus, and Trophic Level chlorophyll *a*. Further, removal of the wall alongside even the most ambitious reduction in maximum TLI in Lake Rotorua (i.e., 3.8) would require additional water quality management in Lake Rotoiti to achieve the target TLI in Lake Rotoiti of 3.5.

The analysis of available data on the holes in the diversion wall indicates that despite a relatively small number of estimated holes in the wall, the leakage of Ōhau Channel water into Lake Rotoiti is appreciable; i.e., assuming a total of 100 holes along the length of the diversion wall, approximately 3.3% of the Ōhau Channel water was estimated to leak through the holes into Lake Rotoiti. This percentage increased to 9.8% of the Ōhau Channel water when the total number of holes was assumed to be 300. These discharge rates compare well with the hydrodynamic modelled output, where a single 1 × 100-meter hole (the finest scale hole possible within our model grid) in the Ōhau Channel diversion wall was shown to reduce the effectiveness of the wall in preventing the accumulation of Ōhau-derived water within the lake by 29.3-55.0%. However, the study's estimates are conservative and limited by the model resolution. Given uncertainties in the number of holes, the focus was on estimating water discharge rather than assessing nutrient load or water quality impacts.

Overall, the evaluation of water quality in Lake Rotoiti, including a systematic analysis of long-term datasets and detailed 3-D hydrodynamic-ecological modelling, shows that improvements in water quality in the lake were evident following the construction of the diversion wall. This study shows that the Ōhau Channel diversion wall was critical in preventing the degradation of Lake Rotoiti, but meeting the TLI target in the lake will be challenging if the removal of the wall occurs, even if TLI targets in Lake Rotorua are met.

TECHNICAL SUMMARY

Introduction

Lake Rotoiti is a large-monomictic mesotrophic lake (Trophic Level Index; 3.8) located in the central North Island of New Zealand. Lake Rotoiti experienced considerable degradation in water quality from the 1960s to the early 2000s, primarily due to nutrient-laden waters flowing from Lake Rotorua via the Ōhau Channel. Consequently, in the mid-2000s an in-lake diversion wall was designed and constructed, with construction completed in mid-2008, to prevent the nutrient-laden Ōhau Channel flow from entering the main basin of the lake and instead short-circuiting the water down the Kaituna River. However, improvements in water quality in Lake Rotorua during this period, attributed to enhanced catchment management practices and alum dosing, raise questions about the continued necessity of the diversion wall for preventing water quality decline in Lake Rotoiti, with respect to both its current Trophic Level Index (TLI) of 3.8 and target TLI of 3.5.

This report presents the findings and implications of a comprehensive study commissioned by the Bay of Plenty Regional Council (BoPRC) to evaluate the impact of the Ōhau Channel diversion wall on the water quality of Lake Rotoiti, New Zealand. The study, guided by specific research questions outlined in the “Terms of Reference: Ōhau wall: 7-year review”, aimed to assess the effectiveness of the wall in improving water quality, its influence on achieving TLI targets, and its impact on the quality of the Kaituna River. Additionally, the study investigated the potential consequences of removing the diversion wall, considering the altered water residence time and its effects on bottom water dissolved oxygen (DO) levels. To address these aims, a multifaceted approach was employed, including: 1) a water quality review, which included a comprehensive analysis of observed data, and 2) water quality modelling, which included the configuration and calibration of a 3-D model for pointed scenario testing. In addition, an assessment of the holes in the diversion wall was also carried out to understand the amount of water leaking through the wall into Lake Rotoiti, and the potential implications for water quality.

Methods

To address the above research questions, the study consisted of three main components: 1) water quality data analysis, 2) lake system modelling, and 3) assessment of holes in the diversion wall.

1. This study utilised a combination of statistical and analytical techniques to investigate the impact of the Ōhau Channel diversion wall on water quality in Lake Rotoiti. Descriptive statistics and graphical aids were employed to explore long-term changes in water quality parameters, including trends and patterns. Correlation analysis was conducted to examine the relationship between Lake Rotorua and Lake Rotoiti, as well as between Lake Rotoiti and the Kaituna River, using Pearson correlation coefficients and least square linear regression. This analysis aimed to identify any changes in the association between the water quality of these systems before and after the diversion construction of the diversion wall. Intervention analysis using generalized least squares regression models was used to detect changes in water quality variables, including total nitrogen (TN), total phosphorus (TP), chlorophyll *a*, and Secchi depth. The models incorporated terms for time, intervention, and post-intervention time, enabling the detection of both immediate (step changes) and gradual (change in trend direction and slope) changes in water quality.
2. Lake system modelling was carried out using the Aquatic Ecosystem Model (AEM3D), a 3-D hydrodynamic–ecological model, which allowed the temporal and spatial behaviour of Lake Rotoiti to be well captured. The model was configured to run at a 100-m² horizontal grid and uniform 1-m vertical layer, on a 2-min timestep, in trade-off between model resolution and runtime. The hydrodynamic-ecological model was configured to include two phytoplankton

groups, cyanobacteria (summer-adapted; buoyant) and diatoms (and other; winter-adapted; non-buoyant). Hydrodynamic model simulations were applied to investigate changes in the accumulation, retention, and behaviour of Ōhau Channel inflow-derived water within the lake and the removal of the existing water in the lake, with and without the wall in place.

Correspondingly, two scenarios were tested, including: 1) wall-out, 2) and wall-in.

Hydrodynamic-ecological model simulations were applied to investigate changes in TLI with and without the wall in place, and without the wall in place under three Ōhau Channel inflow water quality regimes. Correspondingly, four scenarios were tested, including: 1) wall-in (with Ōhau Channel water quality parameters as measured), 2) wall-out (with Ōhau Channel water quality parameters as measured); 3) wall-out, with Ōhau Channel water quality measures scaled to a maximum TLI of 4.2 (equivalent to a 15.5% reduction in nitrogen, phosphorus, and chlorophyll *a*); and 4) wall-out, with Ōhau Channel water quality measures scaled to a maximum TLI of 3.8 (equivalent to a 39.0% reduction in nitrogen, phosphorus, and chlorophyll *a*). As simulations are initialised with measured data, wall-out scenarios for the hydrodynamic-ecological model (which was initialised in 2014; 7-8 years post-wall construction) represent the removal of the Ōhau Channel diversion wall. Hydrodynamic simulations were run across 19 limnological years from 1-Jul-2003 through 30-Jun-2022, whereas coupled-hydrodynamic-ecological simulations were run across 8 limnological years from 1-Oct-2014 through 30-Jun-2022.

3. Assessment of wall holes involved data analysis and hydrodynamic model scenario testing to evaluate their impact on Lake Rotoiti. To facilitate a quantitative estimation of the water flow through the holes in the diversion wall, BoPRC commissioned Greenfield Diving Services & Maintenance Engineering to assess the condition of the wall, which included measuring the size of the holes, using a 100 × 100-mm square welded wire mesh. Thirty-two holes were assessed, yielding a total measured hole area of 1.13 m² and an average hole size of 0.035 m². Flow velocity measurements were taken at 100-meter intervals along the wall in February 2024. The distance-weighted average velocity was 0.156 m s⁻¹, with a maximum velocity of 0.456 m s⁻¹, and a minimum velocity of -0.074 m s⁻¹. Notably, measurements from 900 meters downstream from the Ōhau Channel delta onwards were all negative, indicating water flowing from Lake Rotoiti into the Ōhau Channel through the holes. The total number of holes was estimated to calculate the volume of water flowing through the holes, which was compared to the average discharge in the Ōhau Channel during February 2024. Hydrodynamic modelling was based on the same calibrated and configured hydrodynamic model used to quantify changes in hydrodynamics with and without the wall, except for the addition of a single 1 × 100-m hole (the finest scale hole possible within our model grid). To account for the simplified representation of the holes, six different configurations of the single 1 × 100-m hole were simulated to provide a range of potential values, which included holes at 300-400 m, 600-700 m, and 1000-1100 m along the wall, at 1 m and 2 m below the surface. To investigate whether and to what extent a 1 × 100-m hole affects the rate of accumulation, rate of retention, and wall efficiency, the six scenarios with a 100-m hole, and the regular wall-in and wall-out scenarios were run for one limnological year from Jul-2003 through Jun-2004.

Findings

The data analysis of existing water quality data for Lake Rotoiti, employing a three-step approach (in increasing levels of complexity and inference), revealed nuanced insights into the impacts of the Ōhau Channel diversion wall (Table I). While descriptive statistics (i.e., approach 1) indicated an overall improvement in water quality post-wall construction in Lake Rotoiti, correlation analysis (i.e., approach 2) between water quality in Lake Rotorua and Rotoiti suggested limited statistical significance in observed differences, except for Secchi depth, indicating altered connectivity between

Lake Rotorua and Rotoiti. An intervention analysis (i.e., approach 3), employing interrupted time series analysis, detected significant step changes in TN, Secchi depth, and TLI post-wall construction, suggesting immediate positive effects on lake water quality persisting throughout the study period. The estimated improvements due to the diversion wall were a decrease in TN by 203 mg m⁻³, an increase in Secchi depth by 2.5 m, and a decrease in TLI by 0.59 units. The data analysis supports the long-held observations of the Lake Rotoiti community, who have noticed a visible improvement in water quality immediately following the construction of the diversion wall. The data analysis revealed that the diversion wall has had no significant impact on bottom water DO demand in Lake Rotoiti, as measured by volumetric hypolimnetic oxygen demand, which remained largely unchanged. Any year-to-year variations are likely attributed to changes in prevailing in-lake and meteorological conditions.

Table I Summary of findings for the water quality data analysis

Approach	Outcome					
	TLI	TN	TP	Chlorophyll <i>a</i>	Secchi depth (SD)	Overall impact in Rotoiti WQ
Descriptive statistics	N/A	Improvement	Improvement	Improvement	Improvement	Improvement in all variables post-wall.
Correlation analysis	N/A	No improvement	No improvement	No improvement	Significant improvement	Significant change post-wall in SD only.
Intervention analysis	Significant improvement (down 0.59 units)	Significant improvement (down 203 ppb)	No improvement	No improvement	Significant improvement (up 2.5 m)	Significant step change post-wall in TLI, TN, & SD.

Hydrodynamic model simulations illustrated that the wall was effective in reducing the accumulation of Ōhau Channel inflow in the system, increasing the fraction of Ōhau Channel inflow short-circuited down the Kaituna River, and consequently, increasing the residence time of Lake Rotoiti (Table II). In terms of accumulation of Ōhau Channel-derived water in Lake Rotoiti, the wall resulted in a substantial reduction as evidenced by an annual cumulative contribution of Ōhau Channel water to Lake Rotoiti of 22.0% without a wall in place, but 0.3% with a wall in place. Concerning the fraction of Ōhau Channel-derived water short-circuited down the Kaituna River, the wall resulted in a substantial increase, as evidenced by the proportion of Ōhau Channel water being diverted down the Kaituna River being 55.2% without a wall in place, but 99.3% with a wall in place. Regarding the residence time in Lake Rotoiti, the wall resulted in a substantial increase, i.e., a factor of 3.3, as evidenced by a residence time of 8.2 years without a wall in place, but 26.9 years with a wall place.

Table II Summary of findings for the hydrodynamics lake system modelling

Scenario	Outcome		
	Fraction of Lake Rotoiti water derived from Ohau channel in an average year	Fraction of Ohau channel water diverted down the Kaituna River	Residence time in Lake Rotoiti
Wall-in	0.3%	99.3%	26.9 years
Wall-out	22.0%	55.2%	8.2 years

Coupled hydrodynamic-ecological model simulations revealed the removal of the wall (c.f., wall-in, base scenario) would lead to a small deterioration of water quality in Lake Rotoiti (Table III). However, this deterioration could be mitigated with improvements in water quality in the Ōhau Channel inflow (Table III). Specifically, removal of the wall with Ōhau Channel water quality parameters as measured, i.e., maximum TLI of 4.41, resulted in a small deterioration to water quality (i.e., increase in TLI of 0.02 units) in Lake Rotoiti due to small increases to Trophic Level nitrogen (TLn; 0.08), Trophic Level chlorophyll *a* (TLC; 0.07), but a slight decrease in Trophic Level phosphorus (TLp; 0.09). Removal of the wall with Ōhau Channel water quality measures scaled to a maximum TLI of 4.2 (equivalent to a 15.5% reduction in nitrogen, phosphorus, and chlorophyll *a*), resulted in an improvement to water quality (i.e., decrease in TLI of 0.02 units) in Lake Rotoiti, due to slight increases to TLn (0.02), TLC (0.04), but a decrease in TLp (0.12). Removal of the wall with Ōhau Channel water quality measures scaled to a maximum TLI of 3.8 (equivalent to a 39.0% reduction in nitrogen, phosphorus, and chlorophyll *a*), resulted in an improvement to water quality (i.e., decrease in TLI of 0.08 units) in Lake Rotoiti, due to decreases to TLn (0.07), TLp (0.16), TLC (0.02). Consequently, removing the wall alongside maintaining a maximum TLI in Lake Rotorua of ~4.3 would likely be required to maintain the current TLI in Lake Rotoiti. However, removing the wall alongside maintaining a maximum TLI in Lake Rotorua of ~4.0 would likely be required to maintain the current TLI as well as TLn, TLp, and TLC in Lake Rotoiti. Furthermore, even with the most ambitious reduction in maximum TLI in Lake Rotorua (i.e., 3.8), additional water quality management in Lake Rotoiti would be required to achieve the target TLI of 3.5.

Table III Summary of findings for the water quality lake system modelling wall-out scenarios

Wall-out scenario (c.f. wall-in scenario), as Ōhau Channel inflow water quality	Outcome (8-years post wall removal)					
	TLI	TLn	TLp	TLC	Overall impact in Rotoiti WQ*	Does Rotoiti meet TLI target of 3.5
<i>Simulated scenario</i>						
Wall-out with max TLI of 4.41 (i.e., as measured)	Increase of 0.02	Increase of 0.08	Decrease of 0.09	Increase of 0.07	Small decline (TLI = 3.96)	No
Wall-out with max TLI of 4.2 (i.e., as a 15.5% reduction in WQ parameters)	Decrease of 0.02	Increase of 0.02	Decrease of 0.12	Increase of 0.04	Small improvement (TLI = 3.92)	No
Wall-out with max TLI of 3.8 (i.e., as a 39% reduction in WQ parameters)	Decrease of 0.08	Decrease of 0.07	Decrease of 0.16	Decrease of 0.02	Improvement (TLI = 3.86)	No
<i>Inferred scenario</i>						
Wall-out with max TLI of 4.3	Expected hold	Expected hold	Expected decrease	Expected increase	Expected hold in TLI, but not all of TLn, TLp, & TLC	No
Wall-out with max TLI of 4.0	Expected decrease	Expected decrease	Expected decrease	Expected hold	Expected hold in TLI, & each of TLn, TLp, & TLC	No

* Modelled TLI, thus to be interpreted relative to equivalent modelled 'wall-in' scenario TLI of 3.94.

Based on the hydrodynamic-ecological model scenario testing, water quality improvements in Lake Rotoiti expected from improved the Ōhau Channel inflow water quality appear to be buffered against by internal processes (e.g., internal loading of N and P). This was demonstrated by a reduction to TLn, TLp, and TLC, as well as TN, TP, and chlorophyll *a* concentrations in the Ōhau Channel inflow,

not directly correlating with changes in Lake Rotoiti. Moreover, even accounting for the Ōhau-derived contribution of water in the lake, realised improvements in water quality were less than what would be expected based on concentration of the Ōhau Channel inflow and dilution and dispersion of the Ōhau Channel inflow within Lake Rotoiti. It is likely that this buffering is attributed to nitrogen (N) and phosphorus (P) legacies in the system released from the sediments during anoxia, and/or N and P derived from a substantive unquantified groundwater-based geothermal flux. Consequently, future improvement to the water quality in Lake Rotoiti may require additional water quality management measures in Lake Rotorua, and within Lake Rotoiti itself.

The analysis of available data of the holes in the diversion wall indicated that despite a relatively small number of estimated holes in the wall, the leakage of Ōhau Channel water into Lake Rotoiti is appreciable; i.e., assuming a total of 100 holes along the length of the diversion wall, approximately 3.3% of the Ōhau Channel water was estimated to leak through the holes into Lake Rotoiti. This percentage increased to 9.8% of the Ōhau Channel water when the total number of holes was assumed to be 300. These discharge rates compare well with the hydrodynamic modelled output, where a single 1×100 -meter hole (the finest scale hole possible within our model grid) in the Ōhau Channel diversion wall was shown to reduce the effectiveness of the wall in preventing the accumulation of Ōhau-derived water within the lake by 29.3-55.0%. Although the study's estimates are conservative and limited by the model resolution, the corroboration of the measured and modelled data provides sufficient evidence that all holes in the wall collectively, although small individually, can result in a substantial flux of Ōhau Channel-derived water and ultimately accumulation within the lake. Given uncertainties in the number of holes, the focus was on estimating water discharge rather than assessing nutrient load or water quality impacts.

This research, as with Priscu et al. (1986) and Hamilton et al. (2005), demonstrated nutrient dynamics in Lake Rotoiti are complex and not well understood. Nutrient-related dynamics in Lake Rotoiti that would benefit from a further understanding are primarily related to: 1) processes driving the $\text{NH}_4\text{-NO}_3\text{-NH}_4$ succession in the hypolimnion of Lake Rotoiti; 2) geothermal fluxes relating to temperature, pH, and most notably P and N, and their constituents; and 3) atmospheric deposition of P and N, and their constituents. This research, although ambitious, was limited by the current state of computing, modelling capabilities, and understanding of certain scientific processes (e.g., the unique N succession in the hypolimnion of Lake Rotoiti). Despite this, continued advancement in computational power and lake model capabilities, and breakthrough and advancement of critical scientific processes will enable more ambitious scenario testing and more advanced simulations in the coming years. Finally, this research also highlights that future work might endeavour to explore the impact of a greater variety of Ōhau Channel inflow scenarios, the impact of future climate scenarios, and the interplay of these two factors.

Conclusions

A comprehensive evaluation of water quality in Lake Rotoiti involved a systematic analysis of long-term datasets and detailed 3-D hydrodynamic-ecological modelling to better understand the impacts of the Ōhau Channel diversion wall and the potential effects of its removal on the lake. Data analysis revealed clear improvements in water quality in Lake Rotoiti, with TN, Secchi depth, and the TLI exhibiting a significant change following the wall's construction. This underscores the critical role of the Ōhau Channel diversion wall in preventing degradation in Lake Rotoiti. Hydrodynamic modelling illustrated that the wall was effective in reducing accumulation of Ōhau Channel inflow in the system, increasing the fraction of Ōhau Channel inflow short-circuited down the Kaituna River, and consequently, increasing the residence time of Lake Rotoiti. Hydrodynamic-ecological simulations illustrated that removal of the wall (c.f., wall-in, base scenario) would lead to a small deterioration of

water quality in Lake Rotoiti, which could be mitigated with improved water quality in the Ōhau Channel inflow. An assessment of the effects of holes in the diversion wall using the best available data and hydrodynamic modelling suggested that a significant amount of Ōhau Channel water is leaking into Lake Rotoiti. However, considerable uncertainty remains in this assessment as the total number of holes remains unknown.

Answers to research questions outlined in the “Terms of Reference: Ōhau wall: 7-year review”

Water quality review:

Has the wall achieved its objective of improving water quality?

Evidence suggests that the diversion wall has led to enhanced water quality in Lake Rotoiti independent of water quality improvement in Lake Rotorua. Total nitrogen, Secchi depth, and TLI showed a step change after the wall's construction, although there were no shifts in long-term trend slopes.

Has the wall resulted in the lake reaching its TLI target in advance of improvements to Lake Rotorua water quality impacting Lake Rotoiti?

There is some evidence suggesting that water quality in Lake Rotoiti improved before the construction of the wall. Total nitrogen and chlorophyll *a* concentrations, as well as Secchi depth, showed improvement prior to the wall's construction. However, drawing strong conclusions from the data is challenging as the observed patterns in the long-term dataset may or may not be fluctuating cyclically.

Does current monitoring support the continued placement of the wall, diverting Ōhau Channel water?

The TLI in Lake Rotoiti is still above its target. There is also no clear evidence that water quality in the lake is still improving. However, there is some evidence that the TN and TP concentrations are going through a period of increase. This suggests that (together with conclusions drawn from this study's water quality modelling work; see below), the continued placement of the wall is still warranted.

What impact has the diversion wall had on the quality of the Kaituna River.

There is no evidence to suggest that the diversion wall has had an impact on the water quality dynamics in the Kaituna River.

Water quality modelling:

What is the modelled impact of the diversion wall on water quality and ecology?

Modelling showed that the implementation of the diversion wall has resulted in small reductions to TN and chlorophyll *a*, but increases in TP concentrations (Figure 32). Taken together, the wall has resulted in a reduction in TLI in Lake Rotoiti (Figure 34d).

Does this align with the water quality and ecological monitoring of Lake Rotoiti?

Simulated TLI and its constituents over longer-term periods (i.e., 8 years) agree well with the data analysis of even longer-term data sets carried out in this study's water quality review work (see above). Further, the effects of the observed reduction in TLP in Lake Rotorua (because of catchment management practices and alum dosing in Lake Rotorua), and thus the Ōhau Channel inflow entering Lake Rotoiti, were well captured by model simulations through simulating a decrease in TLP in Lake Rotoiti as the Lake Rotorua-derived water accumulated within the lake.

The diversion wall is expected to be in place for 50 to 100 years. Once it has been removed what is the likely water quality expectation for Lake Rotoiti if Lake Rotorua meets the TLI of 4.2 +, when Lake Rotoiti is expected to meet a TLI of 3.5?

Simulations run from 2014-2022 in which the Ōhau diversion wall was removed in conjunction with water quality in Lake Rotorua equivalent to a maximum annual TLI of 4.2, resulted in a TLI in Lake Rotoiti after eight years of 4.2. Although eight years is ample time for the lake to reach a new equilibrium, this assumes all other inputs are at baseline, and thus no concomitant in-lake or catchment management practices implemented in Lake Rotoiti. Therefore, removal of the wall alongside a maximum annual TLI in Lake Rotorua of 4.2, without additional measures, will be insufficient to have Lake Rotoiti meet its TLI target of 3.5.

The diversion wall has effectively changed the water residence time in Lake Rotoiti from about 1.5 years to 5+ years. How does this impact Lake Rotoiti water quality, potentially having an impact on bottom water dissolved oxygen levels and especially the western arm of the lake?

Simulations suggest residence times (determined as the time to clear 95% of existing water) are substantially longer than 1.5 and 5+ years for wall-out and wall-in scenarios, respectively. Simulations instead indicated residence times of 8.2 and 26.9 years for wall-out and wall-in scenarios. Nevertheless, model simulations in the eastern (i.e., Narrows) and western (i.e., Crater) basins demonstrated the wall-in scenario, compared to the wall-out scenario, maintains a small increase of <0.1-0.2 mg DO L⁻¹ in the bottom waters during the stratified period., which is well within the range of uncertainty of the model simulations. There was no clear evidence of any changes in bottom water DO levels in the monitoring data in Lake Rotoiti at sites 3 and 4.

TABLE OF CONTENTS

1	Introduction.....	17
1.1	Project Scope.....	17
1.2	Background.....	17
1.3	Aims and objectives	19
2	Study Site.....	20
3	Methods.....	21
3.1	Part 1: Water quality data analysis	21
3.1.1	Data sources	21
3.1.2	Statistical analysis.....	21
3.2	Part 2: Lake system modelling	23
3.2.1	Data sources	23
3.2.2	Modelling.....	23
3.3	Part 3: Assessment of holes in the diversion wall	31
3.3.1	Calculations.....	31
3.3.2	Modelling.....	32
4	Results.....	34
4.1	Part 1: Water quality data analysis	34
4.1.1	Descriptive statistics	34
4.1.2	Correlation analysis.....	37
4.1.3	Intervention analysis	40
4.2	Part 2: Lake system modelling	42
4.2.1	Hydrodynamics	42
4.2.2	Water quality.....	51
4.3	Part 3: Assessment of holes in the diversion wall	68
4.3.1	Calculations.....	68
4.3.2	Modelling.....	68
5	Discussion.....	71
5.1	Water quality data analysis.....	71
5.2	Lake system modelling: hydrodynamics scenario testing	72
5.3	Lake system modelling: water quality scenario testing	73
5.4	Assessment of holes in the diversion wall.....	74
5.5	Lake system modelling: calibration.....	75
5.6	Implications and future work.....	76
5.7	Conclusions	78
5.7.1	Overview.....	78
5.7.2	Answers to research questions	78
6	Acknowledgements.....	80
7	References.....	81
8	Appendices.....	86

LIST OF TABLES

Table 1 Configuration of light, oxygen, nitrogen, phosphorus, and organic matter for the water quality model.	24
Table 2 Configuration of phytoplankton groups for the water quality model.....	25
Table 3 Configuration for BIRD Clear Sky Model.....	27
Table 4 Summary of statistical correlation analysis results for water quality variables before and after construction of the diversion wall for Lake Rotorua vs. Lake Rotoiti and Lake Rotoiti vs. Kaituna River.....	38
Table 5 Model coefficients of the interrupted time series analysis carried out as part of the intervention analysis.	41
Table 6 Temperature performance statistics of the hydrodynamic model at Site 4. Statistics include Pearson correlation (R), root mean squared error (RMSE), and mean absolute error (MAE). Calibration period 1-Jul-2003 through 30-Jun-2004; Validation period 1-Jul-2004 through 30-Jun-2005.	42
Table 7 Temperature performance statistics of the hydrodynamic-ecological model at Site 4. Statistics include Pearson correlation (R), root mean squared error (RMSE), and mean absolute error (MAE). Calibration period 1-Sep-2014 through 31-Aug-2015; Validation period 1-Sep-2015 through 31-Aug-2016.	51
Table 8 Dissolved oxygen performance statistics of the hydrodynamic-ecological model at Site 4. Statistics include Pearson correlation (R), root mean squared error (RMSE), and mean absolute error (MAE). Calibration period 1-Sep-2014 through 31-Aug-2015; Validation period 1-Sep-2015 through 31-Aug-2016.	53
Table 9 Phosphorus, nitrogen, and chlorophyll <i>a</i> performance statistics of the hydrodynamic-ecological model at Site 4. Statistics include Pearson correlation (R), root mean squared error (RMSE), and mean absolute error (MAE). Calibration period 1-Sep-2014 through 31-Aug-2015; Validation period 1-Sep-2015 through 31-Aug-2016.	55

LIST OF FIGURES

Figure 1: Lake Rotoiti study site showing sampling Sites (circles) 1 and 2, the Ōhau River inflow and the 17 minor inflows (triangles), the Kaituna River outflow (square), and the Ōhau Channel diversion wall.....	20
Figure 2: Cartesian mesh of, a) Lake Rotoiti, and b) the western reaches of Lake Rotoiti, demonstrating the boundary condition for the Ōhau inflow and Kaituna outflow, and Levee representing the Ōhau Channel diversion wall (wall-in scenarios only).	26
Figure 3: Examples of hole measurements carried out by Greenfield Diving Services & Maintenance Engineering as part of an assessment of the condition of the wall in July 2023. The size of the square mesh is 100 × 100-mm.....	32
Figure 4: a) Cartesian mesh of the western reaches of Lake Rotoiti, demonstrating the boundary condition for the Ōhau inflow and Kaituna outflow, and Levee representing the Ōhau Channel diversion wall (wall-in scenarios only) with sections of wall with holes (wall-in with hole scenarios only) identified; and b) vertical grid of Levee representing the diversion wall (n.b. only upper 6 cells represented) showing placement of holes under the six configurations for wall-in with a hole scenarios.....	33
Figure 5: Median values of water quality parameters in Lakes Rotorua (Site 5) and Rotoiti (Site 3) before and after the Ōhau Channel diversion wall construction. Vertical lines inside the boxes denote the medians; boxes denote the 25th and 75th percentile; the whiskers denote the smallest and largest observation greater than or equal to lower/upper box-1.5× interquartile range. Units for all nutrient chlorophyll <i>a</i> concentrations are mg m ⁻³ , Secchi depth is m, and turbidity is NTU.	34
Figure 6: Time series all four water quality variables included in the TLI at Lake Rotoiti Site 3. Turquoise line represents data collected before and red line represents data after the construction of the Ōhau Channel diversion wall. The blue line is a loess smoother to visually indicate trends of water quality in the lake.....	35
Figure 7: Monthly volumetrically averaged hypolimnetic oxygen concentrations in Lake Rotoiti (Site 4 top, and Site 3 bottom) for all monitoring years where oxygen profiled were consistently available. For Site 3, the years 2003-2004, 2004-2005, and 2008-2009 have been omitted due to spurious temperature profiles during those year affecting calculations.	36
Figure 8: Bi-plots of annual average water quality variables in Lakes Rotorua (Site 5) and Rotoiti (Site 3) for all four water quality variables included in the TLI. Turquoise line and points represents data collected before, and red line and points represents data after the construction of the Ōhau Channel diversion wall. The corresponding Pearson correlation coefficient (R), t statistic, P value, and number of samples for each correlation are also shown. A P value <0.05 indicates a significant correlation.	37
Figure 9: Time series of total nitrogen and total phosphorus concentrations in the Kaituna River at the Lake Rotoiti outlet. Turquoise line represents data collected before and red line represents data after the construction of the Ōhau Channel diversion wall. The blue line is a loess smoother to visually indicate trends of water quality in the lake.	39
Figure 10: Bi-plots of annual average water quality variables in the Kaituna River (at Rotoiti outflow) and Lake Rotoiti (Site 3) for total nitrogen and total phosphorus. Turquoise line and points represents data collected before, and red line and points represents data after the construction of the Ōhau Channel diversion wall. The corresponding Pearson correlation coefficient (R), t statistic, P value, and number of samples for each correlation are also shown. A P value <0.05 indicates a significant correlation.	39

Figure 11: Time series graphs of intervention analysis results using generalized linear modelling of annual average values for all four water quality variables included in the TLI for data collected between 1995 and 2023. Black line represents linear trends (± 95 confidence interval, green shade) for pre and post wall periods calculated from data shown by grey points. A counterfactual trend line (extrapolation of the pre-wall trend line) is shown as red dotted line (± 95 confidence interval, red shade) is compared with the post-wall trend to estimate the immediate and longer-term impact of the diversion wall (see results in Table 5). 40

Figure 12: Time series graphs of intervention analysis results using generalized linear modelling of the TLI for data collected between 1995 and 2023. Black line represents linear trends (± 95 confidence interval, green shade) for pre and post wall periods calculated from data shown by grey points. A counterfactual trend line (extrapolation of the pre-wall trend line) is shown as red dotted line (± 95 confidence interval, red shade) is compared with the post-wall trend to estimate the immediate and longer-term impact of the diversion wall (see results in Table 5)..... 41

Figure 13: Measured vs modelled water level (as Height, Moturiki datum), during the calibration and validation periods. Data are daily measurements taken at 00:00 hours. Calibration period 1-Jul-2003 through 30-Jun-2004 (light grey), Validation 1-Jul-2004 through 30-Jun-2005 (mid grey). 42

Figure 14: Measured vs modelled Temperature (T) at Site 4, during the calibration and validation periods, at a) 1, b) 10, c) 20, d) 30, e) 40, and f) 60 m depth. Calibration period 1-Jul-2003 through 30-Jun-2004 (light grey), Validation 1-Jul-2004 through 30-Jun-2005 (mid grey)..... 43

Figure 15: Simulated annual (i.e., single year) accumulation of Ōhau Channel-derived water (tracer value = 1) with the Ōhau Channel diversion wall in place over each limnological year from 2003-2004 through 2021-2022. Dates in figure represent the tracer value on the final day of the limnological year. N.b. entire lake shown, but subsequent analysis excludes area within wall (with and without the wall in place) and the Okare Arm. 44

Figure 16: Simulated annual (i.e., single year) accumulation (i.e., % of Lake Rotoiti water derived from the Ōhau Channel over a single year) of Ōhau Channel-derived water (tracer value = 1) without the wall in place over each limnological year from 2003-2004 through 2021-2022. Dates in figure represent the tracer value on the final day of the limnological year. N.b. entire lake shown, but subsequent analysis excludes area within wall (with and without the wall in place) and the Okare Arm. 45

Figure 17: Simulated comparison of 1) the accumulation (i.e., % of Lake Rotoiti water derived from the Ōhau Channel over a single year) of Ōhau Channel-derived water, and b) the retention (i.e., % of Ōhau Channel water entering Lake Rotoiti, which remained in the Lake Rotoiti over a single year) of Ōhau Channel-derived water, with and without the wall in place over each limnological year from 2003-2004 through 2021-2022..... 46

Figure 18: Simulated Ōhau Channel-derived water (tracer value = 1) without a wall at a) Site 3 and b) Site 4, and with the Ōhau Channel diversion wall at c) Site 3 and d) Site 4, from 1-Jul-2003 through 30-Jun-2022. Values represent that of a tracer which decays at a rate of 0.5 per week. N.b. Variable tracer scale across panels ‘a’ through ‘d’..... 47

Figure 19: Simulated annual (i.e., within a single year) retention (i.e., % of Lake Rotoiti water not replaced by water derived from outside the lake over a single year) of Lake Rotoiti water with the Ōhau Channel diversion wall in place, represented by removal of tracer (initial value = 1) over each limnological year from 2003-2004 through 2021-2022. Dates in figure represent the tracer value on the final day of the limnological year. N.b. entire lake shown, but subsequent analysis excludes area within wall (with and without the wall in place) and the Okare Arm; retention used to determine removal as 1 less retention. 48

Figure 20: Simulated annual (i.e., within a single year) retention (i.e., % of Lake Rotoiti water not replaced by water derived from outside the lake over a single year) of Lake Rotoiti water without the

wall in place, represented by removal of tracer (initial value = 1) over each limnological year from 2003-2004 through 2021-2022. Dates in figure represent the tracer value on the final day of the limnological year. N.b. entire lake shown, but subsequent analysis excludes area within wall (with and without the wall in place) and the Okare Arm; retention used to determine removal as 1 less retention. 49

Figure 21: Simulated comparison of the removal (as % of Lake Rotoiti water replaced by water derived from outside the lake over a single year) of Lake Rotoiti water with and without the wall in place over each limnological year from 2003-2004 through 2021-2022. 50

Figure 22: Simulated comparison of residence time, as determined as the number of years to reach < 5% of Rotoiti water, with and without the wall in place. Dotted grey line denotes 5% threshold. 50

Figure 23: Measured vs modelled temperature (T) at Site 4, during the calibration and validation periods, at a) 1 m, b) 10 m, c) 20 m, d) 30 m, e) 40 m, and f) 60 m depth. Calibration period 1-Oct-2014 through 30-Sep-2015 (light grey), Validation 1-Oct-2015 through 30-Sep-2016 (mid grey). 52

Figure 24: Measured vs modelled dissolved oxygen (DO) at Site 4, during the calibration and validation periods, at a) 1 m, b) 10 m, c) 20 m, d) 30 m, e) 40 m, and f) 60 m depth. Calibration period 1-Oct-2014 through 30-Sep-2015 (light grey), Validation 1-Oct-2015 through 30-Sep-2016 (mid grey). 54

Figure 25: Measured vs modelled phosphate (PO₄) and total phosphorus (TP) at Site 4, during the calibration and validation periods, with a) surface water PO₄, b) bottom water (80 m) PO₄, c) surface water TP, and d) bottom water TP. Calibration period 1-Oct-2014 through 30-Sep-2015 (light grey), Validation 1-Oct-2015 through 30-Sep-2016 (mid grey). 56

Figure 26: Measured vs modelled ammonium (NH₄), nitrate (NO₃), and total nitrogen (TN) at Site 4, during the calibration and validation periods, with a) surface water NH₄, b) bottom water (80 m) NH₄, c) surface water NO₃, and d) bottom water NO₃, e) surface water TN, and f) bottom water TN. Calibration period 1-Oct-2014 through 30-Sep-2015 (light grey), Validation 1-Oct-2015 through 30-Sep-2016 (mid grey). 57

Figure 27: a) Measured vs modelled chlorophyll *a* (Chl *a*) at Site 4, and b) modelled cyanobacteria and diatoms, during the calibration and validation periods. Measured and modelled data as surface water. Calibration period 1-Oct-2014 through 30-Sep-2015 (light grey), Validation 1-Oct-2015 through 30-Sep-2016 (mid grey)..... 58

Figure 28: Measured vs modelled Trophic Level phosphorus (TLp), TL nitrogen (TLn), TL chlorophyll *a* (TLc), and Trophic Level Index (TLI) at Site 4, during the calibration and validation periods. Measured and modelled data as surface water. Calibration period 1-Oct-2014 through 30-Sep-2015 (light grey), Validation 1-Oct-2015 through 30-Sep-2016 (mid grey)..... 59

Figure 29: Simulated cumulative (i.e., year after year, over eight years) removal of Lake Rotoiti water with wall in place (left) and without the wall in place (right), represented by dilution of tracer (initial value = 1) over each limnological year at the mid-point of each year. Mid-point for 2014-15 year (1-10-2014 through 30-6-2015) was 15-02-2015; Mid-point for all other years was 31-12 of the given year..... 61

Figure 30: Simulated cumulative removal of Lake Rotoiti water 1) with and 2) without the wall in place over each limnological year during the hydrodynamic-ecological simulation period. Date represents mid-point of each simulation year. Mid-point for 2014-15 year (1-10-2014 through 30-6-2015) was 15-02-2015; Mid-point for all other years was 31-12 of the given year. 62

Figure 31: Simulated Surface total phosphorus (TP), total nitrogen (TN), and chlorophyll *a* at Site 4, as limnological year means, for the 1) wall-in, 2) wall-out, 3) wall-out with TLI max of 4.2, and 4) wall-out with TLI max of 3.8 configurations, across the 2014-15 through 2021-22 limnological years (i.e., 1-Jul through 30-Jun of the subsequent year). N.b. variable vertical scale. 63

Figure 32: Simulated relative change—i.e., to the simulated ‘wall-in’ configuration—in Surface total phosphorus (TP), total nitrogen (TN), and chlorophyll *a* at Site 4, as limnological year means, for the 1) wall-out, 2) wall-out with TLI max of 4.2, and 3) wall-out with TLI max of 3.8 configurations, across the 2014-15 through 2021-22 Limnological years (i.e., 1-Jul through 30-Jun of the subsequent year). N.b. variable vertical scale..... 64

Figure 33: Simulated Trophic Level phosphorus (TLp), TL nitrogen (TLn), TL chlorophyll *a* (TLc), and TL Index (TLI) at Site 4, as limnological year means, for the 1) wall-in, 2) wall-out, 3) wall-out with TLI max of 4.2, and 4) wall-out with TLI max of 3.8 configurations, across the 2014-15 through 2021-22 Limnological years (i.e., 1-Jul through 30-Jun of the subsequent year). N.b. variable vertical scale. 66

Figure 34: Simulated relative change—i.e., to the simulated ‘wall-in’ configuration— in Trophic Level phosphorus (TLp), TL nitrogen (TLn), TL chlorophyll *a* (TLc), and TL Index (TLI) at Site 4, as limnological year means, for the 1) wall-out, 2) wall-out with TLI max of 4.2, and 3) wall-out with TLI max of 3.8 configurations, across the 2014-15 through 2021-22 Limnological years (i.e., 1-Jul through 30-Jun of the subsequent year). N.b. variable vertical scale..... 67

Figure 35: Summary of calculations of discharge through the holes in the Ōhau Channal diversion wall. Percent discharge of Ōhau Channal water was based on measurements of average hole size and flow velocities through the holes, using different estimated of the total number of holes (which is currently unknown). 68

Figure 36: Simulated contribution of Ōhau Channel (tracer value = 1) derived water with the wall in place and a 1 × 100-m hole in the wall; a) hole 300-400 m along the wall at ~0-1 m depth, b) hole 300-400 m along the wall at ~1-2 m depth, c) hole 600-700 m along the wall at ~0-1 m depth, d) hole 600-700 m along the wall at ~1-2 m depth, e) hole 1000-1100 m along the wall at ~0-1 m depth, and f) hole 1000-1100 m along the wall at ~1-2 m depth. Left column contains scenario, and right column contains control, as wall in with no hole in the wall. 69

Figure 37: Simulated comparison of a) the contribution of Ōhau Channel-derived water, b) the retention of Ōhau Channel-derived water, and c) wall efficiency, with combinations of holes in the wall at 300-400 m, 600-700 m, or 1000-1100 m along the wall, and ~0-1 m depth or ~1-2 m depth. N.b. For reference, short-dashed line equals wall-out, and long dashed lines equals wall-in (with no holes)..... 70

LIST OF ABBREVIATIONS & ACRONYMS

AEM3D	Aquatic Ecosystem Model
BoPRC	Bay of Plenty Regional Council
CC	Cloud cover
DO	Dissolved oxygen
DOCL	Dissolved organic carbon – labile
DONL	Dissolved organic nitrogen – labile
DOPL	Dissolved organic phosphorus – labile
DRP	Dissolved reactive phosphorus
IN _{Cyan}	Cyanobacteria internal nitrogen
IN _{Diat}	Diatom internal nitrogen
IP _{Cyan}	Cyanobacteria internal phosphorus
IP _{Diat}	Diatom internal phosphorus
MAE	Mean absolute error
N	Nitrogen
NH ₄	Ammonium
NO ₃	Nitrate
NO _x	Oxides of nitrogen
P	Phosphorus
PO ₄	Phosphate
POCL	Particulate organic carbon – labile
PONL	Particulate organic nitrogen – labile
POPL	Particulate organic phosphorus – labile
RMSE	Root mean squared error
SWR	Shortwave radiation
TL _c	Trophic level chlorophyll <i>a</i>
TLI	Trophic level index
TL _n	Trophic level nitrogen
TL _p	Trophic level phosphorus
TN	Total nitrogen
TP	Total phosphorus
VHOD	Volumetric hypolimnetic oxygen demand

1 INTRODUCTION

1.1 Project Scope

The Bay of Plenty Regional Council (BoPRC) requested a thorough review of the available data for Lake Rotoiti, along with a modelling analysis, to assess the impact of the Ōhau Channel diversion wall on the lake's water quality. This study was directed by the research questions outlined in the "Terms of Reference: Ōhau wall: 7-year review", listed below:

Water quality review:

- Has the wall achieved its objective of improving water quality?
- Has the wall resulted in the lake reaching its Trophic Level Index (TLI) target in advance of improvements to Lake Rotorua water quality impacting Lake Rotoiti?
- Does current monitoring support continued placement of the wall, diverting Ōhau Channel water?
- What impact has the diversion wall had on the quality of the Kaituna River?

Water quality modelling:

- What is the modelled impact of the diversion wall on water quality and ecology?
- Does this align with the water quality and ecological monitoring of Lake Rotoiti?
- The diversion wall is expected to be in place for 50 to 100 years. Once it has been removed what is the likely water quality expectation for Lake Rotoiti if Lake Rotorua meets the TLI of 4.2 +, when Lake Rotoiti is expected to meet a TLI of 3.5?
- The diversion wall has effectively changed the water residence time in Lake Rotoiti from about 1.5 years to 5+ years. How does this impact Lake Rotoiti water quality, potentially having an impact on bottom water dissolved oxygen (DO) levels and especially the western arm of the lake?

In addition to reviewing water quality and conducting modelling, an evaluation was conducted on the leakage of water from the Ōhau Channel into Lake Rotoiti through multiple small holes in the wall near the lake surface.

1.2 Background

Lakes comprise 87% of surface freshwater existing in a liquid state on Earth (Gleick, 1996), and as such their management is integral to managing the integrity of earth's ecosystems. In recent decades, however, lakes have deteriorated at an alarming rate (Dixit et al., 1999; Schallenberg et al., 2013) primarily as a result of poor management and mitigation of anthropogenic-related inputs (Carpenter et al., 2011; Hamilton et al., 2016). Of these anthropogenic-related inputs, nitrogen (N) and phosphorus (P) are of particular concern owing to their driving eutrophication (i.e., over-enrichment) of the system, and subsequently resulting in bottom-water deoxygenation and surface-water phytoplankton blooms (Carpenter et al., 2011; Conley et al., 2009). Resultant phytoplankton blooms often also result in discoloration and reduced transparency of lake surface waters (Paerl et al., 2001). Further, blooms comprised of toxin-producing species may result in the death of flora and fauna and thus declining biodiversity and food web resilience within the lake; as well as sickness and death of livestock, wildlife, and humans reliant on lakes as a source of water (Carmichael & Boyer, 2016; Harke et al., 2016; Woodhouse et al., 2014).

A variety of in-lake restoration methods exist, designed to prevent further degradation and/or restore lake systems. These can include, for example, coagulant application (e.g., Alum or Phoslock; Smith et al., 2016), hydraulic flushing (Zhang et al., 2020), or artificial aeration (Antenucci et al., 2005). One method often simulated, although seldom applied, is that of inflow diversion, which primarily acts by stopping or reducing the scale of the nutrient-laden inflow entering a given system (Liu et al., 2014; Zhang et al., 2016). As such, the applicability of inflow diversion as a management strategy is dictated by the velocity of the inflow, the location of the inflow and outflow, the water quality properties (namely N and P) of the inflow and receiving system, and resultant changes to in-lake hydrodynamics (Gao et al., 2015; Yang et al., 2021). The largest scale inflow diversion in New Zealand is that of the in-lake inflow diversion wall in Lake Rotoiti, which largely prevents nutrient-laden water from the eutrophic Lake Rotorua entering via the Lake Rotoiti's primary inflow, the Ōhau Channel, and transiting to the main basin of the lake by instead short-circuiting the water down lakes primary outflow, the Kaituna River (Hamilton et al., 2005).

Lake Rotoiti (38°02'02.3"S; 176°24'34.4"E) is a large-monomictic mesotrophic lake (TLI; 3.8) located in the central North Island of New Zealand, that underwent considerable deterioration in water quality from the 1960s through the early 2000s. Deterioration during this time was primarily attributable to delivery of nutrient-laden waters from Lake Rotorua (TLI; 4.3), a large-monomictic eutrophic lake, via the Ōhau Channel (Vincent et al., 1984; Vincent et al., 1991; von Westernhagen et al., 2010). Consequently, in the mid-2000s an in-lake diversion wall was designed and constructed, with construction completed in mid-2008, to prevent the nutrient-laden Ōhau Channel flow from entering the main basin of the lake and instead short-circuiting the water down the Kaituna River (Hamilton et al., 2009). Following the wall's completion, water quality measures in Lake Rotoiti were shown to improve through 2009-10, before plateauing off through the early 2020s (BoPRC, unpub. data). During this time, however, water quality measures in Lake Rotorua were also shown to improve, primarily on account of improved catchment management practices, and alum dosing to the lake via the Utuhina and Puarenga Streams (McBride, 2022). Consequently, with improving water quality measures in Lake Rotorua, the question now raised is whether and to what extent the in-lake diversion wall is still required to protect against water quality deterioration in Lake Rotoiti, at its current TLI and target TLI of 3.5 (*Lakes Rotorua and Rotoiti Action Plan Action Plan*, 2009).

Lakes are complex systems influenced by a variety of internal and external processes, which have been shown to be well captured by highly parametrised numerical models (Bruce et al., 2006). These numerical models typically take the form of a 1-dimensional (1-D) (e.g., GLM; Hipsey et al., 2019) or 3-dimensional (3-D) (e.g., AEM3D; Hodges & Dallimore, 2018) hydrodynamic model which may or may not be coupled to an ecological model (or module; Hodges et al., 2000). Hydrodynamic models allow fine-resolution simulation of the temporal and spatial behaviour of physical properties in waterbodies subject to environmental forcing by inflows, outflows, surface heat fluxes, and wind stress (Hodges & Dallimore, 2018). In addition, these models when coupled to an ecological model allow for additional fine-resolution simulation of an array of chemical and biological variables, and an assessment of interactions amongst variables, for example, nutrients and phytoplankton growth and dynamics (Chan & Hamilton, 2001). Importantly, these models have been successfully applied to lakes from a range of latitudes and markedly different morphometries (Hodges et al., 2000; León et al., 2005; Romero et al., 2004). Consequently, when accurately configured and calibrated, these highly parameterised coupled hydrodynamic-ecological models present a powerful means to quantify the impact of various restoration and prevention measures, and in the case of this present study that of an in-lake diversion wall.

1.3 Aims and objectives

The aim of this study was to investigate the effects of the in-lake Ōhau Channel diversion wall on water quality measures and targets in Lake Rotoiti and the potential implications of removing the wall. This was addressed in three parts; 1) water quality data analysis, 2) lake system modelling, and 3) assessment of the flow of water through the holes in the diversion wall, as outlined below:

1. Water quality data analysis component, involving a series of statistical evaluations of existing data.
 - a. A series of summary statistics of existing water quality data for Lake Rotoiti were derived to better understand the broad changes of water quality in the lake before and after the wall was built.
 - b. Correlation analysis between key water quality parameters in Lake Rotorua, Lake Rotoiti, and Kaituna River to understand if and how the diversion wall has changed the connectivity of water quality between these systems. This part of the analysis is analogous to the previous 7-year review conducted by the University of Waikato (M Lehmann, 2015 unpub. data).
 - c. A formal intervention analysis was used to quantify the water quality changes in Lake Rotoiti in response to the construction of the Ōhau Channel diversion wall. In this analysis, we looked for the presence of (i) a step change immediately after the wall was built, which would indicate that the wall effectively caused a sudden change in water quality in Lake Rotoiti and (ii) a slope/trend change after the wall construction, which would indicate that over time, the presence of the wall gradually changed water quality in the lake.
2. The lake system modelling component, involving configuration and calibration of a 3-D hydrodynamic and coupled hydrodynamic-ecological model (AEM3D) of Lake Rotoiti, and subsequent scenario testing.
 - a. The hydrodynamic model scenarios were used to determine changes in the accumulation, retention, and behaviour of Ōhau Channel inflow-derived water within the lake and the removal of existing water in the lake, with and without the wall in place. These scenarios were run over 19 years, from 2003-04 through 2021-22.
 - b. The coupled hydrodynamic-ecological scenarios were used to determine changes in the Tropic Level Index with and without the wall in place, and without the wall in place under three Ōhau Channel inflow water quality regimes. These scenarios were run over 8 years, from 2014-15 through 2021-22.
3. Assessment of the holes in the diversion wall, involving analysis of data and hydrodynamic model scenario testing.
 - a. Available data were analysed to estimate the average hole size along the wall's length and calculate the total volume of water flowing from Ōhau Channel into Lake Rotoiti through the holes.
 - b. Modelling of scenarios using the calibrated hydrodynamic model, developed in step 2a, to determine whether and to what extent the holes affect the rate of accumulation and retention of the Ōhau Channel inflow-derived water within the lake, and changes in the wall's efficiency at limiting the passage of Ōhau Channel inflow-derived water into the main basin of the lake. These scenarios were run over 1 year, from 2003-04 through 2004-05.

2 STUDY SITE

Lake Rotoiti (38°02'02.3"S; 176°24'34.4"E) is a large warm-monomictic lake in Rotorua, The Bay of Plenty, New Zealand (Figure 1) (Gibbs, 1992). The climate of the region is temperate, with monthly median rainfall of ~85 mm in summer (Dec–Feb) and ~141 mm in winter (Jun–Aug) (Rotorua Aero Aws [1770], 2003–2022, MetService, New Zealand). The lake has a direct catchment area of 117.2 km², and an additional indirect catchment area of 478.0 km² (i.e., from Lake Rotorua, via the Ōhau Channel) (McBride et al., 2021). The catchment includes approximately 37% exotic forest, 21% native forest, and 8% agricultural land (McBride et al., 2021). At full water storage capacity, Lake Rotoiti has a volume of 1,042,300 ML, area of 33.7 km², and mean and maximum depths of 30.9 and ~120 m, respectively (McBride et al., 2021). The lake’s morphometry comprises a shallow eastern and deep western basin (Fish & Chapman, 1969). The lake’s primary inflow, the Ōhau Channel, enters at the eastern side of the eastern basin, with ~20 additional minor rivers, streams, and drains entering across both the eastern and western basins (Muraoka et al., 2010). Several of these inflows are geothermally derived, emanating from the Tikitere Geothermal Field. In addition, the lake receives a lakebed-based geothermal inflow within the lakes eastern basin, with an estimated hydraulic input of 350 L s⁻¹ (McBride et al., 2021). Outflow is via the Kaituna River, of which is controlled via the Okere Control Gate structure with the objective of maintaining lake level between a minimum and maximum water level of 278.89 and 279.44 m (Moturiki datum; Muraoka et al., 2010). Construction of an in-lake diversion wall—officially ‘The Ōhau Channel diversion wall’—was completed in mid-2008. The wall inserts at the shoreline just south of the Ōhau Channel inflow and extends ~1275 m northwards approximately parallel to the shoreline into the ‘Okere Arm’ and towards the Kaituna Outflow (von Westernhagen et al., 2010), thus preventing nutrient-laden Ōhau Channel derived-water from entering the main basin of the lake by instead short-circuiting the water down the Kaituna River. The lake stratifies for ~9–10 months between September and June (Gibbs et al., 2003), with surface waters during this time typified by having low concentrations of bioavailable N (i.e., dissolved inorganic N; DIN) and P (i.e., dissolved reactive P; DRP). The phytoplankton community is typically Diatom-dominated, except for during mid-Spring though late-Summer when diatom and cyanobacteria abundance are similar (BoPRC, unpub. data). Chlorophyll *a* concentrations typically peak during winter following turnover, typically coinciding with peak diatom abundance (BoPRC, unpub. data).

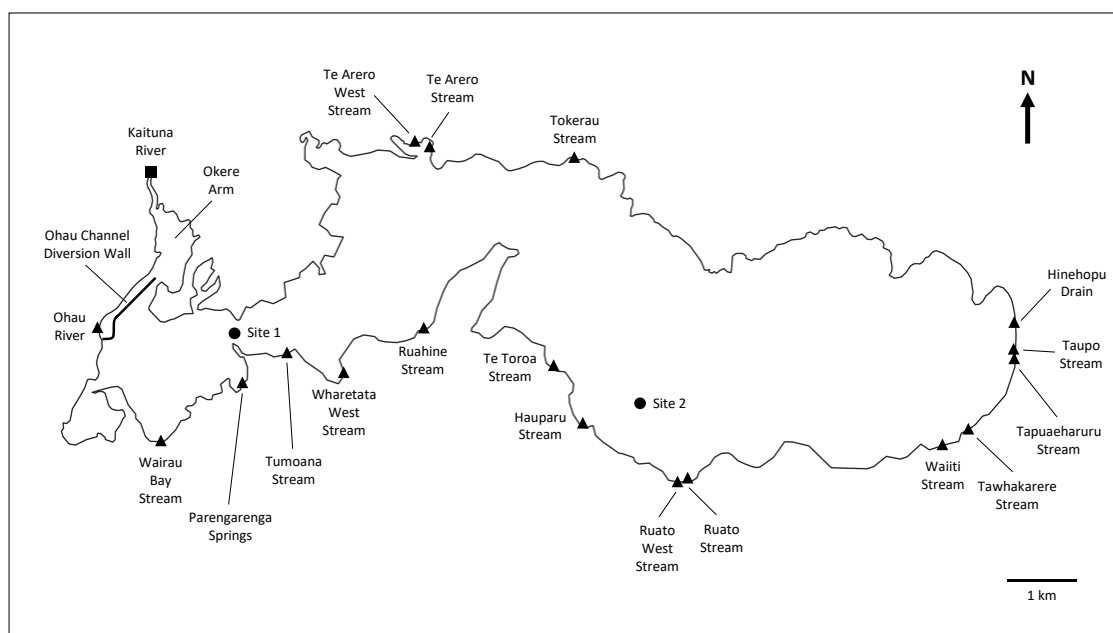


Figure 1: Lake Rotoiti study site showing sampling Sites (circles) 1 and 2, the Ōhau River inflow and the 17 minor inflows (triangles), the Kaituna River outflow (square), and the Ōhau Channel diversion wall.

3 METHODS

3.1 Part 1: Water quality data analysis

3.1.1 Data sources

All water quality data was sourced from the BoPRC. This analysis focused primarily on data collected in Lake Rotorua at Site 5, Lake Rotoiti at Site 3, and Kaituna River at the Lake Rotoiti outlet. Description of lake sampling methodology, and changes in laboratory analysis methods are described in detail in Hamill (2022). Wherever possible, all available data were used for analysis, unless otherwise stated.

3.1.2 Statistical analysis

Descriptive statistics

Several descriptive statistics were used to explore any long-term changes in water quality in Lake Rotoiti. Graphical aids were used to visualise the differences between water quality before and after the construction of the Ōhau Channel diversion wall and time series graphs (including indicative long-term trends) to understand the trajectory of water quality in the lake. Additionally, hypolimnetic DO dynamics were interrogated to understand better if the construction of the wall has changed internal processes in the lake. For this, the volumetric hypolimnetic oxygen demand (VHOD) was calculated for each hydrological year at sites 3 and 4. The VHOD measures oxygen depletion and integrates oxygen demand in the hypolimnion at the sediment-water interface due to organic matter breakdown and respiration and, therefore, encompasses several internal lake processes into a single indicator.

Correlation analysis

In a previous examination of the Ōhau Channel diversion wall (Lehmann, 2015, unpub. data), a correlation in water quality between Lakes Rotorua and Rotoiti was observed before the wall was built. The earlier study speculated that alterations in the association between the water quality of Lake Rotorua and Lake Rotoiti before and after the diversion wall installation would indicate an inherent adjustment in the water quality dynamics influencing Lake Rotoiti, which would be detectable by a correlation analysis of water quality between the two lakes. Consequently, a stronger correlation between the two lakes would be anticipated before the diversion wall's construction compared to the period following its installation, during which the majority of the Ōhau Channel flow was redirected downstream into the Kaituna River.

In this study, the correlation analysis methodology was expanded from 2015 to include data from more years (up to 2023) to address the relatively limited sample size post-diversion wall highlighted in the earlier review. A Pearson correlation coefficient was computed for all four variables constituting the TLI (total nitrogen, total phosphorus, chlorophyll *a*, and Secchi depth) using yearly average values from data obtained at Site 5 in Lake Rotorua and Site 3 in Lake Rotoiti. Given their proximity, these sites are presumed to exhibit the strongest correlation compared to other water quality monitoring sites in these lakes. Correlation coefficients were calculated for the period preceding the wall's construction (1995-2007) and the period following its installation (2008-2023). In addition, we also conducted least square linear regression of the data to determine the slope and intercept of the regression lines. A deviation in the slope of the relationships of the regression was interpreted as a modification in the connectivity between the two lakes, while a shift in the intercept was interpreted as a change in overall water quality in Lake Rotoiti. Interpretation of slopes and intercept was done using least square linear regression analysis in R using the 'lm' function, where the effects of the wall were included as an interaction term in the model formulation. Testing for differences in intercepts between pre- and post-wall periods was not done when there are differences

in slopes, because changing the slope also changes the intercept, which can then not be attributed to the effects of the wall.

Furthermore, the correlation analysis was extended to evaluate the impact of the diversion wall on Kaituna River water quality. Any change in the relationship between the water quality of Lake Rotoiti and the Kaituna River before and after the diversion wall would be ascribed to the wall's influence. It was anticipated that the correlation of water quality between these two systems would be stronger before the wall's construction compared to the post-diversion wall period. It is noted that only total phosphorus (TP) and total nitrogen (TN), but not chlorophyll *a* or Secchi depth, was used for this analysis, as these two water quality variables were deemed most comparable between the lake and river system.

Intervention analysis

To answer the question of whether the diversion wall has achieved its objective of improving water quality in Lake Rotoiti, causal inference must be drawn from analysing the observations from routine monitoring data before and after the wall. The challenge here is to compare the water quality state of the lake in the presence of the intervention (i.e., the diversion wall in this instance) with the state of the lake that would have existed if the intervention never occurred. A valid conclusion of causal inference from this comparison requires strong assumptions to ensure that other extrinsic factors (e.g., climate variability) did not cause any observed changes, which can be achieved by including a control site that was monitored during the same period and was itself not affected by the intervention. If any change in water quality was driven by extrinsic factors, the true effect of the intervention might be falsely under- or overestimated, or it could be falsely concluded that there was an effect even though in reality there was not, which highlights the importance of the control site.

A useful approach for drawing inference about the effect of an intervention is interrupted time series analysis using generalized least squares, which can be employed to assess whether the values of a quantity (e.g., water quality variables) have changed significantly in response to some form of intervention. At the core of this analysis lies the concept of a counterfactual, which in this case is the water quality that would have been observed in the absence of the intervention (i.e., the diversion wall). Statistical modelling using generalized least squares regression was utilised to estimate what did happen (the factual scenario) and what would have been expected to occur (the counterfactual scenario) if the diversion wall had never been installed. Considerable effort was dedicated to identifying a potential control site for this analysis. Lake Rotorua, among all other Te Arawa Rotorua Lakes, would have been the most logical choice as a control site due to its hydrological connection with Lake Rotoiti and empirical evidence indicating that water quality in these lakes was interconnected before the installation of the wall (refer to results of correlation analysis below). However, Lake Rotorua itself has undergone significant water quality management, including alum dosing that commenced around the time the diversion wall was installed. This rendered Lake Rotorua unsuitable for this purpose, as documented improvements in water quality in the lake would have influenced inferences about changes in Lake Rotoiti. No other Te Arawa Lake was deemed an adequate control site.

Generalized least squares regression models were constructed for all four water quality variables in the TLI, as well as for the TLI itself. The basic models incorporated terms for time, time of intervention, and post-intervention time. This model design facilitated the detection of water quality changes in two forms: (i) a step change immediately after the intervention, for instance, if the wall was so effective that water quality suddenly improved, and (ii) a slope/trend change after the

intervention, indicating gradual changes in water quality over time in Lake Rotoiti. Alternatively, there could be an initial step change in water quality followed by a gradual return to previous levels due to, for example, alterations in internal dynamics in Lake Rotoiti. The counterfactual (i.e., what would have happened without the wall) was modelled using the basic model without the intervention and post-intervention arguments, enabling the extrapolation of the pre-intervention trend beyond the intervention time point. The intervention analysis was conducted on annual average values of all water quality variables to avoid the need for more complex time series models that would have necessitated accounting for autocorrelation in the model formulation. All analyses were performed in the R statistical environment.

3.2 Part 2: Lake system modelling

3.2.1 Data sources

Bathymetric data were collected from a comprehensive bathymetric survey using depth soundings on 2006, by BoPRC. Water level measurements (BoPRC Site FL289316; 15-min resolution), for Jun-2003 through Dec-2022, were provided by BoPRC. Ōhau Channel inflow (BoPRC Site FL150407, daily resolution [1-Jun-2003–29-Oct-2010]; BoPRC Site FL230406, ~weekly resolution [8-Nov-2010–31-Dec-2022]) and Kaituna outflow (BoPRC Site FL334833, daily resolution) flow data, for Jun-2003 through Dec-2022, were provided by BoPRC. Ōhau Channel inflow water quality data (BoPRC Site FL230406, ~weekly resolution), for Jun-2003 through Dec-2022, were provided by BoPRC. Minor inflow flow and water quality data (for site listing see Appendix 1; monthly to sub-yearly resolution) for the limnological years (i.e., 1 July through 30 June of the following year) 1993-94 (flow only), 2005-06, and 2009-10, were provided by BoPRC. Meteorological data (MetService Site 1770 [Rotorua Aero Aws], 1-h resolution), including air temperature, atmospheric pressure, cloud cover (CC), rainfall, relative humidity, shortwave radiation (SWR), and wind speed and wind direction, for Jun-2003 through Dec-2022, were provided by MetService, New Zealand. In-lake water quality data for Site 3 (i.e., BoPRC Rotoiti Site 3; FL479468) and Site 4 (i.e., BoPRC Rotoiti Site 4; GL051366), for Jun-2003 through Dec-2022, were provided by BoPRC. Water quality data included temperature, DO, pH, specific conductivity, DRP, TP, ammonium (NH_4), oxides of N (NO_x) or nitrate (NO_3), TN, and chlorophyll *a*. Preliminary analysis indicated NO_3 composed 95-100% of NO_x , thus NO_3 and NO_x were pooled as NO_3 . Water quality data was taken at a single depth for inflows, and as a surface-integrated sample (variable depth) and bottom water sample (variable depth) in-lake. Temperature, DO, and specific conductivity, nutrients, and chlorophyll *a* were determined per Hamill (2022). Phytoplankton assemblage and count data (quarterly resolution) in Lake Rotorua (BoPRC Rotorua Site 5)—used as a proxy for the Ōhau Channel—and in Lake Rotoiti for Site 4 (BoPRC Rotoiti Site 4; GL051366), for Jul-2003 through Jun-2012, were provided by BoPRC.

3.2.2 Modelling

3.2.2.1 Model description

The Aquatic Ecosystem Model (AEM3D; v 1.1.2; Hodges & Dallimore, 2018) used to simulate the hydrodynamics in Lake Rotoiti. AEM3D is a 3-dimensional hydrodynamic–ecological model that simulates the temporal and spatial behaviour of stratified waterbodies subject to environmental forcing (inflows, outflows, surface heat fluxes, and wind stress). The 3-D nature of the AEM3D lends itself well to simulating complex spatially variable systems. The hydrodynamic module is based on the Estuary and Lake Computer Model (ELCOM) which has been applied to lakes from a range latitudes and markedly different morphometries (Chung et al., 2009; León et al., 2005; Romero et al., 2004), including Lake Rotoiti (Muraoka et al., 2010; Von Westernhagen, 2010). The model applies the unsteady Reynolds-averaged Navier-Stokes equations for incompressible flow, with a Boussinesq approximation for density differences and a hydrostatic assumption for pressure (Hodges et al., 2000). The hydrodynamic algorithms are based on the Euler-Lagrange method for advection of momentum,

and a conservative ULTIMATE QUICKEST (Leonard, 1991) approach for active (e.g., temperature) and passive (e.g., tracer) scalar transport (Hodges et al., 2000; Romero et al., 2004).

3.2.2.2 Model set-up

The model was configured to run at a 100-m² horizontal grid and uniform 1-m vertical layer, on a 2-min timestep, in trade-off between model resolution and runtime. The hydrodynamic model was configured with a photosynthetic active radiation extinction coefficient of 0.4. The hydrodynamic-ecological model was configured to not simulate resuspension, particulate inorganics, or refractory particulate organics (i.e., only labile particulate organics) because resuspension was assumed to be negligible in Lake Rotoiti and no data was available to adequately parametrise particulate matter. In addition, the hydrodynamic-ecological model was configured to include two phytoplankton groups, cyanobacteria (summer-adapted; buoyant) and diatoms (and other; winter-adapted; non-buoyant), of which growth and respiration functions for salinity, silica, and photoinhibition were disabled. Light, oxygen, N, P, and organic matter were parameterised as presented in Table 1, and the phytoplankton groups parameterised as presented in Table 2.

Table 1 Configuration of light, oxygen, nitrogen, phosphorus, and organic matter for the water quality model.

Parameter (as key string)	Unit	Value
Light		
uva_base_extinction	m ⁻¹	1.5
uvb_base_extinction	m ⁻¹	2.5
nir_base_extinction	m ⁻¹	1
par_base_extinction	m ⁻¹	0.2
Oxygen		
temperature_DO_sedflux_multiplier	Dimensionless	1.05
DO_sedflux_coefficient	g m ⁻² day ⁻¹	2
O2_DO_sedflux_half_saturation	mg L ⁻¹	0.25
Nitrogen		
<i>Sediment parameters</i>		
temperature_NH4_sedflux_multiplier	Dimensionless	1.05
NH4_sedflux_coefficient	g m ⁻² d ⁻¹	0.047
O2_NH4_sedflux_half_saturation	mg L ⁻¹	2.75
temperature_NO3_sedflux_multiplier	Dimensionless	1.05
NO3_sedflux_coefficient	g m ⁻² d ⁻¹	0
O2_NO3_sedflux_half_saturation	mg L ⁻¹	2.75
<i>Water-column parameters</i>		
temperature_nitrification_multiplier	Dimensionless	1.08
nitrification_coefficient	d ⁻¹	0.11
O2_nitrification_half_saturation	mg L ⁻¹	2.5
temperature_denitrification_multiplier	Dimensionless	1.08
denitrification_coefficient	d ⁻¹	0.125
O2_denitrification_half_saturation	mg L ⁻¹	0.3
temperature_mineralisation_multiplier	Dimensionless	1.08
mineralisation_coefficient	d ⁻¹	0.013
O2_mineralisation_half_saturation	mg L ⁻¹	1.5
Phosphorus		
<i>Sediment parameters</i>		
temperature_PO4_sedflux_multiplier	Dimensionless	1.05
PO4_sedflux_coefficient	g m ⁻² d ⁻¹	0.011
O2_PO4_sedflux_half_saturation	mg L ⁻¹	2.75
<i>Water-column parameters</i>		
temperature_mineralisation_multiplier	Dimensionless	1.08
mineralisation_coefficient	d ⁻¹	0.045
O2_mineralisation_half_saturation	mg L ⁻¹	1.5
Organic matter		
labile_density	kg m ⁻³	1050
labile_diameter	m	1.25E-05
labile_settling_model	-	STOKES
temperature_labile_decomposition_multiplier	Dimensionless	1.08
labile_decomposition_coefficient	d ⁻¹	0.005
O2_labile_decomposition_half_saturation	mg L ⁻¹	1.5
labile_light_attenuation	m ⁻¹	0.02

Table 2 Configuration of phytoplankton groups for the water quality model.

Parameter (as key string)	Unit	Value	
		Cyanobacteria	Diatoms
<i>General parameters</i>			
min_biomass	$\mu\text{g chl } a \text{ L}^{-1}$	0.1	0.1
carbon_Chla_ratio	Dimensionless	40	40
sediment_decay_rate	d^{-1}	0.5	0.5
salinity_growth_function_type	-	NONE	NONE
salinity_respiration_function_type	-	NONE	NONE
<i>Growth parameters</i>			
growth_coefficient	d^{-1}	0.54	1.4
light_growth_initial_curve_slope	$\mu\text{mol m}^{-2} \text{ s}^{-1}$	140	1
temperature_growth_multiplier	Dimensionless	1.05	1.05
temperature_growth_standard	$^{\circ}\text{C}$	17	9
temperature_growth_optimum	$^{\circ}\text{C}$	32	19
temperature_growth_maximum	$^{\circ}\text{C}$	39	34
P_Chla_ratio_min	$\text{mg P mg chl } a^{-1}$	0.2	0.25
P_Chla_ratio_max	$\text{mg P mg chl } a^{-1}$	1.8	1.3
P_max_uptake_rate	$\text{mg P mg chl } a^{-1} \text{ d}^{-1}$	0.33	0.1
P_growth_half_saturation	mg P L^{-1}	0.01	0.013
N_Chla_ratio_min	$\text{mg N mg chl } a^{-1}$	4.4	4
N_Chla_ratio_max	$\text{mg N mg chl } a^{-1}$	10	8
N_max_uptake_rate	$\text{mg N mg chl } a^{-1} \text{ d}^{-1}$	2.95	3.35
N_growth_half_saturation	mg N L^{-1}	0.028	0.035
<i>Loss parameters</i>			
respiration_coefficient	d^{-1}	0.0378	0.077
temperature_respiration_multiplier	Dimensionless	1.05	1.05
mortality_coefficient	d^{-1}	0.0081	0.0165
excretion_coefficient	d^{-1}	0.0081	0.0165
<i>Other parameters</i>			
migration_type	-	CONSTANT	CONSTANT
settling_velocity	m s^{-1}	3.23E-07	2.91E-06
density	kg m^{-3}	990	980
diameter	m	1.50E-04	8.00E-06
light_attenuation	m^{-1}	0.014	0.014

Lake geometry input was compiled in the pre-processor model, and included input relating to 1) lake bathymetry, 2) inflow and outflow boundary conditions, 3) update boundary conditions, 4) levee boundary conditions. Lake bathymetry was input as a 3-dimensional cartesian mesh, with uniform cell spacing of 100 m in each of the horizontal dimensions (x and y) and at 1 m in the vertical dimension (z). Lake bathymetry was generated in QGIS v. 3.16.14 (QGIS.org, 2023) by resampling data from the bathymetric survey conducted in 2006. Inflow and outflow boundary conditions, as flow direction and x, y, and z placement within the bathymetric grid, were stipulated for the Ōhau Channel inflow, the Kaituna outflow, 17 minor surface inflows, the groundwater-based geothermal flux in the main crater and northern reaches of the eastern-basin, and a residual outflow (for balancing of the water budget). In the absence of an explicit means to simulate atmospheric deposition, inflow boundary conditions also stipulated in the hydrodynamic-ecological model for an ‘atmospheric deposition’ inflow, which was applied as a set of 39 boundary conditions spaced appropriately equally around the periphery of the bathymetric grid. Update boundary conditions (i.e., user defined cells, which enables scalar values to be arbitrarily updated), as x, y, and z placement within the bathymetric grid, were stipulated to encompass the entire lake to allow labelling of the lake with a tracer, and thus quantify removal of existing lake water and ultimately residence time (N.b. hydrodynamic model and hydrodynamic-ecological wall-in and wall-out ‘baseline’ only). Levee boundary conditions (i.e., user defined cells, which places a solid wall between cells), as x, y, and z placement within the bathymetric grid, were stipulated to model the Ōhau Channel diversion wall (N.b., wall-in scenarios only).

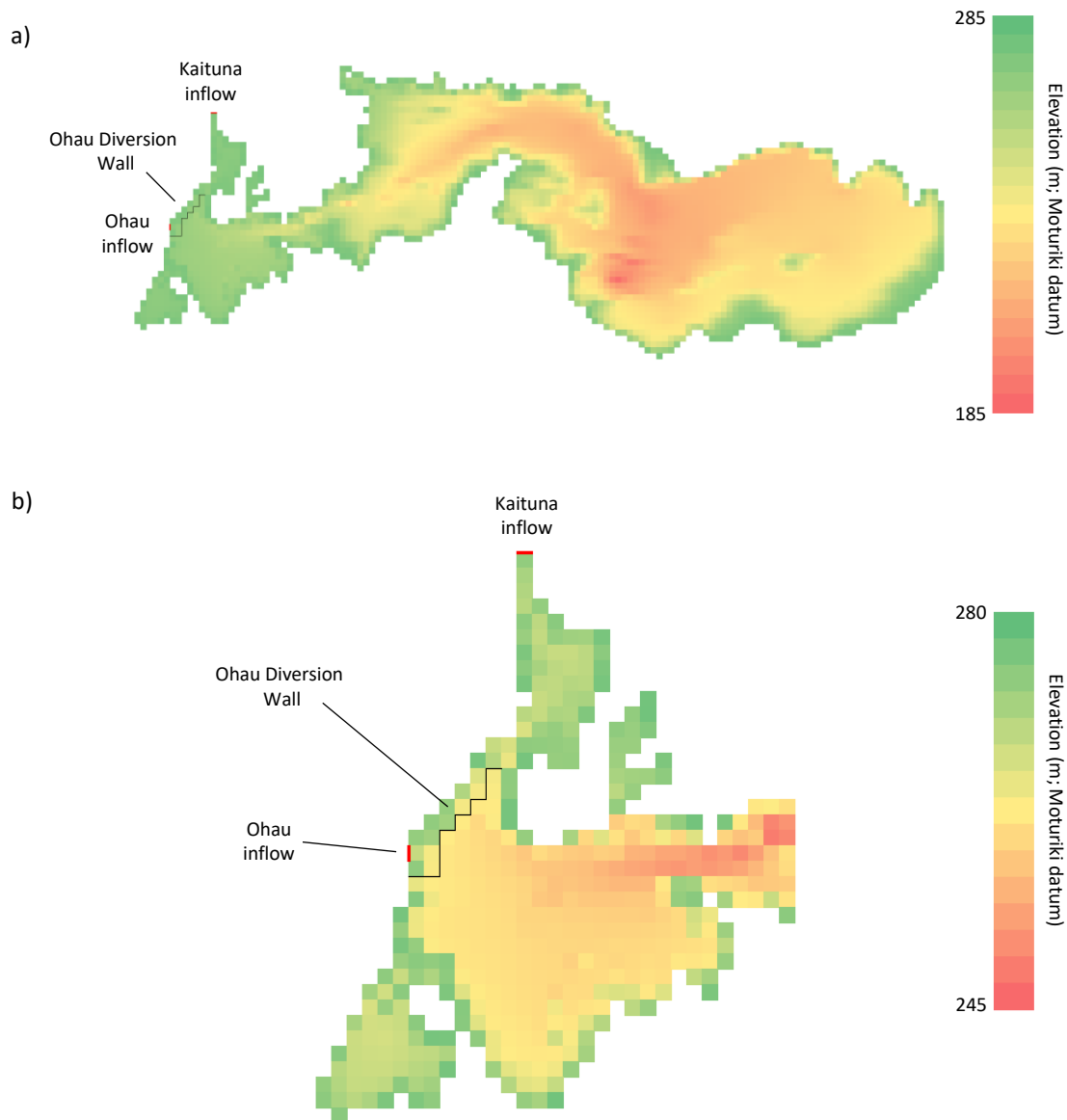


Figure 2: Cartesian mesh of, a) Lake Rotoiti, and b) the western reaches of Lake Rotoiti, demonstrating the boundary condition for the Ōhau inflow and Kaituna outflow, and Levee representing the Ōhau Channel diversion wall (wall-in scenarios only).

Initial profile conditions for temperature, DO, and specific conductivity were determined from measured SONDE profiles, and input at 1 m intervals from 1 m to 100 m depth. Salinity (psu) was determined as $0.4665 \times SC^{1.0878}$ where specific conductivity is in $mS\ cm^{-1}$ (Williams, 1986). Initial profile conditions for pH, phosphate (PO_4 , as DRP), dissolved organic P – labile (DOPL), particulate organic P – labile (POPL), NH_4 , NO_3 , dissolved organic N – labile (DONL), particulate organic N – labile (PONL), dissolved organic carbon – labile (DOCL), particulate organic carbon – labile (POCL), cyanobacteria, cyanobacteria internal P (IP_{Cyan}), cyanobacteria internal N (IN_{Cyan}), diatoms, diatom internal P (IP_{Diat}), diatom internal N (IN_{Diat}) were determined as the mean of surface and bottom water measurements for all other parameters. Particulate P (i.e., $POPL + IP_{Cyan} + IP_{Diat}$) and DOPL were apportioned as 0.73 and 0.27 of TP less DRP, respectively. In the absence of direct measurements of the nutrient species, this was based on a ratio determined from a mean monthly value taken across a

12-month period in Lake Wivenhoe, Australia (Prentice, unpub. data). Particulate N (i.e., PONL + IN_{Cyan} + IN_{Diat}) was determined as particulate P multiplied by 1.4, a ratio determined from monthly N and P values taken from bottom waters across a 24-month period in Lake Rotoiti (Priscu et al., 1986). Dissolved organic nitrogen – labile was determined as TN less DIN and particulate N. Phytoplankton N and P stores were determined as their respective chlorophyll *a* value multiplied by their configured N_Chla_ratio_max and P_Chla_ratio_max values, respectively. Particulate organic nitrogen – labile was determined as particulate N less IN_{Cyan} and IN_{Diat}, and POPL was determined as Particulate P less IP_{Cyan} and IP_{Diat}. Particulate organic carbon – labile was determined as TIN less DIN, multiplied by 7.29; and DOCL as DIN multiplied by 7.29 (Abell et al., 2015). Initial profiles at the start of the simulations were applied uniformly to all horizontal grids in the lake.

Meteorological data were determined from that measured at MetService Site 1770 (Rotorua Aero Aws), and included air temperature, atmospheric pressure, rainfall, relative humidity, SWR, wind speed and wind direction (for daily time series see Appendix 2 and Appendix 3). Data was input hourly, with missing data filled by linear interpolation in Python 3.11 (Van Rossum & Drake, 2009), and applied uniformly across all horizontal grids. In addition, CC was determined from SWR (Luo et al., 2010), from a subset of measured CC and SWR data collected across a 10 year period during 2013–2023. Here, measured CC was sorted into bins at 0.01 increments between 0 and 1, and the mean (cloud) obstructed fraction of SWR for each bin calculated and plotted as a 2nd order polynomial ($R^2 = 0.9843$), given as (Equation 1):

$$CC = (-1.4859 \cdot O_{SWR}^2) + (2.4098 \cdot O_{SWR}) \quad 1$$

where CC is cloud cover, and O_{SWR} is the (cloud)obstructed fraction of SWR. O_{SWR} is given as (Equation 2):

$$O_{SWR} = 1 - \left(\frac{M_{SWR}}{CS_{SWR}} \right) \quad 2$$

where M_{SWR} is the measured SWR, and CS_{SWR} is the theoretical “clear-sky” SWR (i.e., SWR under cloud-free conditions). CS_{SWR} was determined using the BIRD Clear Sky model (Bird & Hulstrom, 1981; Myers), and parametrised per Table 3. Cloud cover was input daily and applied uniformly across all horizontal grids.

Table 3 Configuration for BIRD Clear Sky Model.

Parameter	Unit	Value	Reference
Latitude	decimal degrees	-38.0398	N/A
Longitude	decimal degrees	176.3465	N/A
Timezone	GMT offset	12	N/A
Pressure	mB	982.01	MetService
Ozone	cm	0.296	Luo et al. (2010)
Total Colum Water Vapour	cm	1.5	Default
Aerosol Optical Depth @500 nm	cm	0.0254	Luo et al. (2010)
Aerosol Optical Depth @380 nm	cm	0.0290	Luo et al. (2010)
Ba	Dimensionless	0.85	Default
Albedo	Dimensionless	0.2	Default

Ōhau Channel inflow and the Kaituna outflow were input as daily, by linearly interpolating available measurements. The groundwater geothermal inflow was input as a constant daily flow of 350 L s^{-1} (McBride et al., 2021), apportioned as 225 L s^{-1} to the main crater and 125 L s^{-1} to the northern reaches of the eastern basin. Minor surface inflows ($n = 17$) were input daily, as the positive unknown term in a daily water balance of known sources, of which included the Ōhau Channel inflow (measured), Kaituna outflow (measured), the groundwater geothermal inflow (constant, as above), rainfall (measured), evaporation (calculated; from air temperature, atmospheric pressure, relative humidity, wind speed, and surface water temperature). The negative term of the water balance was assigned as a groundwater outflow. The flow assigned to each of the minor inflows was calculated as (Equation 3):

$$QM_X = U \cdot \left(\frac{Q_X}{Q_T} \right) \quad 3$$

where QM_X is the modelled flow for a given minor flow, U is the positive unknown term in the water balance, Q_X is the mean measured daily flow for a given site, and Q_T is the mean measured daily flow across all 17 sites. Q_X and Q_T were determined as the mean value across three limnological years (1993-94, 2005-06, 2009-10), with mean values for each year determined from daily-linearly interpolated data, and each year indexed to the largest flow, i.e., Waiti Stream (BOP120009). The flow assigned to the groundwater outflow, was applied to 23 cells east of Site 3 per a $1 \times 1 \text{ km}$ grid.

Ōhau Channel inflow water quality data were input as daily, by linearly interpolating available measurements. Salinity (psu) was determined as $0.4665 \times SC^{1.0878}$ where specific conductivity is in mS cm^{-1} (Williams, 1986). Water quality data for the minor inflows were input as daily values based on a generalised seasonal model for each flow. These generalised seasonal models were determined as the mean daily value from one or both 2005-06 and 2009-10 limnological years, in turn determined as the 90-day mean from daily interpolated bi-weekly to multi-monthly data. Particulate P (i.e., POPL, IP_{Cyan} , IP_{Diat}) and DOPL were determined as TP less DRP, multiplied by 0.5 (Abell et al., 2015). Particulate N (i.e., PONL, IN_{Cyan} , IN_{Diat}) was determined as TP less DRP, multiplied by 0.6 (Abell et al., 2015). Dissolved organic nitrogen – labile was determined as TP less DRP, multiplied by 0.4 (Abell et al., 2015). Phytoplankton N and P stores were determined as their respective chlorophyll *a* value multiplied by their configured $N_Chla_ratio_max$ and $P_Chla_ratio_max$ values, respectively. Particulate organic nitrogen – labile was determined as Particulate N less IN_{Cyan} and IN_{Diat} , and POPL was determined as Particulate P less IP_{Cyan} and IP_{Diat} . Particulate organic carbon – labile was determined as TIN less DIN, multiplied by 7.29; and DOCL as DIN multiplied by 7.29 (Abell et al., 2015). Particulate organic carbon – labile was determined as TIN less DIN, multiplied by 7.29; and DOCL as DIN multiplied by 7.29.

The groundwater geothermal flow for temperature was input as $115 \text{ }^\circ\text{C}$ and $35 \text{ }^\circ\text{C}$ in the main crater and the northern reaches of the eastern basin, respectively (Muraoka et al., 2010). The groundwater geothermal flow for DO were input daily, as the mean of the four sub-surface geothermal inflows; Te Arero Stream (BOP120261), Parengarenga Springs (BOP120012), Wharetata West Stream (BOP120265), and Wairau Bay Stream (BOP120263), and all other water quality variables input as zero. It is recognised that the groundwater geothermal flow has associated P and N loadings, however with there being no measured flow data, let alone water quality data, it was decided the more conservative approach was to have the nutrient loadings associated with a completely dynamic input, in that of a sediment flux.

The atmospheric deposition flux was input daily. The flux was determined by the average atmospheric deposition of N and P for North Island, New Zealand lakes of 6.37 kg N ha⁻¹ y⁻¹ and 0.34 kg P ha⁻¹ y⁻¹ (Verburg et al., 2018). The inorganic portion was determined as that reported in Lake Taupo of 42% of the N flux and 54% of the P flux (Vant & Gibbs, 2006), with 42% of N applied as equally at 21% as NH₄, and 21% as NO₃, and 54% of P applied as PO₄. The remainder of N and P was apportioned equally between the dissolved organic and particulate organic fractions. Nitrogen and P loads were released as a concentrated flow at a rate of 25 m s⁻¹, divided equally amongst the 39 sites placed appropriately around the lake periphery.

3.2.2.3 *Model calibration and validation*

The hydrodynamic model was calibrated (1-Jul-2003–30-Jun-2004) from measurements of temperature, and the water quality model calibrated (1-Oct-2014–30-Sep-2015) from measurements of temperature, DO, DRP, TP, NH₄, NO₃, TN, and chlorophyll *a*. Model calibration fit was quantified statistically by way of; model fit using Pearson correlation (R), and model accuracy using root mean squared error (RMSE) and mean absolute error (MAE). Temperature and DO were calibrated at 1 m, 10 m, 20 m, 30 m, 40 m, and 60 m. Dissolved reactive phosphorus, P, NH₄, NO₃, TN, and chlorophyll *a* were calibrated in the surface waters (surface-integrated) and bottom waters (discrete depth), at depths consistent with field measurement depths. In addition, an emphasis was given to the concentration of TP and TN on autumn turnover to ensure the model was well calibrated to simulate abrupt increases or decreases in nutrients due to autumn mixing throughout the 8 year simulation period, even if nutrient dynamics during the stratification period were not captured very well. Both the hydrodynamic and hydrodynamic-ecological models were validated, following the same logic as the model calibration, across the 12-month period immediately following the calibration period (1-Jul-2004–30-Jun-2005 for the hydrodynamic model; 1-Oct-2015–30-Sep-2016 for the water quality model).

3.2.2.4 *Model simulations*

Hydrodynamic simulations were initialised on 1-Jun-2003, permitting a 30-day spin-up period, and a simulation period beginning on 1-Jul-2003. Hydrodynamic-ecological simulations were initialised on 19-Aug-2014, permitting a 43-day spin-up period, and a simulation period beginning on 1-Oct-2014. The Hydrodynamic-ecological (c.f., hydrodynamic model) initialisation was determined by the sampling date in which the lake was most vertically homogenous, owing to the water quality model's sensitivity to initialisation of water quality parameters. As simulations were initialised with measured data, wall-out scenarios for the hydrodynamic-ecological model (which was initialised in 2014; 7-8 years post-wall construction) represent the removal of the Ōhau Channel diversion wall. Both the hydrodynamic and coupled hydrodynamic-ecological simulations were analysed within the context of the limnological year (1-Jul through 30-Jun of the subsequent year). In the case of the coupled hydrodynamic-ecological simulations and the 19-Aug-2014 initialisation and spin-up period, the first limnological year represents 9-months from 1-Oct-2014 through 30-Jun-2015.

In the output definition file, temperature and tracers in the hydrodynamic model, and temperature, DO, PO₄, TP, NH₄, NO₃, TN, diatoms, and cyanobacteria in the hydrodynamic-ecological model were stipulated for output. For the purpose of answering the current study's aims and objective, the same variables were stipulated to output: 1) hourly Sites 3 and 4; and 2) daily (at 0000 h) as sheets (i.e., aerial 100-m² grids of the lake) as average (vertically integrated).

Model simulations included both hydrodynamic and coupled hydrodynamic-ecological, as follows:

1. Hydrodynamic model simulations were applied to investigate changes in the accumulation (i.e., % of Lake Rotoiti water derived from the Ōhau Channel over a single year), retention (i.e., % of Ōhau Channel water entering Lake Rotoiti, which remained in the Lake Rotoiti over a single year), and behaviour (i.e., trajectory) of Ōhau Channel inflow-derived water within the lake, and the removal (i.e., % of Lake Rotoiti water replaced by water derived from outside the lake over a single year) of existing water in the lake (to determine residence time), with and without the wall in place. Correspondingly, two scenarios were tested including: 1) wall-out, 2) and wall-in. First, this involved applying a unique conservative tracer—for each limnological year—to Ōhau Channel inflow, to investigate the accumulation of Ōhau-derived water within Lake Rotoiti each limnological year. Second, this involved applying a non-conservative tracer (i.e., with a tracer decay rate of 0.5 per week) to the Ōhau Channel inflow, to investigate the insertion and propagation (i.e., as an over-, inter-, or under-flow) of the Ōhau Channel-derived flow within Lake Rotoiti. Third, this involved applying a unique conservative tracer (via an update file, in the pre-processor model)—on day 1 of each limnological year—to Lake Rotoiti, to investigate the loss of Lake Rotoiti water each limnological year, and thus calculate residence time. Simulations were run for 19 years from 1-Jul-2003 through 30-Jun-2022.
2. Hydrodynamic-ecological model simulations were applied to investigate changes in TLI with and without the wall in place, and without the wall in place under three Ōhau Channel inflow water quality regimes. Correspondingly, four scenarios were tested, including: 1) wall-in (with Ōhau Channel water quality parameters as measured, i.e., maximum TLI of 4.41), 2) wall-out (with Ōhau Channel water quality parameters as measured, i.e., maximum TLI of 4.41); 3) wall-out, with Ōhau Channel water quality measures scaled to a maximum TLI of 4.2 (equivalent to a 15.5% reduction in N, P, and chlorophyll *a*); and 4) wall-out, with Ōhau Channel water quality measures scaled to a maximum TLI of 3.8 (equivalent to a 39.0% reduction to N, P, and chlorophyll *a*). For the wall-in and wall-out under baseline conditions, this also involved applying a unique conservative tracer to Ōhau Channel inflow, to investigate accumulation of Ōhau-derived water within Lake Rotoiti from 1-Oct-2014 through 30-Jun-2022; and applying a unique conservative tracer (via an update file, in the pre-processor model)—on day 1 of the model simulation (i.e., 1-Oct-2014)—to Lake Rotoiti, to investigate loss of Rotoiti water from 1-Oct-2014 through 30-Jun-2015. Simulations were run from 1-Oct-2014 through 30-Jun-2022.

3.2.2.5 Model output

Model simulations included both hydrodynamic and coupled hydrodynamic-ecological, as follows:

1. Hydrodynamic model output: Calibration and validation per Profile at Site 4. Insertion and propagation (i.e., as an over-, inter-, or under-flow) of the Ōhau-derived flow within Lake Rotoiti was visualised per ‘Profiles’ placed Site 3 and Site 4. Accumulation of Ōhau Channel inflow in Lake Rotoiti and removal of Lake Rotoiti water (for calculation of residence time) was determined per average ‘Sheet’ across the lake (here defined as the entire lake less the area inside the diversion wall and north of the wall into the Okare arm of the lake), given as (Equation 4):

$$Z = \frac{\sum_{i=1}^n t_i \cdot d_i}{\sum_{i=1}^n 1 \cdot d_i} \quad 4$$

where *Z* represents the proportion of water as Ōhau Channel-derived water (i.e., when calculating Ōhau Channel-derived water accumulation) or removal of Rotoiti water (i.e.,

when calculating Lake Rotoiti water removal, and thus residence time), t_i represents the value of the tracer at Site i , d_i represents the depth at Site i . Removal (i.e., % of Lake Rotoiti water replaced by water derived from outside the lake over a single year) was determined as 1 less the ‘raw’ modelled output value which represented retention (i.e., % of Lake Rotoiti water *not* replaced by water derived from outside the lake over a single year) of Lake Rotoiti water.

2. Hydrodynamic-ecological model output: Calibration and validation per Profile at Site 4. Loss of Lake Rotoiti water (for calculation of residence time) was determined per average ‘Sheet’ across the lake (Equation 4). Analysis of change in water quality parameters per Profile at Site 4.

3.3 Part 3: Assessment of holes in the diversion wall

This section involved two components: (i) calculations of plausible flow rates through the holes based on hole size and flow measurements, and (ii) hydrodynamic modelling, which quantified the reduction in wall efficiency with a single 1×100 -m hole in the wall—the finest scale hole possible within our model grid—relative to an uncompromised wall.

3.3.1 Calculations

To facilitate a quantitative estimation of the water flow through the holes in the diversion wall, BoPRC commissioned Greenfield Diving Services & Maintenance Engineering to assess the condition of the wall, which included measuring the size of the holes. The measurements were conducted by placing a square welded wire mesh (100×100 -mm) over each hole (see Figure 3). The number of mesh squares covering each hole was counted and recorded as square meters. In total, 32 holes were assessed, with a total of 113 mesh squares counted. This resulted in a total hole area of 1.13 m^2 across all 32 holes, yielding an average hole size of 0.035 m^2 . Additionally, BoPRC conducted flow velocity measurements through the holes at approximately 100-meter intervals along the entire length of the wall in February 2024. The distance-weighted average velocity through the holes was 0.156 m s^{-1} , with a maximum velocity of 0.456 m s^{-1} (approximately 100 meters downstream from the Ōhau Channel delta) and a minimum velocity of -0.074 m s^{-1} (approximately 1200 meters downstream from the Ōhau Channel delta). It is noteworthy that flow velocity measurements from approximately 900 meters downstream from the Ōhau Channel delta onwards were all negative, indicating water flowing from Lake Rotoiti into the Ōhau Channel through the holes. The total number of holes in the diversion wall is currently unknown and needed to be estimated in this study to calculate the volume of water flowing through the holes. This estimated leakage volume was then compared to the average discharge in the Ōhau Channel during February 2024 to better understand the potential impacts of the holes on Lake Rotoiti.

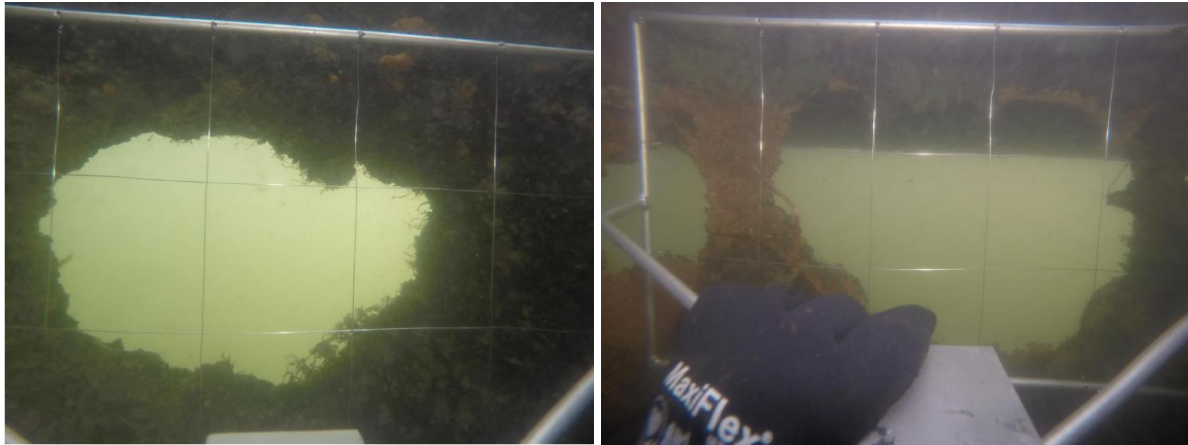


Figure 3: Examples of hole measurements carried out by Greenfield Diving Services & Maintenance Engineering as part of an assessment of the condition of the wall in July 2023. The size of the square mesh is 100×100 -mm.

3.3.2 Modelling

Hydrodynamic modelling was based on the same calibrated and configured model described in section ‘3.2.2 Modelling’ (and more specifically, ‘3.2.2.2 Model set-up’), except for altering the levee of which represents the diversion wall. Here, the wall with holes was simulated in using a single 1×100 -m hole, i.e., the finest scale hole possible within our model grid. To account for the simplified representation of the holes, six different configurations of the single 1×100 -m hole were simulated to provide a range of potential values, which included holes at 300-400 m, 600-700 m, and 1000-1100 m along the wall (Figure 4a), at 1 m and 2 m below the surface (Figure 4b). Simulations were run for a single year from 1-Jul-2003 through 30-Jun-2004. Model resolution in this study meant that many small (i.e., 0.035 m^2 ; see section ‘3.3.1 Calculations’) holes were ‘pooled’ and simulated as a single 1×100 -m hole, and it is understood that this method is an oversimplification, and the process is far more complex in reality.

To investigate whether and to what extent a 1×100 -m hole affects the rate of accumulation (i.e., % of Lake Rotoiti water derived from the Ōhau Channel over a single year), and rate of retention (i.e., % of Ōhau Channel water entering Lake Rotoiti, which remained in the Lake Rotoiti over a single year) of the Ōhau Channel inflow derived water within the lake. The six scenarios with a 1×100 -m hole, and the regular wall-in and wall-out scenarios (see ‘Model simulations 3.2.2.4’, bullet point 1) were run for one limnological year from Jul-2003 through Jun-2004. This involved applying a unique conservative tracer to Ōhau Channel inflow, to investigate the accumulation, and retention, of Ōhau-derived water within Lake Rotoiti each limnological year. In addition, wall efficiency was calculated in the instance of the six scenarios with holes in the wall, and given as:

$$E = \frac{Z_{wo} - Z_{wi_h}}{Z_{wo} - Z_{wi}} \quad 5$$

where E represents the wall efficiency, where Z_{wo} represents Z per eqn 4 for the wall-out scenario, Z_{wi_h} represents Z per eqn 4 for the wall-in with holes, and Z_{wi} represents Z per eqn 4 for the wall-in (with no holes).

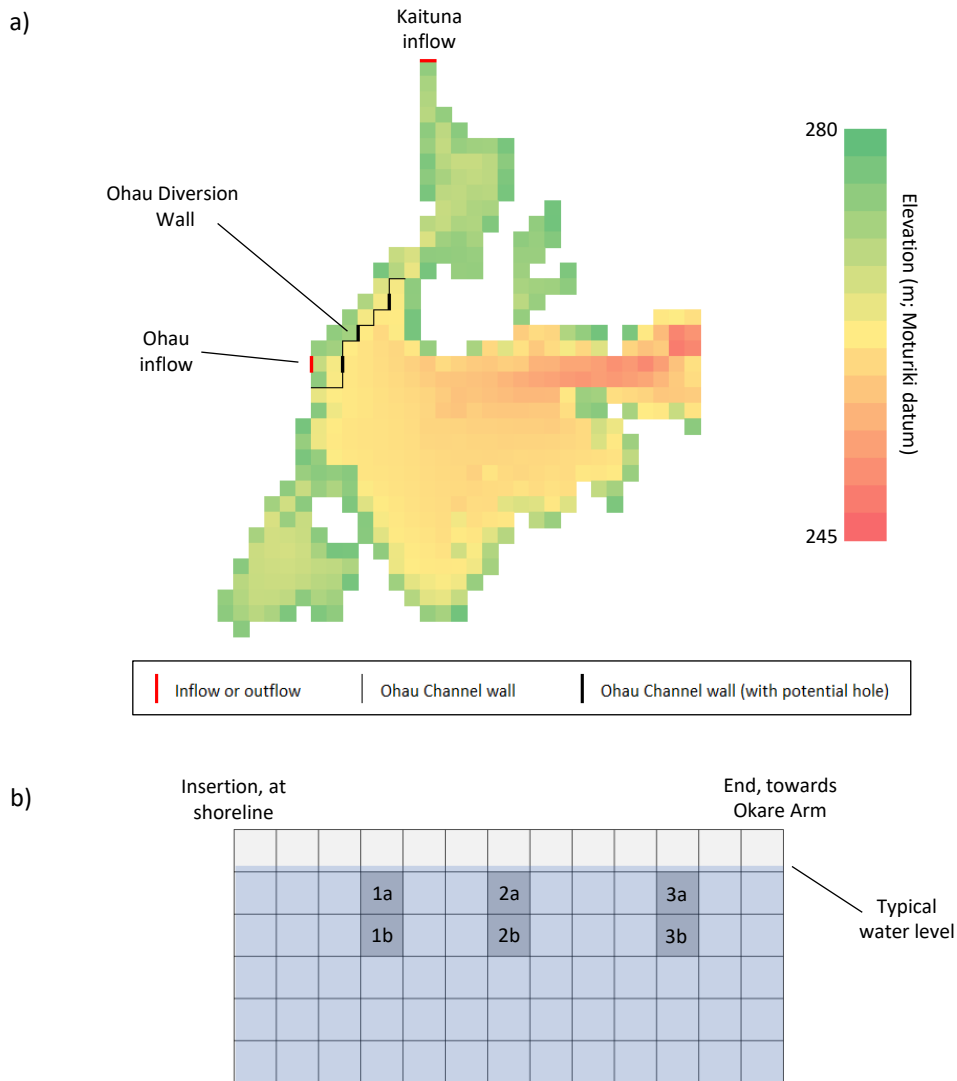


Figure 4: a) Cartesian mesh of the western reaches of Lake Rotoiti, demonstrating the boundary condition for the Ōhau inflow and Kaituna outflow, and Levee representing the Ōhau Channel diversion wall (wall-in scenarios only) with sections of wall with holes (wall-in with hole scenarios only) identified; and b) vertical grid of Levee representing the diversion wall (n.b. only upper 6 cells represented) showing placement of holes under the six configurations for wall-in with a hole scenarios.

4 RESULTS

4.1 Part 1: Water quality data analysis

4.1.1 Descriptive statistics

The monitoring data from Lakes Rotoiti and Rotorua indicate that both lakes experienced changes in water quality over the study period. Lake Rotorua data were incorporated into this analysis to investigate the potential of the lake to serve as a control site for the intervention analysis. Generally, all assessed water quality parameters exhibited improvement in Lake Rotoiti following the construction of the wall (Figure 5). However, this improvement was less noticeable for chlorophyll *a* and TP concentrations. Interestingly, despite not being directly impacted by the diversion wall, Lake Rotorua displayed similar patterns of improvement in water quality and even exhibited a more significant enhancement in DRP and TP compared to Lake Rotoiti. These improvements in Lake Rotorua are likely attributed to the ongoing alum application regime in the Puarenga and Utuhina Streams, as well as enhanced catchment management as part of the implementation of Plan Change 10. However, due to these observed changes in Lake Rotorua, the lake is not an ideal control site for robustly assessing water quality changes in Lake Rotoiti. The remainder of the data analysis largely focused on the four water quality variables included in the TLI, and the TLI itself.

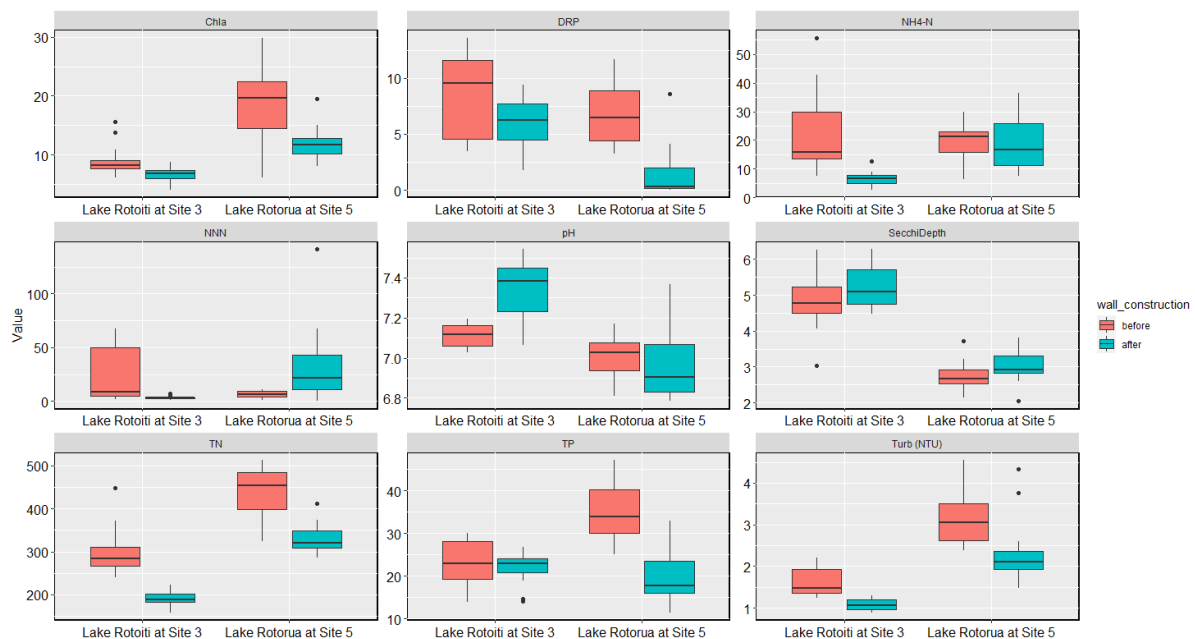


Figure 5: Median values of water quality parameters in Lakes Rotorua (Site 5) and Rotoiti (Site 3) before and after the Ōhau Channel diversion wall construction. Vertical lines inside the boxes denote the medians; boxes denote the 25th and 75th percentile; the whiskers denote the smallest and largest observation greater than or equal to lower/upper box-1.5× interquartile range. Units for all nutrient chlorophyll *a* concentrations are mg m^{-3} , Secchi depth is m, and turbidity is NTU.

Long-term water quality trends in Lake Rotoiti were examined by plotting the monitoring data as a time series (see Figure 6). It is evident that water quality in Lake Rotoiti demonstrates cyclic fluctuations (depicted by the blue line in Figure 6), similar to observations in long-term datasets of this lake and other Rotorua Te Arawa lakes (Hamill, 2022). An observable change in the seasonal pattern of water quality in the lake occurred after the construction of the wall. This change was particularly noticeable in TN concentrations, where observed seasonal fluctuations were less pronounced during the post-wall period. The drivers of this cyclic pattern in the dataset are unclear,

making it challenging to comment on potential mechanisms that would explain the onset of degradation during the latter part of the monitoring period (c. 2017 onwards).

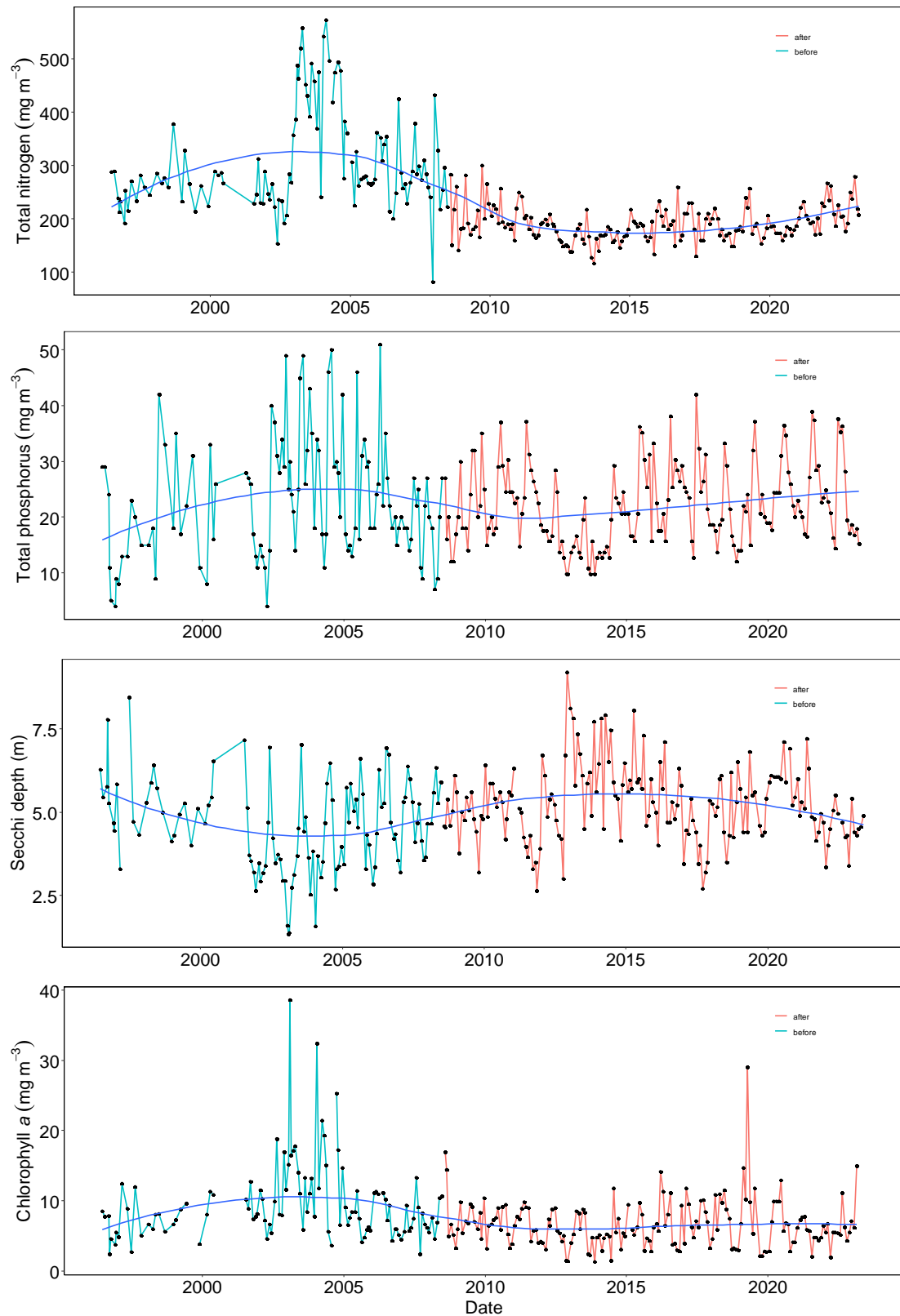


Figure 6: Time series all four water quality variables included in the TLI at Lake Rotoiti Site 3. Turquoise line represents data collected before and red line represents data after the construction of the Ōhau Channel diversion wall. The blue line is a loess smoother to visually indicate trends of water quality in the lake.

Bottom water DO concentrations were examined to understand if the construction of the wall has changed internal processes in Lake Rotoiti (Figure 7). Volumetric hypolimnetic oxygen demand values suggest that there were not changes in internal processes in Lake Rotoiti before and after the construction of the wall. Average VHOD values before the wall construction were $47.33 \text{ g m}^{-3} \text{ d}^{-1}$ ($\pm 6.97 \text{ g m}^{-3} \text{ d}^{-1}$, standard deviation) at Site 4 and $51.27 (\pm 5.77 \text{ g m}^{-3} \text{ d}^{-1}$, standard deviation) at Site 3. Average VHOD values after the wall construction were $45.22 \text{ g m}^{-3} \text{ d}^{-1}$ ($\pm 3.29 \text{ g m}^{-3} \text{ d}^{-1}$, standard deviation) at Site 4 and $41.36 (\pm 12.25 \text{ g m}^{-3} \text{ d}^{-1}$, standard deviation) at Site 3. There was no visual indication of any long-term trends in the data. The lower average VHOD after the wall construction (between 2007 and 2008) at Site 3 is reflective of higher inter-annual variability (as suggested by the comparably high standard deviation), but than a step change or long-term trend in the data.

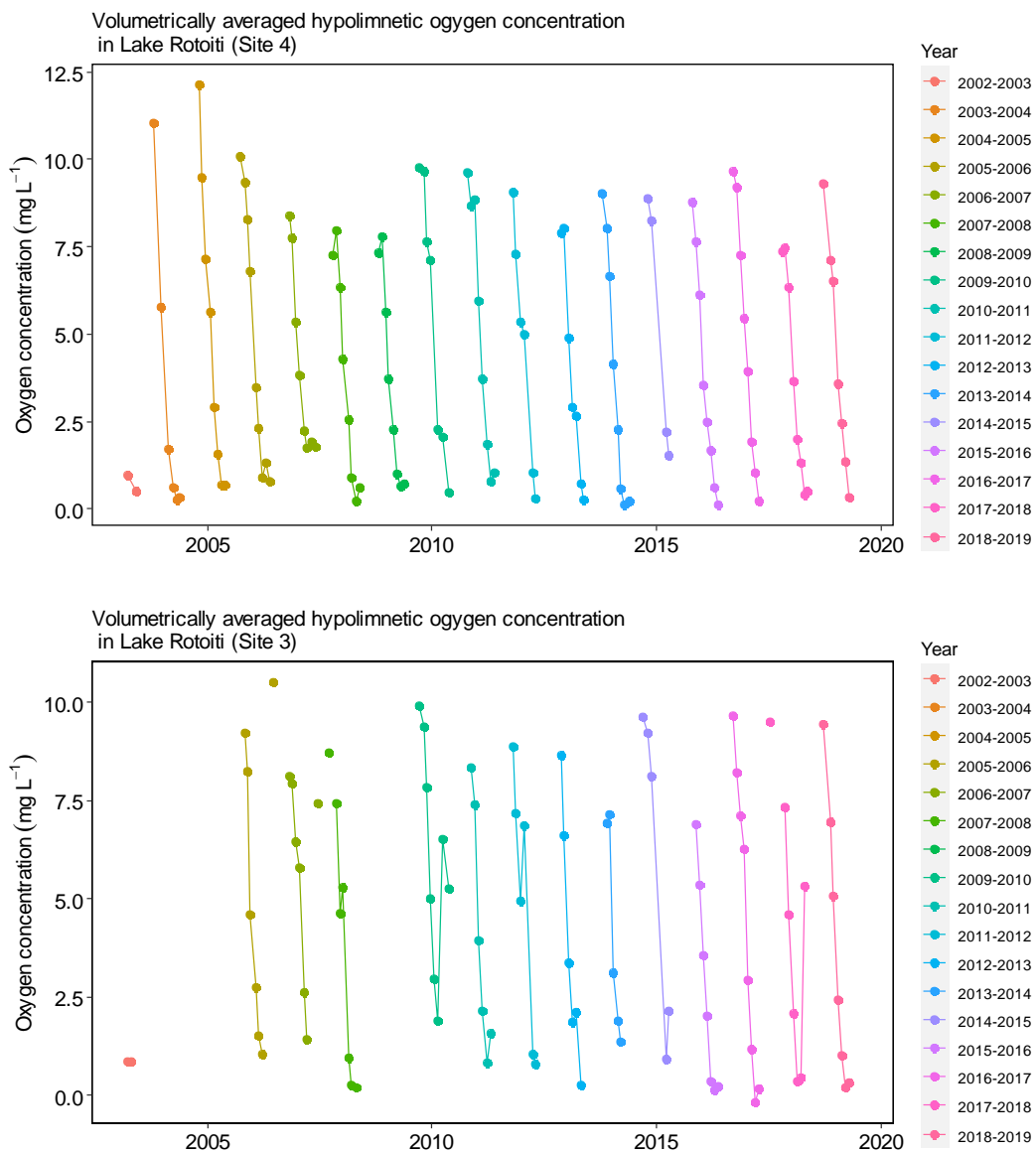


Figure 7: Monthly volumetrically averaged hypolimnetic oxygen concentrations in Lake Rotoiti (Site 4 top, and Site 3 bottom) for all monitoring years where oxygen profile were consistently available. For Site 3, the years 2003-2004, 2004-2005, and 2008-2009 have been omitted due to spurious temperature profiles during those year affecting calculations.

4.1.2 Correlation analysis

The comparison of water quality in Lake Rotorua and Lake Rotoiti using correlation analysis revealed that neither the slope nor the intercept for chlorophyll *a* showed a statistically significant difference. Although the Pearson correlation coefficient during the pre-wall period marginally exceeded that of the post-wall period (Figure 8), reconciling this with the lack of significant changes in other statistical properties of the relationship is challenging (Table 4). For TN, while the slope remained unchanged, the intercept shifted from 169.43 before the wall's construction to 98.04 after its completion. Contrary to expectations, the Pearson correlation coefficient during the post-wall period surpassed that of the pre-wall period (Figure 8). Conversely, for TP, neither the slope nor the intercept exhibited statistically significant differences, possibly due to the comparable variability in TP patterns during both the pre-wall and post-wall periods. The Pearson correlation coefficient between these periods did not appear to differ significantly, with only a slightly higher value observed for the pre-wall period, although neither correlation coefficient was statistically significant. For Secchi depth, statistically significant differences were observed in the slopes, transitioning from 1.38 to -0.40 from the pre-wall to post-wall period. Notably, the post-wall Pearson correlation coefficient was not statistically significant. Overall, the results for Secchi depth suggest that the construction of the wall altered the relationship between Lake Rotorua and Rotoiti, though evidence supporting such alterations for other water quality variables was comparatively weaker.

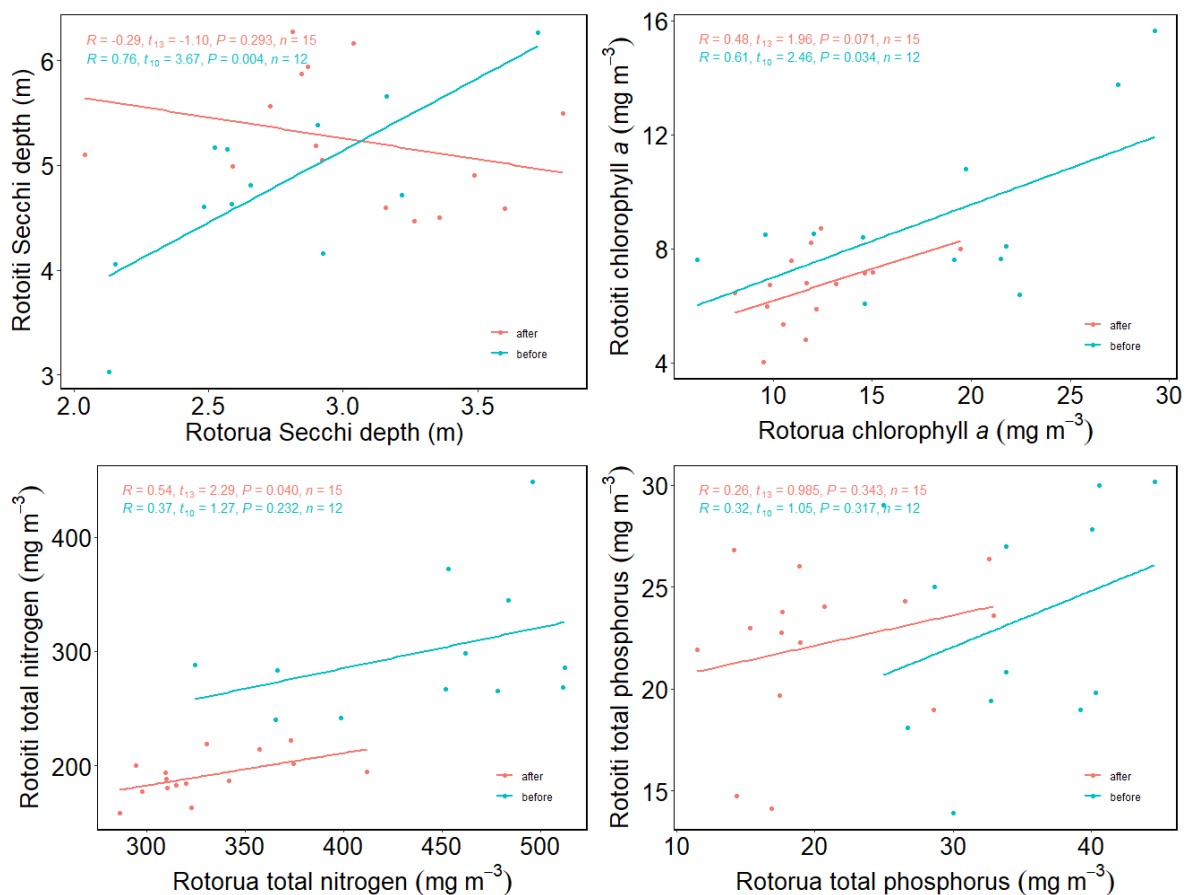


Figure 8: Bi-plots of annual average water quality variables in Lakes Rotorua (Site 5) and Rotoiti (Site 3) for all four water quality variables included in the TLI. Turquoise line and points represents data collected before, and red line and points represents data after the construction of the Ōhau Channel diversion wall. The corresponding Pearson correlation coefficient (R), t statistic, P value, and number of samples for each correlation are also shown. A P value <0.05 indicates a significant correlation.

Table 4 Summary of statistical correlation analysis results for water quality variables before and after construction of the diversion wall for Lake Rotorua vs. Lake Rotoiti and Lake Rotoiti vs. Kaituna River.

Comparison	Variable	Model parameter	Estimate (\pm standard error)	t value	P value
Lake Rotorua vs. Lake Rotoiti	Chlorophyll <i>a</i>	Intercept	3.982 (2.148)	1.854	0.077
		Slope	0.221 (0.174)	1.266	0.218
		Pre- vs. post-wall	0.454 (2.630)	0.172	0.645
		Interaction	0.036 (0.191)	0.186	0.854
	Total nitrogen	Intercept	98.043 (102.592)	0.956	0.349
		Slope	0.283 (0.308)	0.915	0.370
		Pre- vs. post-wall	44.065 (134.349)	0.328	0.746
		Interaction	0.075 (0.365)	0.207	0.838
	Total phosphorus	Intercept	19.138 (3.884)	4.928	<0.05
		Slope	0.149 (0.183)	0.818	0.421
		Pre- vs. post-wall	-5.321 (8.664)	-0.614	0.545
		Interaction	0.126 (0.286)	0.439	0.665
	Secchi depth	Intercept	6.463 (1.092)	5.911	<0.05
		Slope	-0.401 (0.357)	-1.122	0.273
		Pre- vs. post-wall	-5.451 (1.538)	-33.544	<0.05
		Interaction	1.778 (0.528)	3.370	<0.05
Lake Rotoiti vs. Kaituna River	Total nitrogen	Intercept	97.803 (74.900)	1.306	0.206
		Slope	0.316 (0.252)	1.255	0.224
		Pre- vs. post-wall	16.226 (106.523)	0.152	0.880
		Interaction	0.291 (0.357)	0.814	0.425
	Total phosphorus	Intercept	10.093 (6.198)	1.628	0.119
		Slope	0.538 (0.276)	1.974	0.062
		Pre- vs. post-wall	-2.643 (9.047)	-0.292	0.773
		Interaction	0.058 (0.365)	0.159	0.875

The comparison of water quality between Lake Rotoiti and the Kaituna River (Figure 9) revealed that the slope of their relationship remained constant for TN (Figure 10). However, the intercept rose from 97.81 to 200.29 between the pre-wall and post-wall periods. This increase could primarily stem from TN reduction in Lake Rotoiti during the post-wall era, rather than alterations in the Kaituna River. The Pearson correlation coefficients for both periods were not statistically significant. Regarding TP, neither the slope nor the intercept showed statistically significant differences, although the Pearson correlation coefficient was only significant for the post-wall period.

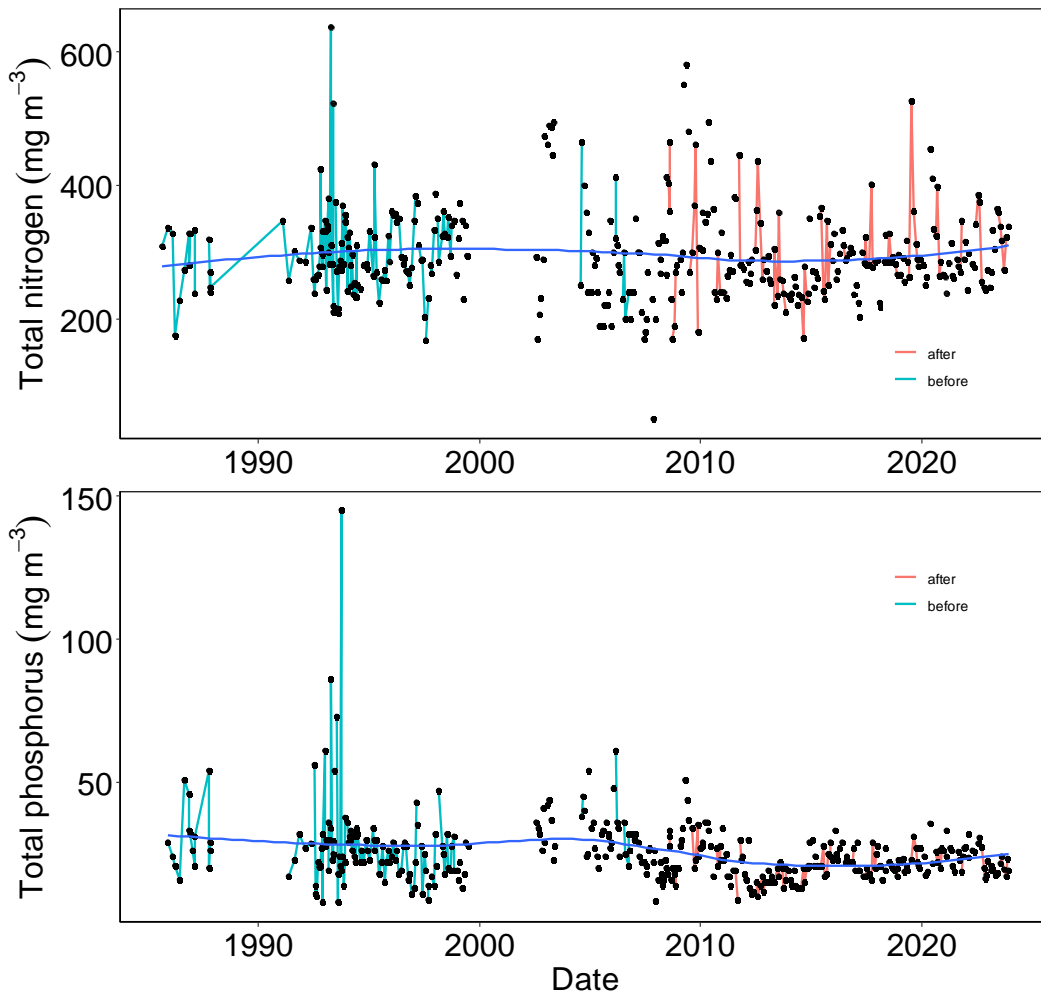


Figure 9: Time series of total nitrogen and total phosphorus concentrations in the Kaituna River at the Lake Rotoiti outlet. Turquoise line represents data collected before and red line represents data after the construction of the Ōhau Channel diversion wall. The blue line is a loess smoother to visually indicate trends of water quality in the lake.

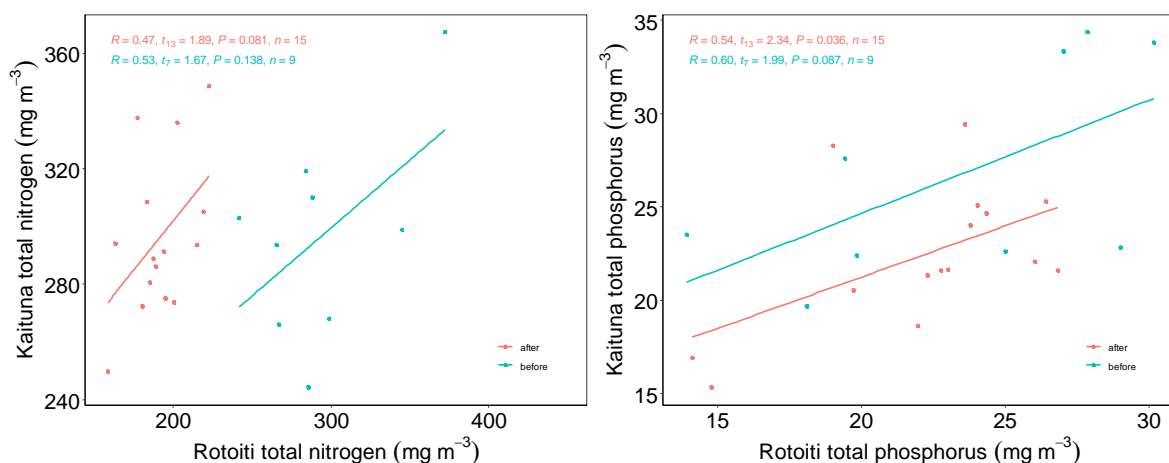


Figure 10: Bi-plots of annual average water quality variables in the Kaituna River (at Rotoiti outflow) and Lake Rotoiti (Site 3) for total nitrogen and total phosphorus. Turquoise line and points represents data collected before, and red line and points represents data after the construction of the Ōhau Channel diversion wall. The corresponding Pearson correlation coefficient (R), t statistic, P value, and number of samples for each correlation are also shown. A P value <0.05 indicates a significant correlation.

4.1.3 Intervention analysis

The findings from the intervention indicate a predominantly positive response of water quality in Lake Rotoiti to the construction of the wall. Figures 11 and 12 depict linear trends for both pre- and post-wall periods alongside a counterfactual trend line, which extrapolates the pre-wall trend. Following the rule of thumb that non-overlapping confidence intervals imply statistically significant differences, conclusions can be drawn regarding step or trend changes in water quality variables attributable to the wall's construction. Statistically significant step changes were identified for TN and Secchi depth (Figure 11, Table 5). However, TP and chlorophyll *a* concentrations did not exhibit statistically significant step changes after the wall's construction (Figure 11), and none of the water quality variables displayed a statistically significant shift in long-term trend. The difference between observed and counterfactual long-term trends at the end of the study period (2023) indicates a decrease in TN by 203 mg m^{-3} and an increase in Secchi depth by 2.5 m.

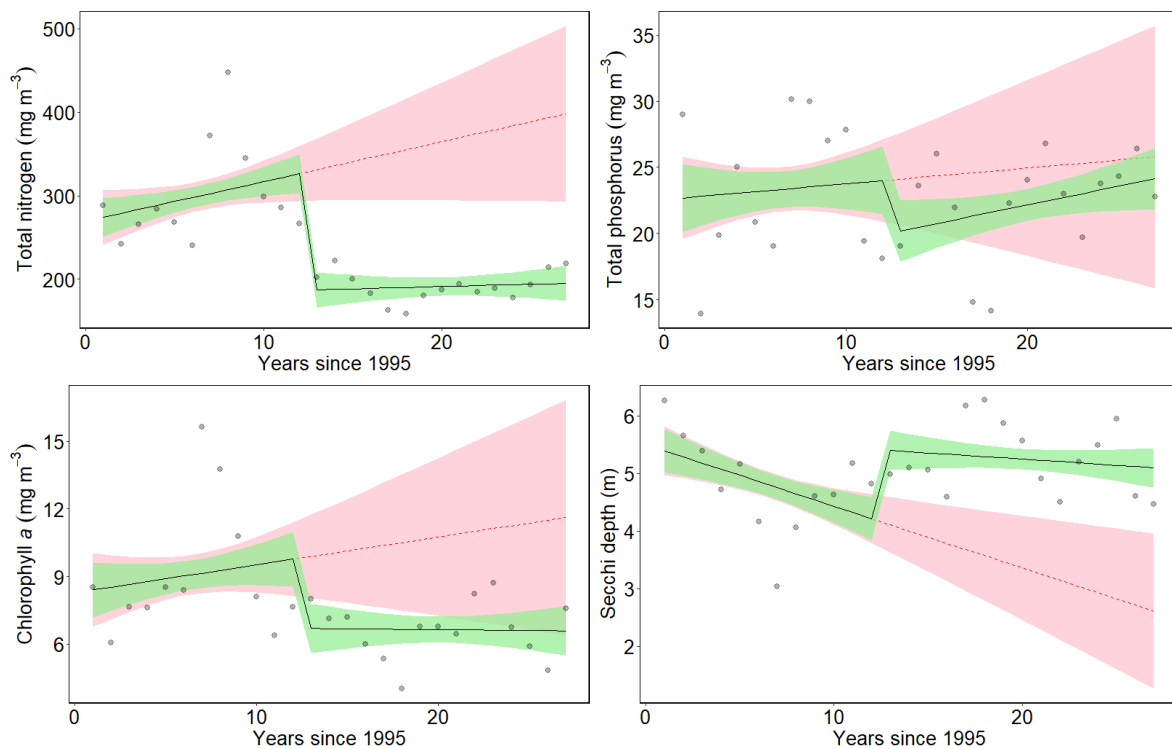


Figure 11: Time series graphs of intervention analysis results using generalized linear modelling of annual average values for all four water quality variables included in the TLI for data collected between 1995 and 2023. Black line represents linear trends (± 95 confidence interval, green shade) for pre and post wall periods calculated from data shown by grey points. A counterfactual trend line (extrapolation of the pre-wall trend line) is shown as red dotted line (± 95 confidence interval, red shade) is compared with the post-wall trend to estimate the immediate and longer-term impact of the diversion wall (see results in Table 5).

The intervention analysis for the TLI showed that there was a statistically significant step change in TLI following the construction of the diversion wall, and significant shift in long-term was observed (Figure 12, Table 5). The difference of TLI values between the observed and counterfactual trend at the end of the study period suggests that the TLI has decreased by 0.58 units following installation of the diversion wall.

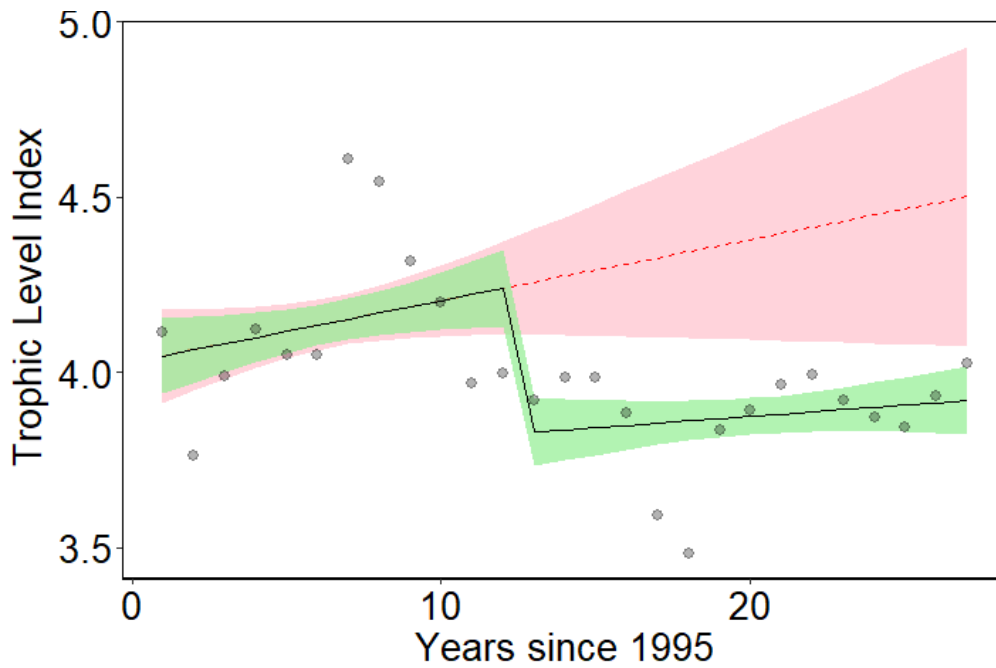


Figure 12: Time series graphs of intervention analysis results using generalized linear modelling of the TLI for data collected between 1995 and 2023. Black line represents linear trends (± 95 confidence interval, green shade) for pre and post wall periods calculated from data shown by grey points. A counterfactual trend line (extrapolation of the pre-wall trend line) is shown as red dotted line (± 95 confidence interval, red shade) is compared with the post-wall trend to estimate the immediate and longer-term impact of the diversion wall (see results in Table 5)

Table 5 Model coefficients of the interrupted time series analysis carried out as part of the intervention analysis.

Attribute	Coefficient	Estimate (\pm standard error)	t value	P value
Total nitrogen	Intercept	269.248 (26.129)	10.305	<0.05
	Time	4.784 (3.550)	1.348	0.191
	Intervention	-137.716 (32.613)	-4.284	<0.05
	Post intervention time	-4.227 (4.364)	-0.969	0.346
Chlorophyll <i>a</i>	Intercept	8.281 (1.368)	6.054	<0.05
	Time	0.124 (0.186)	0.665	0.513
	Intervention	-3.069 (1.707)	-1.798	0.085
	Post intervention time	-0.131 (0.228)	-0.574	0.571
Total phosphorus	Intercept	22.560 (2.892)	7.800	<0.05
	Time	0.119 (0.393)	0.304	0.764
	Intervention	-4.093 (3.610)	-1.134	0.269
	Post intervention time	0.1631 (0.483)	0.338	0.739
Secchi depth	Intercept	5.501 (0.427)	12.865	<0.05
	Time	-0.107 (0.058)	-1.845	0.078
	Intervention	1.206 (0.534)	2.261	<0.05
	Post intervention time	0.085 (0.071)	1.198	0.2429
TLI	Intercept	4.030 (0.122)	32.968	<0.05
	Time	0.017 (0.016)	1.054	0.303
	Intervention	-0.416 (0.153)	-2.729	<0.05
	Post intervention time	-0.011 (0.020)	-0.539	0.595

4.2 Part 2: Lake system modelling

4.2.1 Hydrodynamics

4.2.1.1 Model performance

Hydrodynamic model simulations agreed well with daily measurements of lake height (Figure 13).

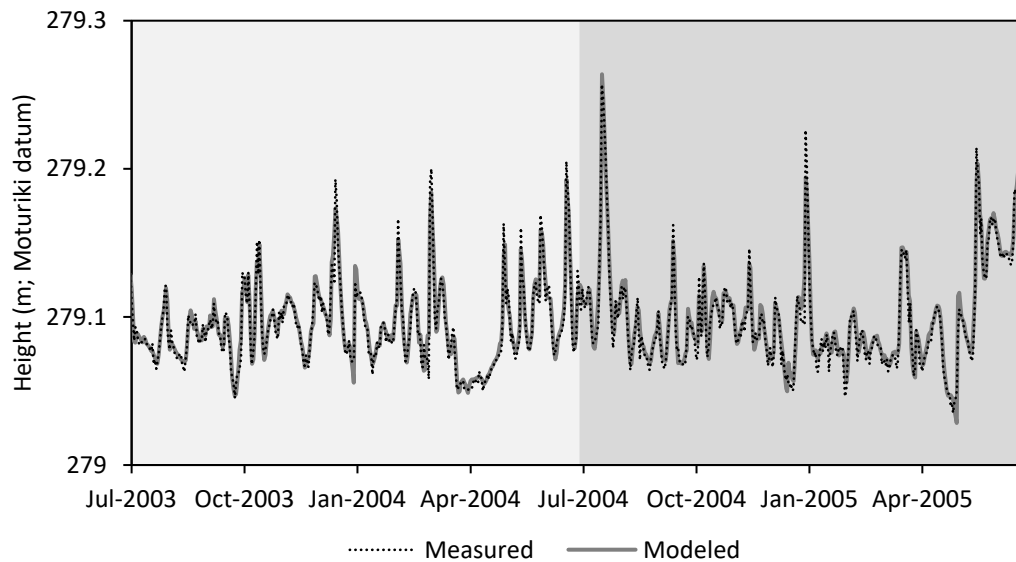


Figure 13: Measured vs modelled water level (as Height, Moturiki datum), during the calibration and validation periods. Data are daily measurements taken at 00:00 hours. Calibration period 1-Jul-2003 through 30-Jun-2004 (light grey), Validation 1-Jul-2004 through 30-Jun-2005 (mid grey).

Hydrodynamic model simulations of lake temperature agreed well with monthly field measurements in the main basin, Site 4, at 1, 10, 20, 30, 40, and 60 m depth (Figure 14), and well captured the monomictic stratification pattern in the lake. The hydrodynamic model calibration was a strong fit as represented by a high R-value of 0.987–0.992, and low RMSE of 0.15–0.55 and MAE of 0.11–0.38, across the 6 depths analysed (Table 6). The validation period returned similarly strong values, with a high R-value of 0.950–0.994, and low RMSE of 0.34–0.81 and MAE of 0.29–0.72, across the 6 depths analysed (Table 6).

Table 6 Temperature performance statistics of the hydrodynamic model at Site 4. Statistics include Pearson correlation (R), root mean squared error (RMSE), and mean absolute error (MAE). Calibration period 1-Jul-2003 through 30-Jun-2004; Validation period 1-Jul-2004 through 30-Jun-2005.

Depth	Calibration			Validation		
	R	RMSE	MAE	R	RMSE	MAE
1 m	0.992	0.45	0.31	0.994	0.53	0.45
10 m	0.991	0.55	0.38	0.995	0.51	0.44
20 m	0.990	0.30	0.20	0.990	0.34	0.29
30 m	0.987	0.22	0.16	0.950	0.81	0.72
40 m	0.991	0.15	0.11	0.972	0.53	0.48
60 m	0.990	0.15	0.12	0.977	0.49	0.45

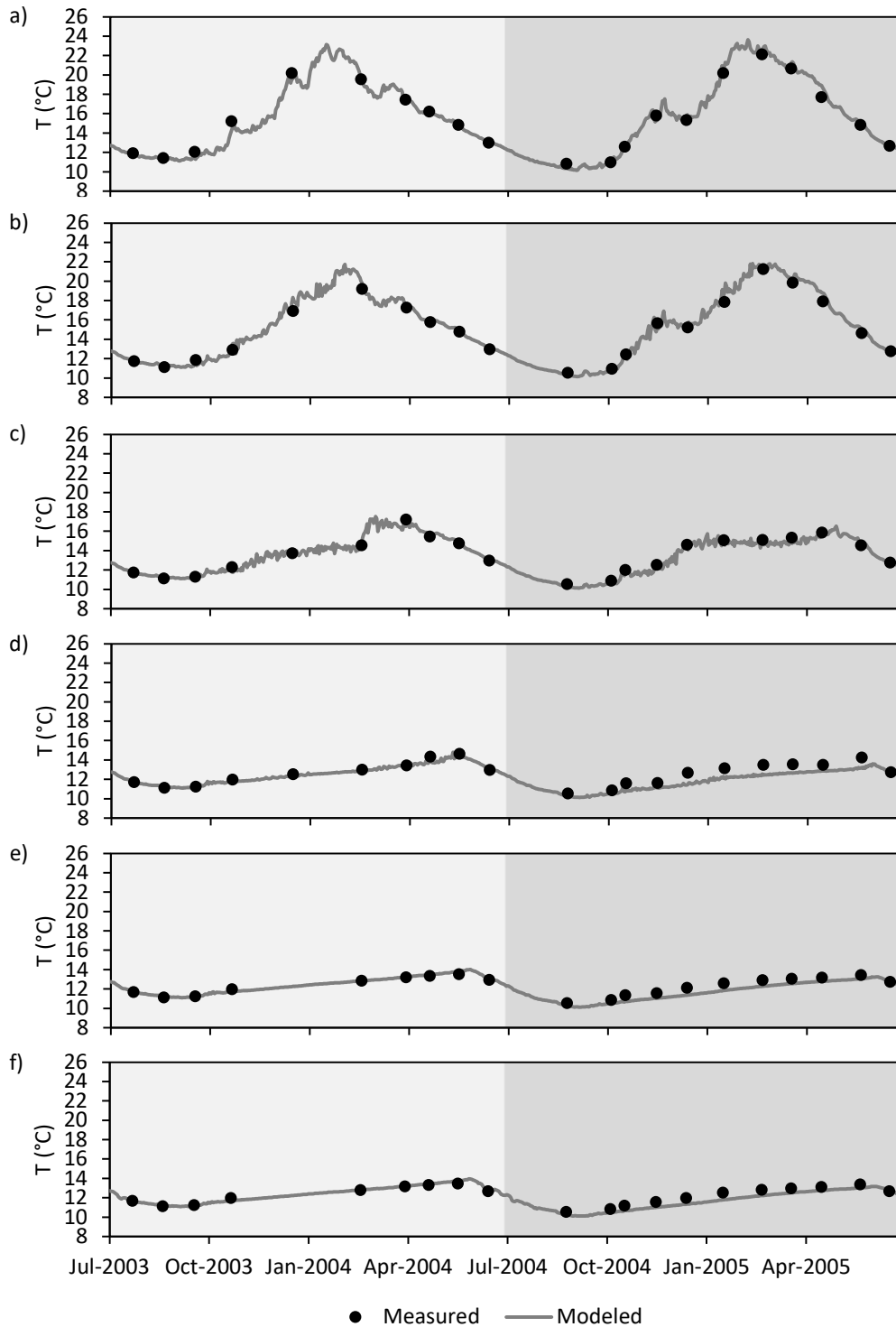


Figure 14: Measured vs modelled Temperature (T) at Site 4, during the calibration and validation periods, at a) 1, b) 10, c) 20, d) 30, e) 40, and f) 60 m depth. Calibration period 1-Jul-2003 through 30-Jun-2004 (light grey), Validation 1-Jul-2004 through 30-Jun-2005 (mid grey).

4.2.1.2 Model output

Model scenarios demonstrated the wall was effective in reducing Ōhau Channel inflow accumulation (i.e., % of Lake Rotoiti water derived from the Ōhau Channel over a single year) throughout the reservoir, from the western through the deeper eastern basin (wall-in [Figure 15]; wall-out [Figure

16]). Specifically, accumulation of Ōhau Channel flow without a wall in place was shown to be consistently high across limnological years between 2003-04 and 2021-22, as represented by a mean annual cumulative contribution of 22.0% ($\pm 2.2\%$, standard deviation) to the lake (Figure 17a). This was driven by a mean (limnological years between 2003-04 and 2021-22) annual retention (i.e., % of Ōhau Channel water entering Lake Rotoiti, which remained in the Lake Rotoiti over a single year) values of 44.8% ($\pm 5.0\%$, standard deviation;), and thus 55.2% of the flow being short-circuited down the Kaituna River (Figure 17b). By contrast, the accumulation of Ōhau Channel flow with the diversion wall in place was consistently low across limnological years between 2003-04 and 2021-22, as represented by a mean annual contribution of 0.3% ($\pm 0.3\%$, standard deviation) to the lake (Figure 17a). This was driven by a mean (limnological years between 2003-04 and 2021-22) annual retention value of 0.7% ($\pm 0.7\%$, standard deviation), and thus 99.3% of the flow being short-circuited down the Kaituna River (Figure 17b). Thus, the diversion wall in place resulted in a reduction of Ōhau-derived water remaining in and accumulating in the lake by factors of ~65.

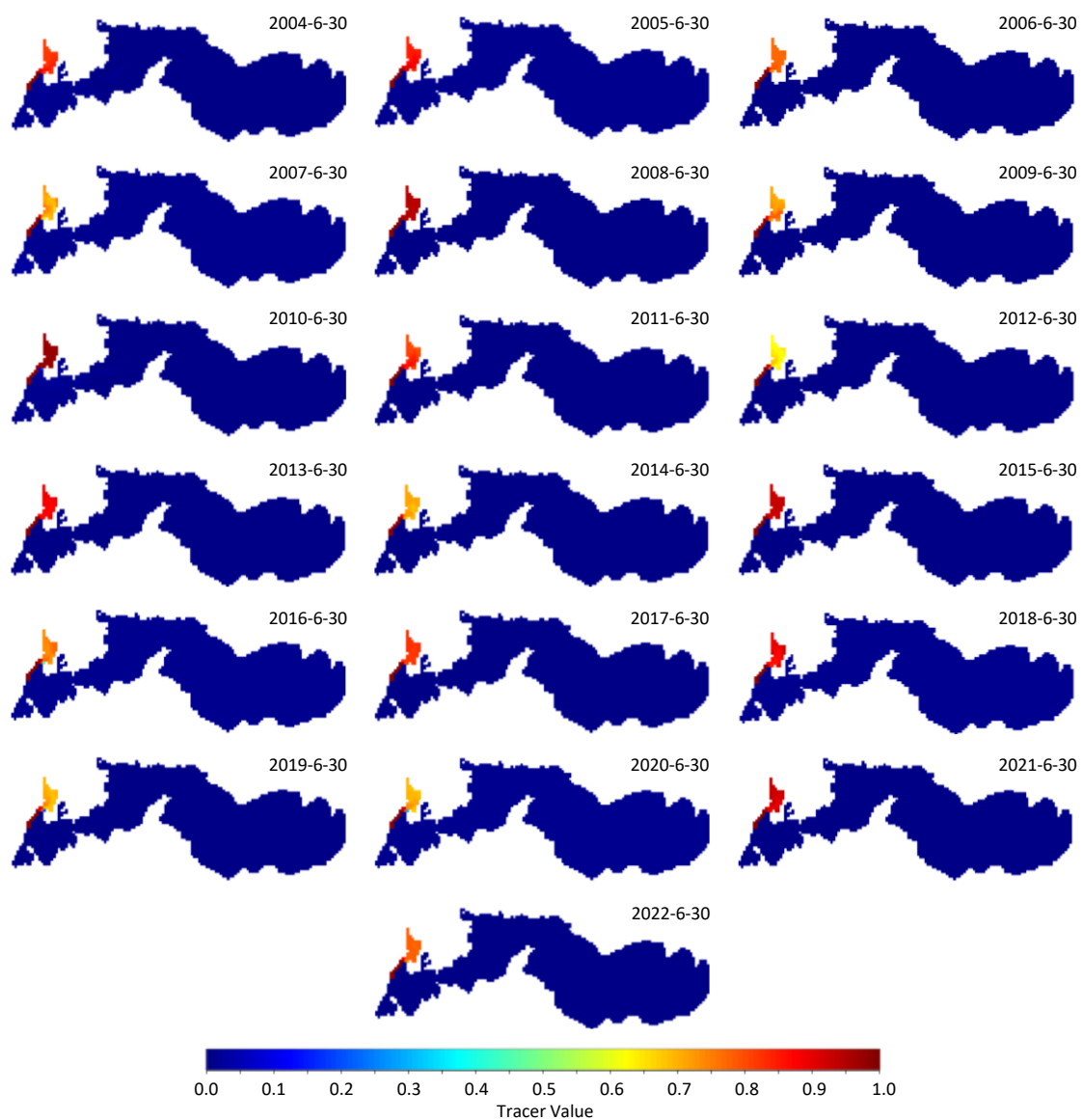


Figure 15: Simulated annual (i.e., single year) accumulation of Ōhau Channel-derived water (tracer value = 1) with the Ōhau Channel diversion wall in place over each limnological year from 2003-2004 through 2021-2022. Dates in figure represent the tracer value on the final day of the limnological year. N.b. entire lake shown, but subsequent analysis excludes area within wall (with and without the wall in place) and the Okare Arm.

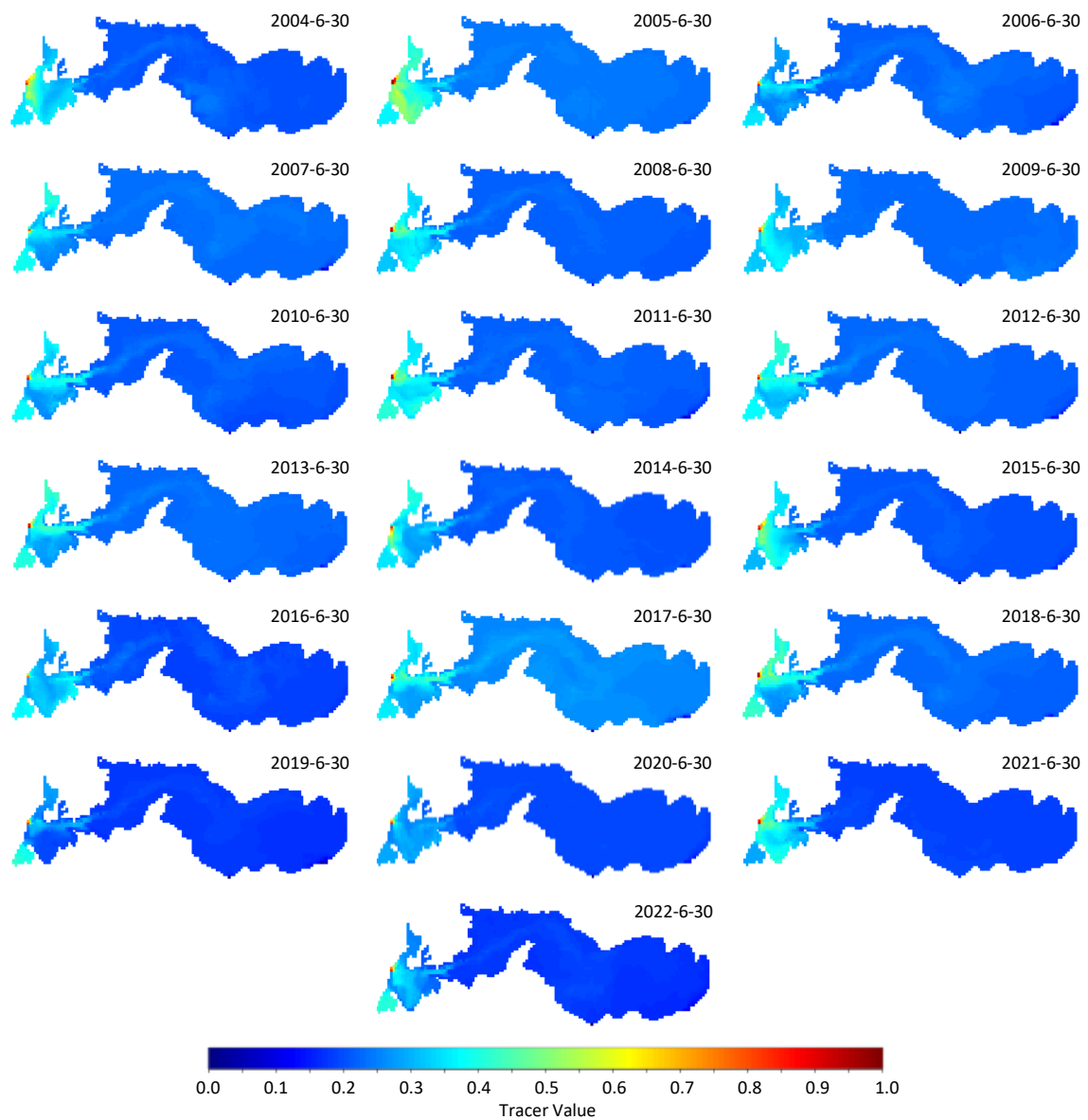


Figure 16: Simulated annual (i.e., single year) accumulation (i.e., % of Lake Rotoiti water derived from the Ōhau Channel over a single year) of Ōhau Channel-derived water (tracer value = 1) without the wall in place over each limnological year from 2003-2004 through 2021-2022. Dates in figure represent the tracer value on the final day of the limnological year. N.b. entire lake shown, but subsequent analysis excludes area within wall (with and without the wall in place) and the Okare Arm.

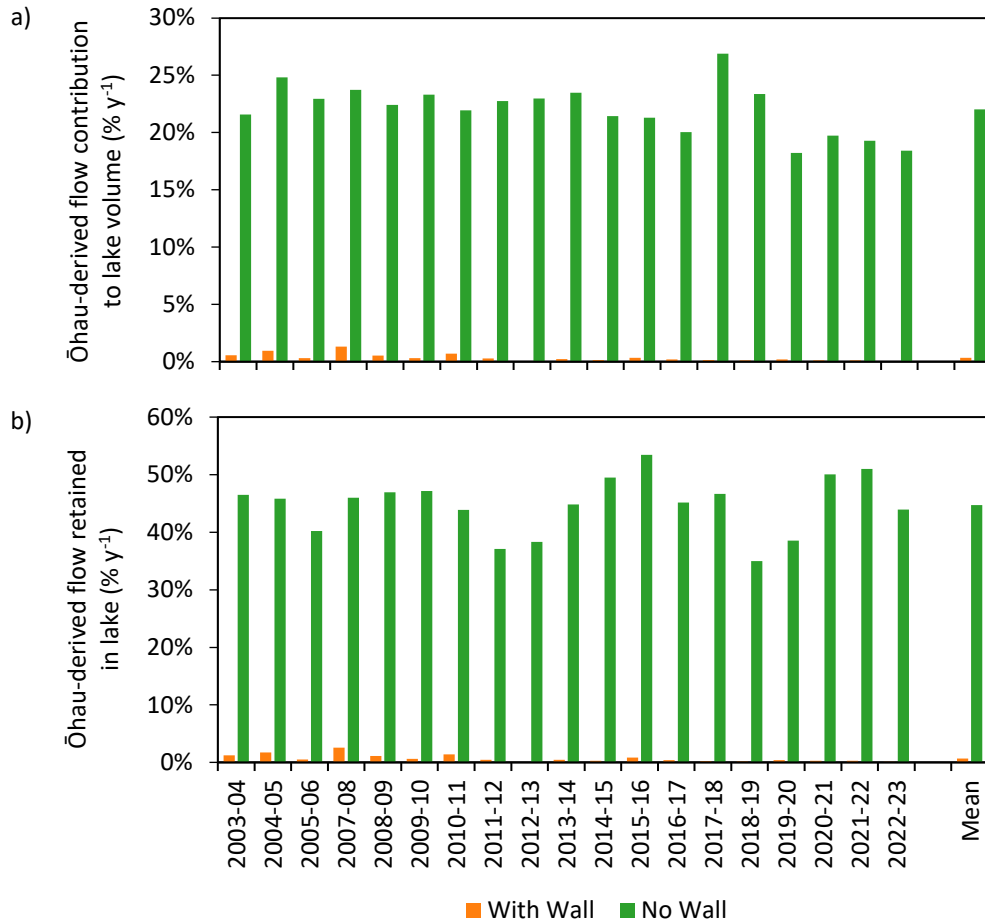


Figure 17: Simulated comparison of 1) the accumulation (i.e., % of Lake Rotoiti water derived from the Ōhau Channel over a single year) of Ōhau Channel-derived water, and 2) the retention (i.e., % of Ōhau Channel water entering Lake Rotoiti, which remained in the Lake Rotoiti over a single year) of Ōhau Channel-derived water, with and without the wall in place over each limnological year from 2003-2004 through 2021-2022.

The model scenario with the wall in place revealed a strong Ōhau Channel inflow signature (i.e., tracer signature) travelling through ‘The Narrows’ and into the eastern basin, which was not observed in the scenario with the wall in place. This flow typically propagated through the lake as an overflow during spring and summer, before transitioning into an interflow during autumn, and finally an underflow during winter (Figure 18a,b). Conversely, the scenario without the Ōhau Channel diversion wall in place presented a substantially muted Ōhau Channel inflow signature, ~2 orders of magnitude (c.f., without the wall in place), and a less regular seasonal trend in the depth at which the water propagated through the lake (Figure 18c,d).

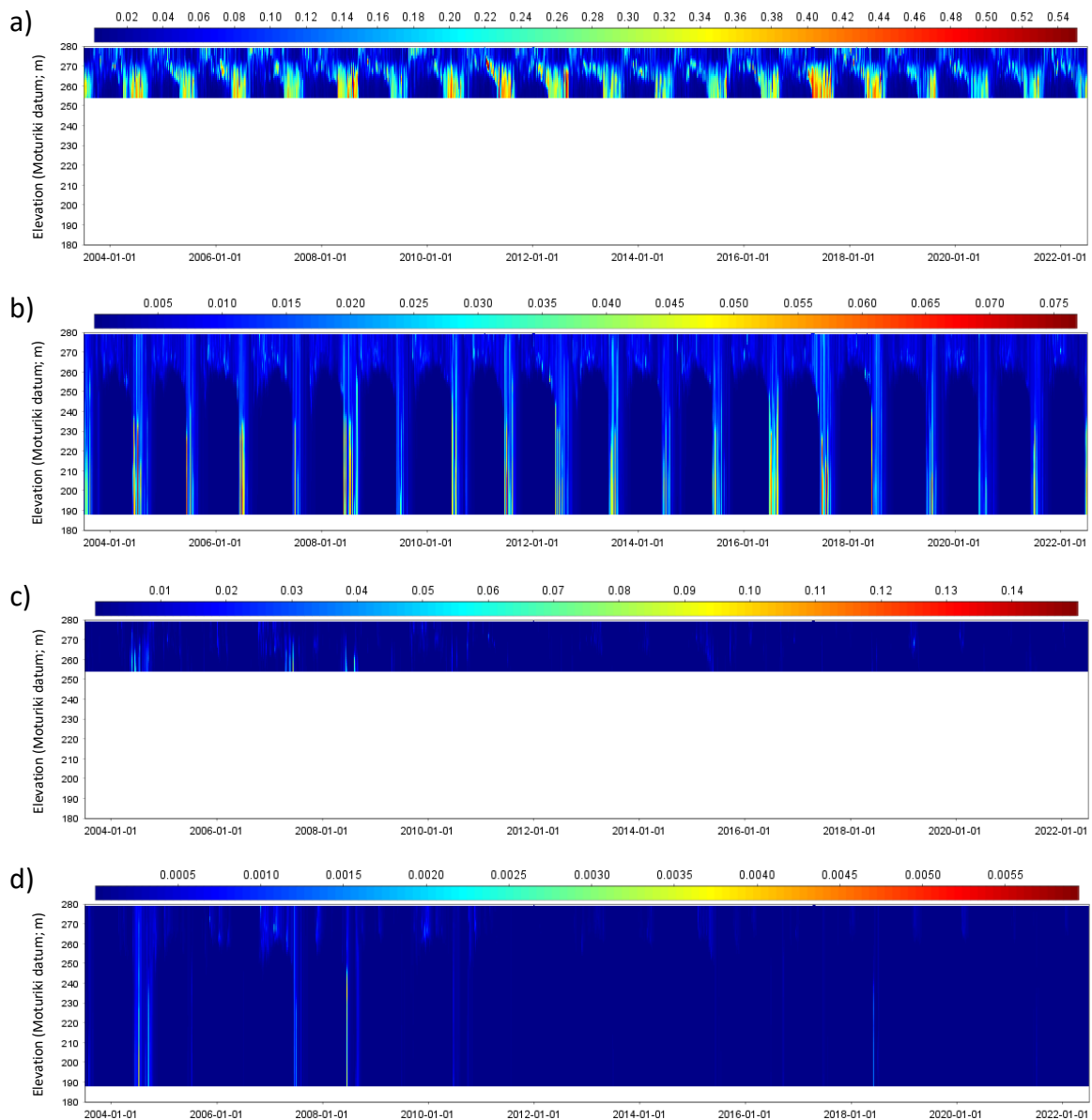


Figure 18: Simulated Ōhau Channel-derived water (tracer value = 1) without a wall at a) Site 3 and b) Site 4, and with the Ōhau Channel diversion wall at c) Site 3 and d) Site 4, from 1-Jul-2003 through 30-Jun-2022. Values represent that of a tracer which decays at a rate of 0.5 per week. N.b. Variable tracer scale across panels ‘a’ through ‘d’.

Model scenarios demonstrated the rate of the removal (i.e., % of Lake Rotoiti water replaced by water derived from outside the lake over a single year) of water originally present in Lake Rotoiti (wall-in [Figure 19]; wall-out [Figure 20]; N.b. retention shown, removal as 1 less retention) was considerably faster without the wall in place. Specifically, the mean annual removal of Lake Rotoiti water, for limnological years between 2003-04 and 2021-22, was 30.67% ($\pm 3.16\%$, standard deviation) without the wall in place and 10.53% ($\pm 2.66\%$, standard deviation) with the wall in place (Figure 21). Scenarios without the wall in place resulted in an increase in the removal of Lake Rotoiti water across any given limnological year by a factor of 2.91.

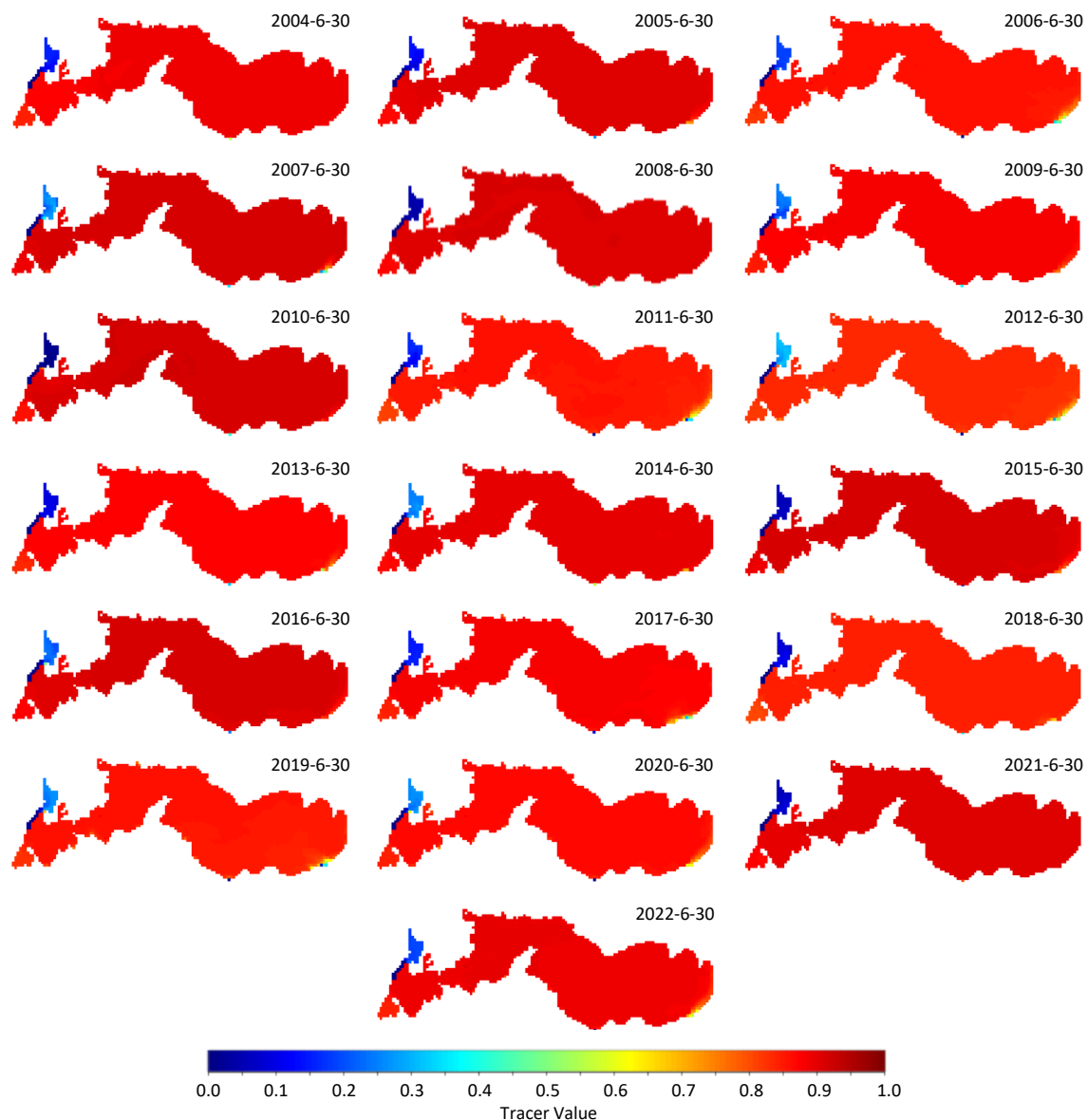


Figure 19: Simulated annual (i.e., within a single year) retention (i.e., % of Lake Rotoiti water not replaced by water derived from outside the lake over a single year) of Lake Rotoiti water with the Ōhau Channel diversion wall in place, represented by removal of tracer (initial value = 1) over each limnological year from 2003-2004 through 2021-2022. Dates in figure represent the tracer value on the final day of the limnological year. N.b. entire lake shown, but subsequent analysis excludes area within wall (with and without the wall in place) and the Okare Arm; retention used to determine removal as 1 less retention.

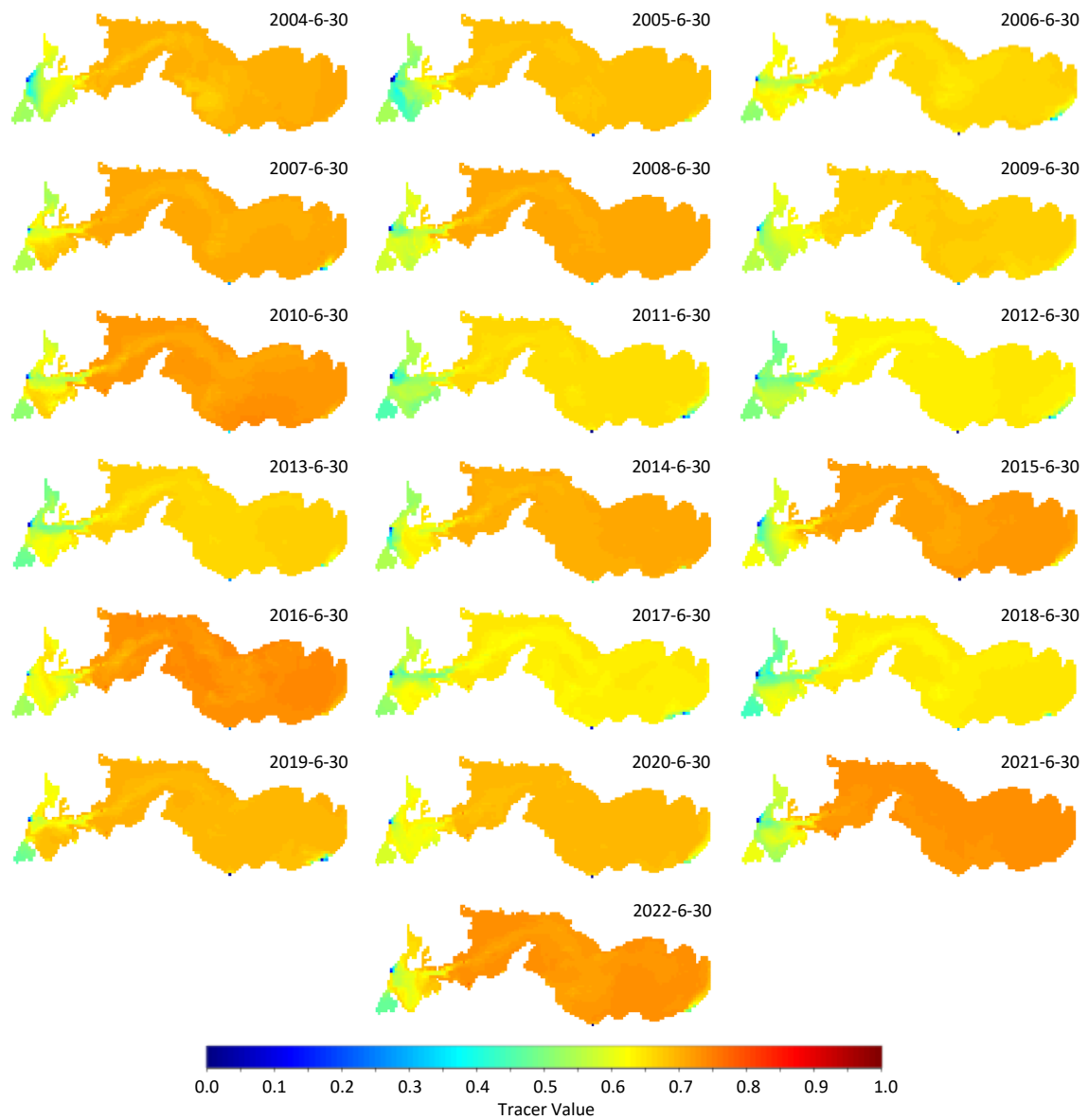


Figure 20: Simulated annual (i.e., within a single year) retention (i.e., % of Lake Rotoiti water not replaced by water derived from outside the lake over a single year) of Lake Rotoiti water without the wall in place, represented by removal of tracer (initial value = 1) over each limnological year from 2003-2004 through 2021-2022. Dates in figure represent the tracer value on the final day of the limnological year. N.b. entire lake shown, but subsequent analysis excludes area within wall (with and without the wall in place) and the Okare Arm; retention used to determine removal as 1 less retention.

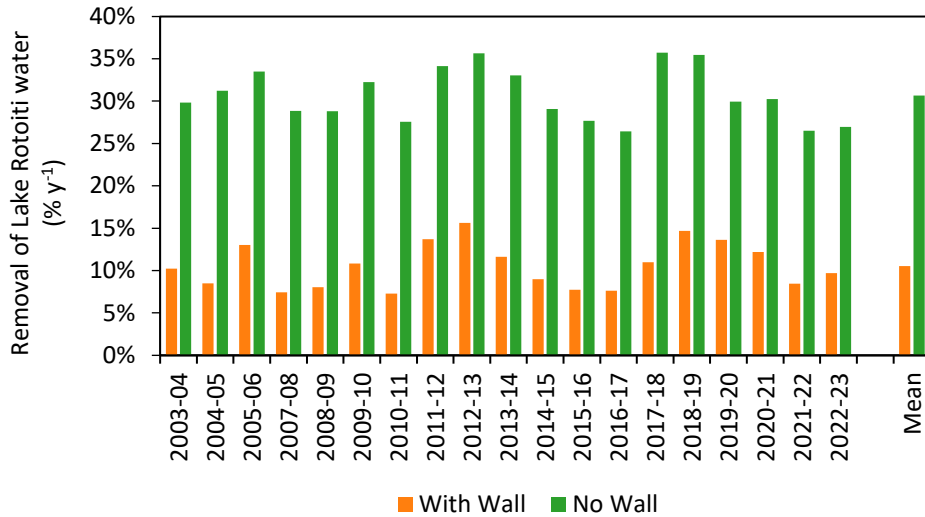


Figure 21: Simulated comparison of the removal (as % of Lake Rotoiti water replaced by water derived from outside the lake over a single year) of Lake Rotoiti water with and without the wall in place over each limnological year from 2003-2004 through 2021-2022.

Assuming the aforementioned mean removal rates of 30.67% without the wall in place and 10.53% with the wall in place (Figure 21), residence times (defined as the time to clear > 95% of the original water) were calculated as 8.18 years without the wall in place and 26.92 years with the wall in place (Figure 22). This equates to the Ōhau Channel diversion wall increasing the residence time in the lake by a factor of 3.29.

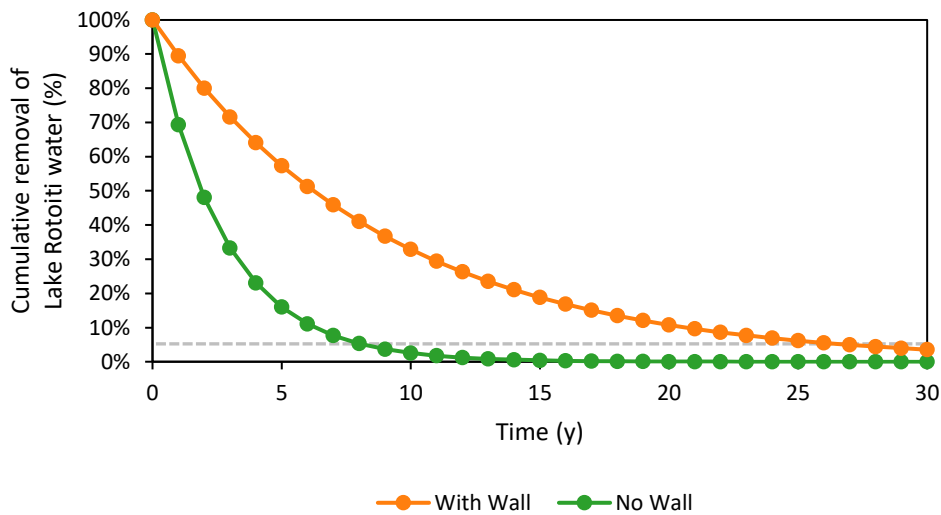


Figure 22: Simulated comparison of residence time, as determined as the number of years to reach < 5% of Rotoiti water, with and without the wall in place. Dotted grey line denotes 5% threshold.

4.2.2 Water quality

4.2.2.1 Model performance

Hydrodynamic-ecological model simulations of lake temperature agreed well with monthly field measurements in main basin, Site 4, at 1, 10, 20, 30, 40, and 60 m depth (Figure 23), and well captured the monomictic stratification pattern in the lake. The hydrodynamic-ecological model temperature calibration was a strong fit as represented by a high R-value of 0.949–0.996, and high accuracy as represented by a low RMSE of 0.34–0.91 and MAE of 0.22–0.71, across the 6 depths analysed (Table 7). The validation period returned similarly strong values, with a high R-value of 0.962–0.999, and low RMSE of 0.20–0.76 and MAE of 0.17–0.60, across the 6 depths analysed (Table 7).

Table 7 Temperature performance statistics of the hydrodynamic-ecological model at Site 4. Statistics include Pearson correlation (R), root mean squared error (RMSE), and mean absolute error (MAE). Calibration period 1-Sep-2014 through 31-Aug-2015; Validation period 1-Sep-2015 through 31-Aug-2016.

Depth	Calibration			Validation		
	R	RMSE	MAE	R	RMSE	MAE
1 m	0.992	0.74	0.58	0.995	0.54	0.43
10 m	0.996	0.91	0.71	0.999	0.60	0.49
20 m	0.964	0.53	0.40	0.974	0.76	0.60
30 m	0.949	0.55	0.37	0.962	0.38	0.32
40 m	0.963	0.39	0.23	0.983	0.22	0.19
60 m	0.973	0.34	0.22	0.987	0.20	0.17

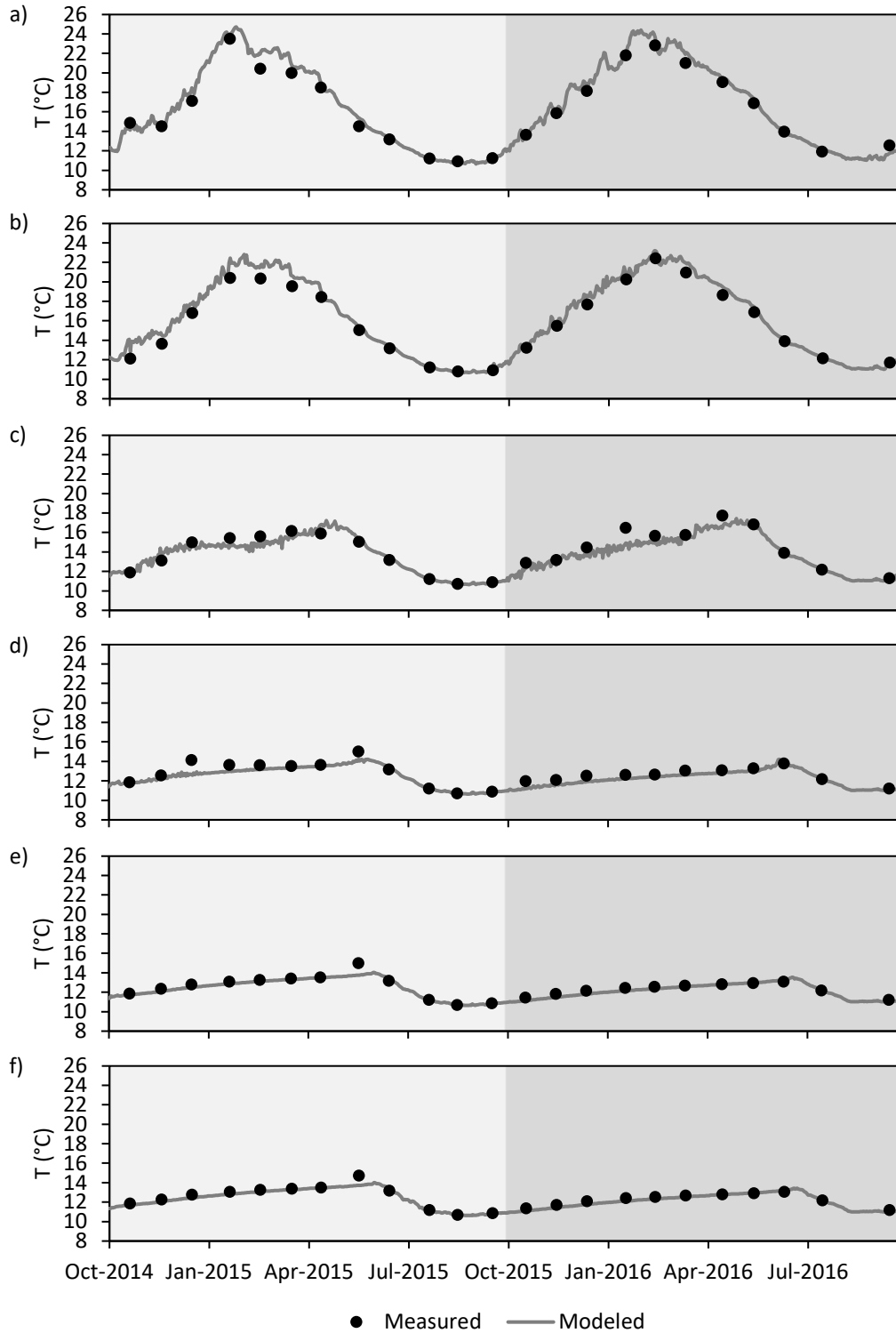


Figure 23: Measured vs modelled temperature (T) at Site 4, during the calibration and validation periods, at a) 1 m, b) 10 m, c) 20 m, d) 30 m, e) 40 m, and f) 60 m depth. Calibration period 1-Oct-2014 through 30-Sep-2015 (light grey), Validation 1-Oct-2015 through 30-Sep-2016 (mid grey).

Hydrodynamic-ecological model simulations of lake DO concentrations agreed well with monthly field measurements in main basin at 30, 40, and 60 m depth, thus capturing the seasonal deoxygenation (Figure 24d,e,f). but to a lesser extent at 1, 10, and 20 m depth (Figure 24a,b,c).

Specifically, the hydrodynamic-ecological model calibration across the 30, 40, and 60 m depths analysed was a strong fit, as represented by high R-value of 0.921–0.966, and low RMSE of 1.22–1.56 and MAE of 0.22–0.37. In contrast, the model calibration across 1, 10, and 20 m depths analysed was a weaker fit, as represented by lower R-values of 0.282–0.747, yet maintained a high accuracy as represented by a low RMSE of 0.97–1.46 and MAE of 0.40–0.71 (Table 8). The validation period (c.f., the calibration) saw a general improvement in R values and RMSE across all depths, including notable improvements at 1 and 10 m, while MAE remained similar (Table 8). Reduced model performance at 1, 10, and 20 m in the calibration period, and throughout the water column relative to the validation period, can in part be attributed to a lack of measured data during December, January, and February of the calibration year.

Table 8 Dissolved oxygen performance statistics of the hydrodynamic-ecological model at Site 4. Statistics include Pearson correlation (R), root mean squared error (RMSE), and mean absolute error (MAE). Calibration period 1-Sep-2014 through 31-Aug-2015; Validation period 1-Sep-2015 through 31-Aug-2016.

Depth	Calibration			Validation		
	R	RMSE	MAE	R	RMSE	MAE
1 m	0.282	1.46	0.58	0.611	1.28	1.13
10 m	0.485	0.97	0.71	0.735	0.84	0.56
20 m	0.747	1.34	0.40	0.744	1.47	1.12
30 m	0.966	1.22	0.37	0.961	0.96	0.72
40 m	0.929	1.52	0.23	0.977	0.78	0.49
60 m	0.921	1.56	0.22	0.980	0.79	0.42

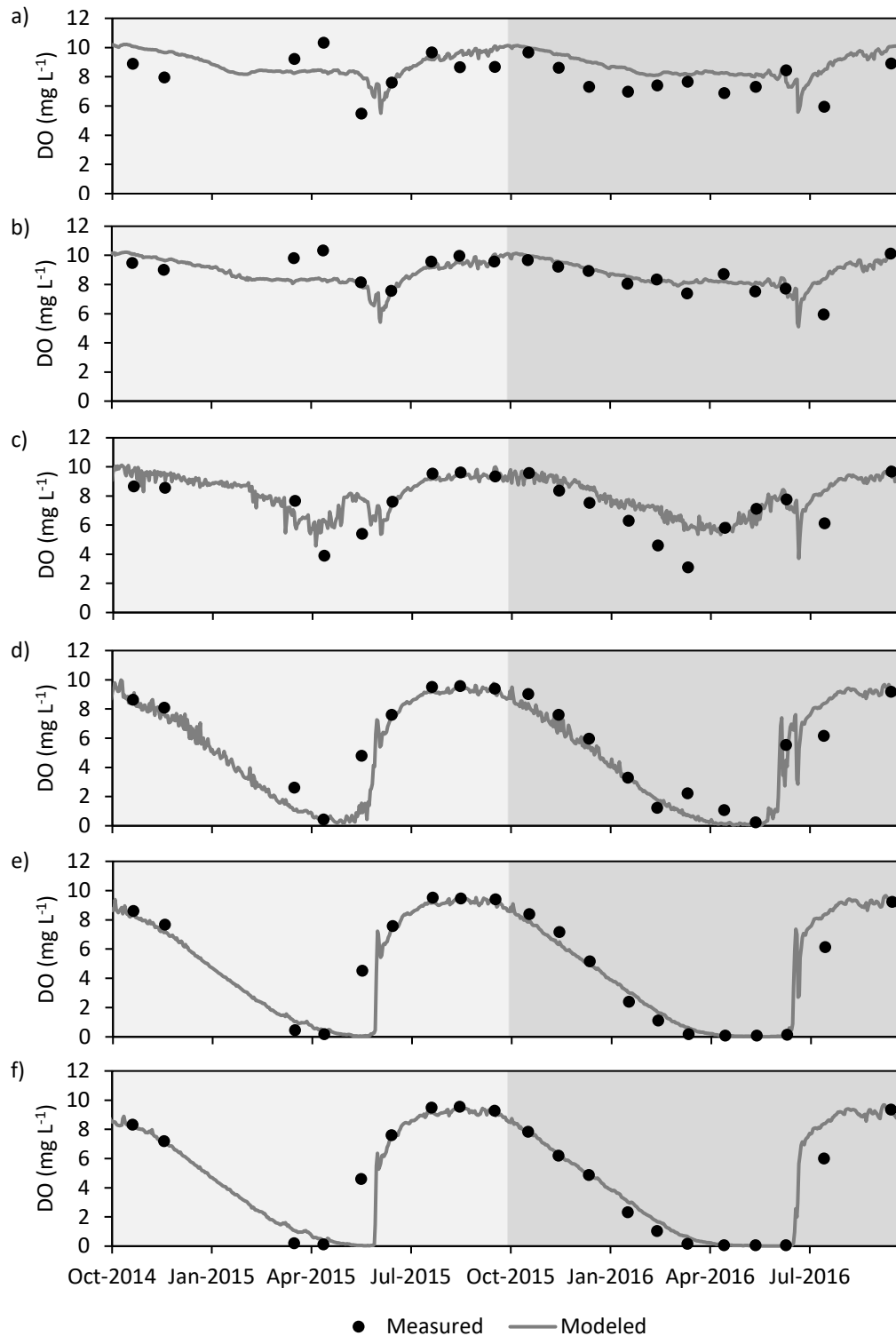


Figure 24: Measured vs modelled dissolved oxygen (DO) at Site 4, during the calibration and validation periods, at a) 1 m, b) 10 m, c) 20 m, d) 30 m, e) 40 m, and f) 60 m depth. Calibration period 1-Oct-2014 through 30-Sep-2015 (light grey), Validation 1-Oct-2015 through 30-Sep-2016 (mid grey).

Hydrodynamic-ecological model simulations of lake P as TP and PO₄ agreed well with monthly field measurements in main basin in the surface and bottom waters (Table 9; Figure 26), capturing the release of PO₄ and the subsequent accumulation of PO₄ and TP in the hypolimnion. Specifically, the

model performance for PO₄ and TP saw a strong fit as represented by high R-values in the surface and bottom waters during the calibration period ≥ 0.960 , and similarly high values during the validation period ≥ 0.914 (Table 9). Despite this, model accuracy as represented by elevated RMSE and MAE demonstrated PO₄ in the surface and bottom waters and TP in the bottom waters to be moderately underestimated. Underestimation of these values is primarily explained by the trade-off with the secondary calibration criteria that nutrients would balance upon autumn turnover, of which was well captured as part of the calibration.

Table 9 Phosphorus, nitrogen, and chlorophyll *a* performance statistics of the hydrodynamic-ecological model at Site 4. Statistics include Pearson correlation (R), root mean squared error (RMSE), and mean absolute error (MAE). Calibration period 1-Sep-2014 through 31-Aug-2015; Validation period 1-Sep-2015 through 31-Aug-2016.

Depth	Calibration			Validation		
	R	RMSE	MAE	R	RMSE	MAE
Phosphate						
Surface	0.985	0.006	0.004	0.933	0.003	0.003
Depth	0.987	0.025	0.021	0.991	0.017	0.014
Total phosphorus						
Surface	0.965	0.004	0.003	0.914	0.006	0.006
Depth	0.960	0.026	0.021	0.968	0.017	0.014
Ammonium						
Surface	0.866	0.011	0.005	-0.118	0.004	0.003
Depth	0.694	0.057	0.041	0.757	0.049	0.034
Nitrate						
Surface	0.105	0.002	0.002	-0.277	0.004	0.003
Depth	0.877	0.065	0.035	0.927	0.073	0.041
Total nitrogen						
Surface	0.001	0.034	0.029	-0.427	0.048	0.044
Depth	0.666	0.070	0.048	0.405	0.064	0.059
Chlorophyll <i>a</i>						
Surface	0.047	2.61	2.18	0.670	2.28	2.00

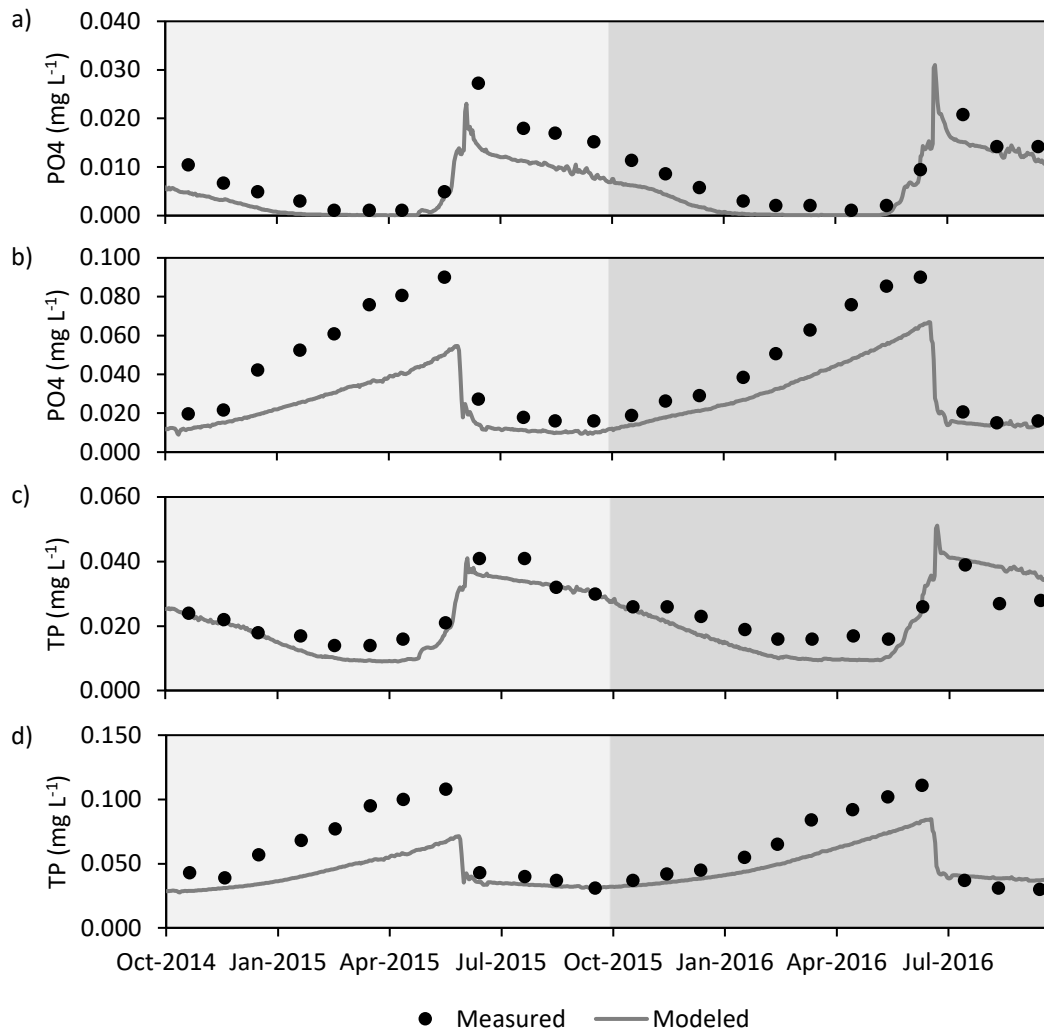


Figure 25: Measured vs modelled phosphate (PO_4) and total phosphorus (TP) at Site 4, during the calibration and validation periods, with a) surface water PO_4 , b) bottom water (80 m) PO_4 , c) surface water TP, and d) bottom water TP. Calibration period 1-Oct-2014 through 30-Sep-2015 (light grey), Validation 1-Oct-2015 through 30-Sep-2016 (mid grey).

Hydrodynamic-ecological model simulations of lake N as TN, NH_4 , and NO_3 agreed sufficiently well with monthly field measurements in main basin in the surface and bottom waters (Table 9; Figure 25). Critically here, a unique and characteristic double peak of NH_4 concentration measured in the lake (see Figure 25)—the first early in and the second later in the stratified period—was not able to be captured in the model simulations. In addition, the magnitude of the peak in NO_3 concentration measured in the lake—present between the two peaks in NH_4 concentration—was also unable to be captured in the model. Consequently, the underestimate of bottom water NH_4 concentrations early in the stratified period, and NO_3 concentrations later in the stratified period, also meant for an underestimate of bottom water TN concentration. This underestimate of N concentration in the bottom waters during stratification also meant for reduced vertical transport of N and its constituents and thus an underestimate of surface water TN, NH_4 , and NO_3 concentrations during the stratified period.

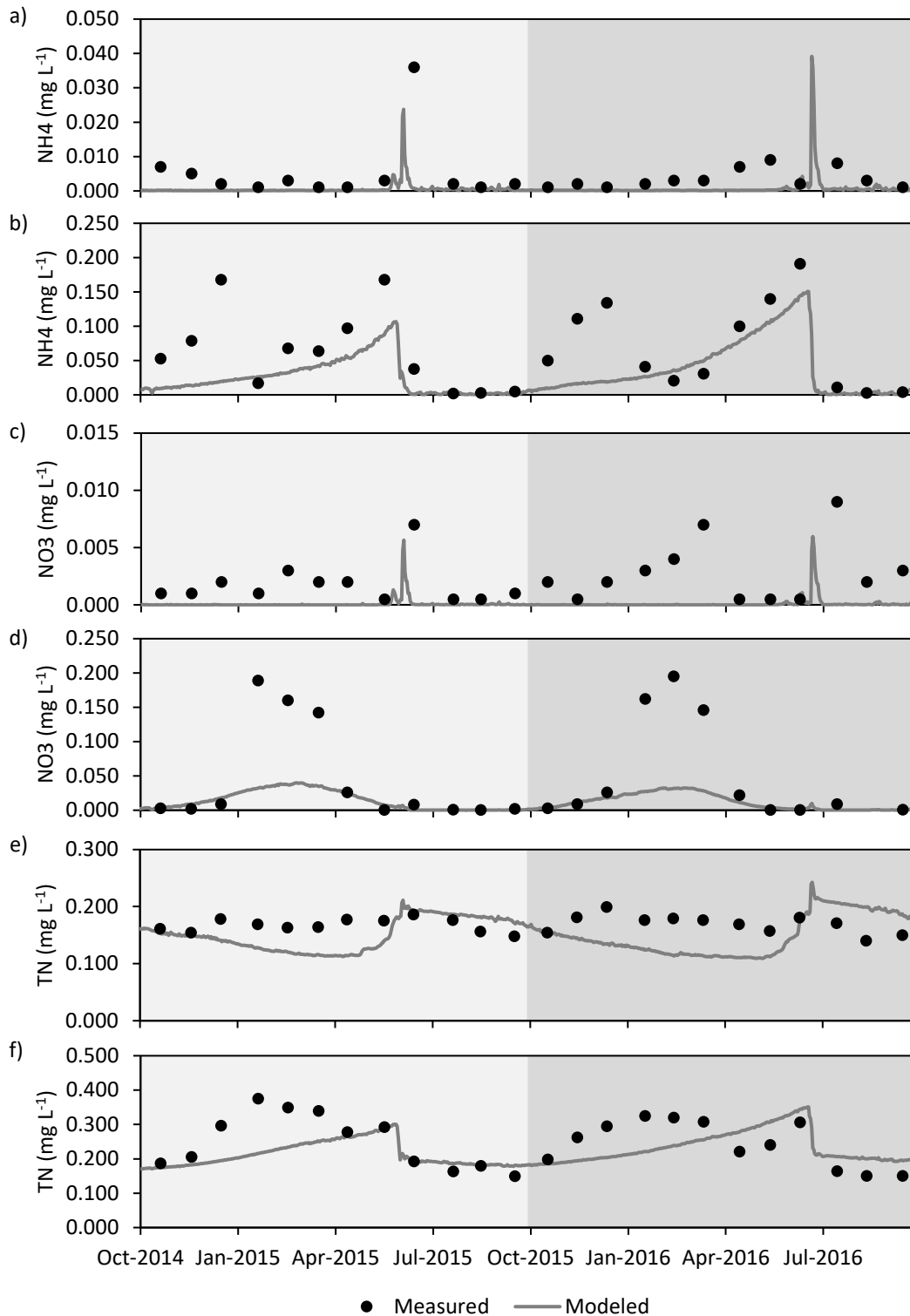


Figure 26: Measured vs modelled ammonium (NH₄), nitrate (NO₃), and total nitrogen (TN) at Site 4, during the calibration and validation periods, with a) surface water NH₄, b) bottom water (80 m) NH₄, c) surface water NO₃, and d) bottom water NO₃, e) surface water TN, and f) bottom water TN. Calibration period 1-Oct-2014 through 30-Sep-2015 (light grey), Validation 1-Oct-2015 through 30-Sep-2016 (mid grey).

Hydrodynamic-ecological model simulations for chlorophyll *a* agreed moderately well with monthly field measurements in main basin (Table 9; Figure 27a). Specifically, the calibration was represented

by a poor fit as represented by a low R-value of 0.047. This low R-value, however, was substantially impacted by the chlorophyll *a* peak in July, which if removed from the analysis would increase the R-value to 0.459. Chlorophyll *a* model fit was substantially stronger during the validation period, as represented by a moderate R-value of 0.670. Calibration (and validation) was represented by relatively strong model accuracy per RMSE values of 2.61 (validation; 2.28) of and MAE of 2.18 (validation; 2.00), with values representing the model's moderate overestimation of chlorophyll *a*. The 'soft calibration' for cyanobacteria and diatoms, owing to the absence of relevant data 1) measured at a monthly or sub-monthly timestep or 2) during calibration and validation period a, well captured the typical seasonality of the two groups measured in years outside our calibration window (e.g., Vincent et al., 1984; BoPRC, unpub) (Figure 27b).

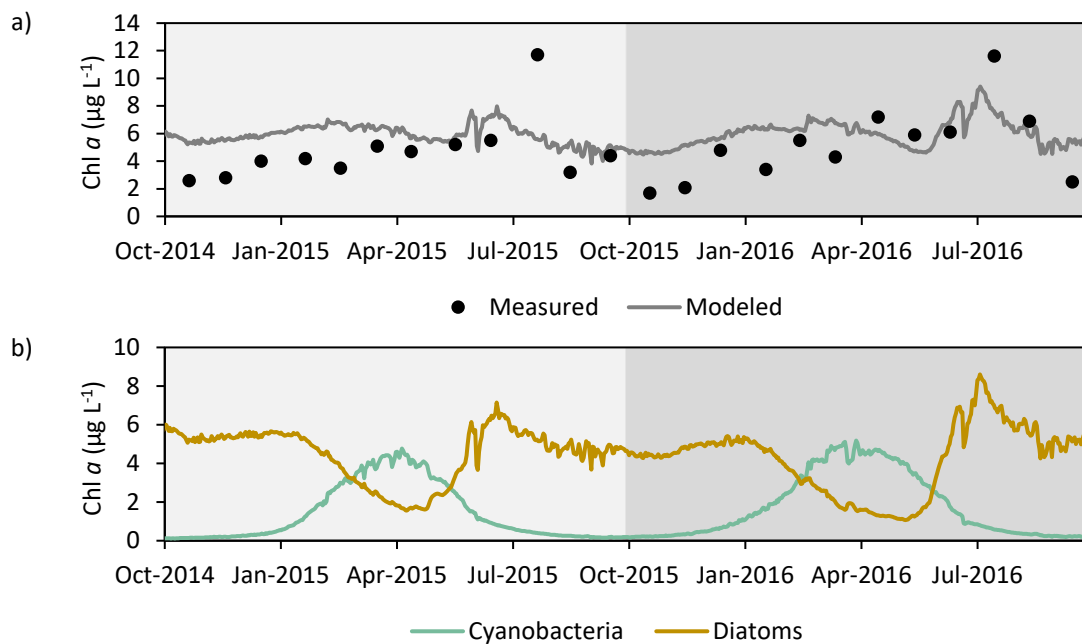


Figure 27: a) Measured vs modelled chlorophyll *a* (Chl *a*) at Site 4, and b) modelled cyanobacteria and diatoms, during the calibration and validation periods. Measured and modelled data as surface water. Calibration period 1-Oct-2014 through 30-Sep-2015 (light grey), Validation 1-Oct-2015 through 30-Sep-2016 (mid grey).

Hydrodynamic-ecological model simulations for TLI agreed well with measured data. This was demonstrated by simulated TLI underestimating measured TLI by only 0.55% during the calibration period (Figure 28d [left]). Moreover, the various TLI constituents too agreed relatively well with measured data throughout the calibration period. Here simulated Trophic Level phosphorus (TLp) overestimated measured data by 3.43%, simulated Trophic Level nitrogen (TLn) overestimated measured data by 6.19%, and Trophic Level chlorophyll *a* (TLc) underestimated measured data by 9.92% (Figure 28a,b,c [left]). The calibration period was confirmed by a validation period that agreed well with measured data. Here simulated TLI was show to underestimate measured TLI by 2.63% (c.f., 0.55% for the calibration), TLp underestimating by 5.15% (c.f., 3.43%), TLn underestimating by 6.75% (c.f., 6.195), and TLc overestimating by 3.24% (c.f., 9.92) (Figure 28a,b,c,d [right]).

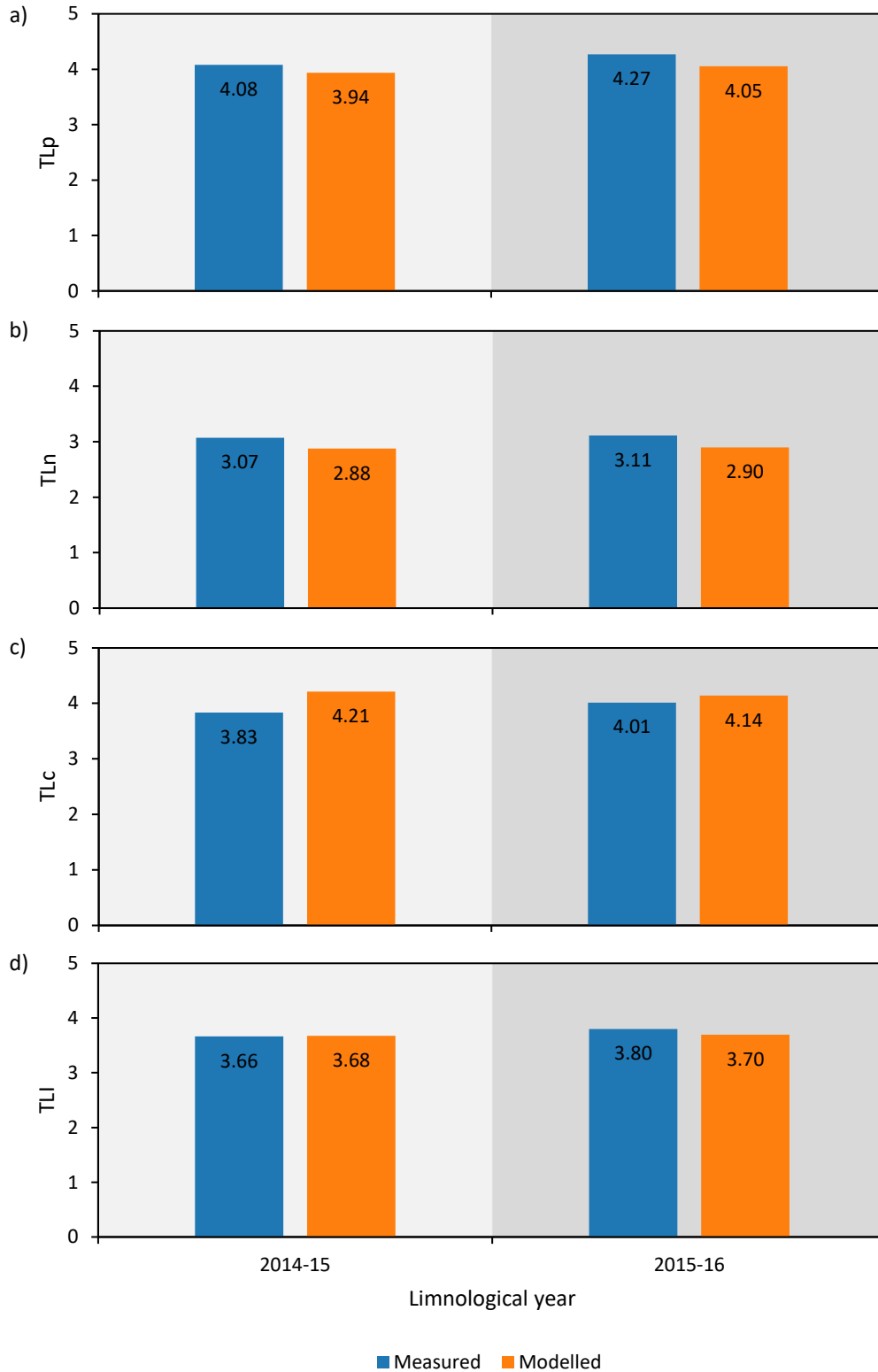


Figure 28: Measured vs modelled Trophic Level phosphorus (TLp), TL nitrogen (TLn), TL chlorophyll *a* (TLc), and Trophic Level Index (TLI) at Site 4, during the calibration and validation periods. Measured and modelled data as surface water. Calibration period 1-Oct-2014 through 30-Sep-2015 (light grey), Validation 1-Oct-2015 through 30-Sep-2016 (mid grey).

4.2.2.2 *Model output*

Simulations demonstrated that removal of the Ōhau Channel diversion wall would result in 70% of the lake's water present at the beginning of the simulation period to be lost by the middle of the fourth limnological year (i.e. 2017-18) (Figure 29 [right]; Figure 30). This would continue with 80%, 86%, 90%, and 93% of the lakes water present at the beginning of the simulation period to be lost by the middle of the fifth (i.e. 2018-19), sixth (i.e. 2019-20), seventh (i.e. 2020-21), and eighth (i.e. 2021-22) limnological years, respectively. By contrast, simulations demonstrating the wall staying in place resulted in water being lost at a substantially lower rate, with only 56% of the lakes water present at the beginning of the simulation period lost by the middle of the eighth (i.e. 2021-22) limnological year (Figure 29 [left]; Figure 30). The cumulative loss of water demonstrated here, agreed well with the mean calculated removal times as demonstrated and calculated in Figure 21 and Figure 22, respectively.

Simulations demonstrated little change between wall-in and wall-out scenarios, for surface water temperature, bottom water temperature, and bottom water DO. Specifically, surface water temperature (i.e., 1 m depth) decreased by 0.05 °C (± 0.07 °C, standard deviation), bottom water temperature decreased by 0.09 °C (± 0.07 °C, standard deviation), and bottom water DO decreased by 0.09 mg L⁻¹ (± 0.27 mg L⁻¹, standard deviation) under wall-out (c.f. wall-in) simulations (data not shown).

Simulations demonstrated TP concentrations to decrease in the surface waters following the removal of the Ōhau Channel diversion wall (Figure 31a; Figure 32a). This was demonstrated in the scenario with the Ōhau Channel at baseline TLI, with the reduction in TP becoming more pronounced in the scenarios in which Ōhau Channel TLI was reduced to a maximum TLI of 4.2 and 3.8. By the eighth year, when ~93% of water existing at the beginning of the simulation period is simulated to have been removed from the lake (Figure 30), TP was simulated to have reduced (relative to the wall-in scenario) by 0.0018 mg L⁻¹ (or 6.9%) under the wall-out scenario with Ōhau Channel inflow at baseline TLI, 0.0022 mg L⁻¹ (or 8.7%) under the wall-out scenario with Ōhau Channel inflow max-TLI of 4.2, and 0.0030 mg L⁻¹ (or 11.6%) under the wall-out scenario with Ōhau Channel inflow max-TLI of 3.8.

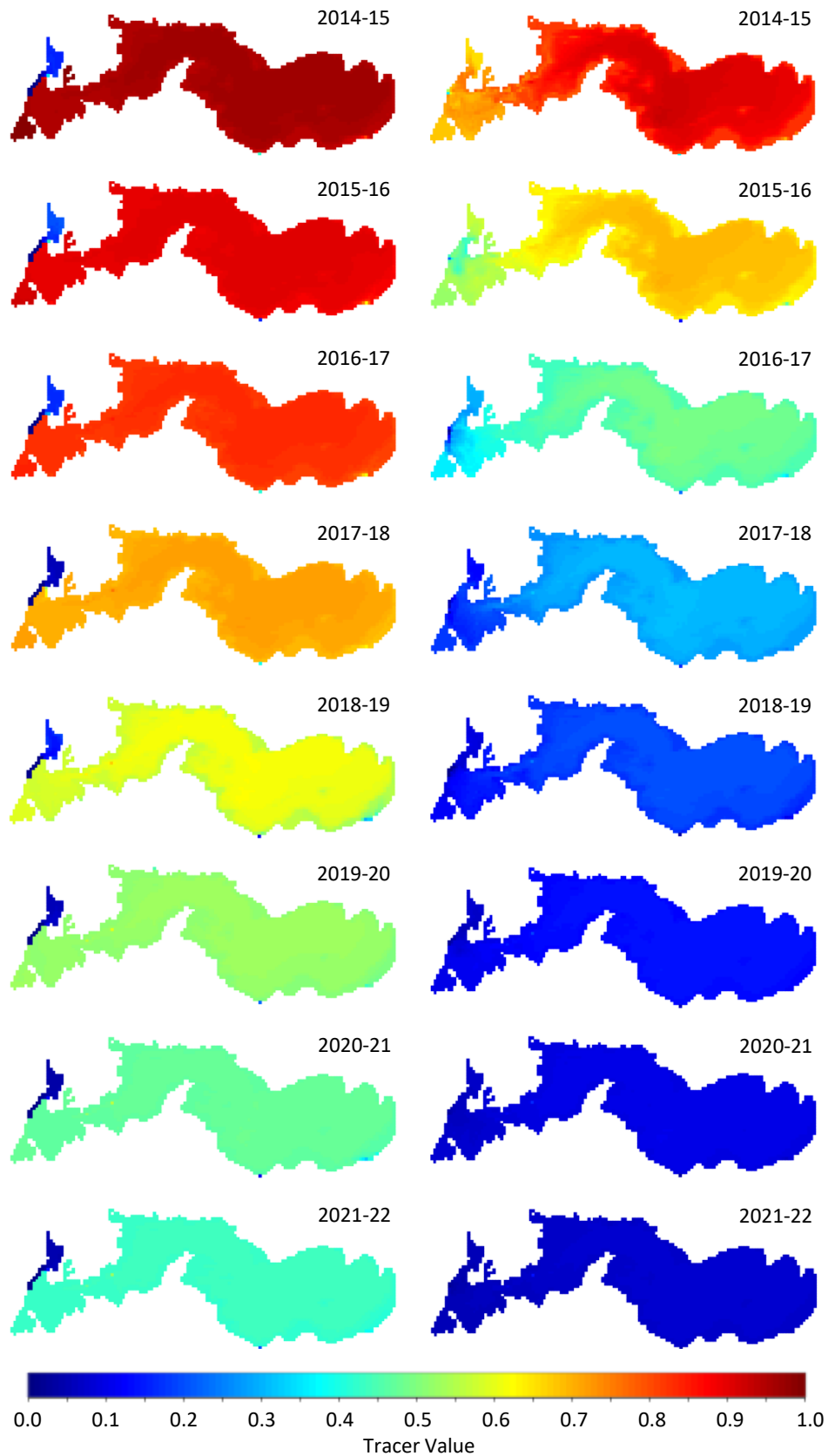


Figure 29: Simulated cumulative (i.e., year after year, over eight years) removal of Lake Rotoiti water with wall in place (left) and without the wall in place (right), represented by dilution of tracer (initial value = 1) over each limnological year at the mid-point of each year. Mid-point for 2014-15 year (1-10-2014 through 30-6-2015) was 15-02-2015; Mid-point for all other years was 31-12 of the given year.

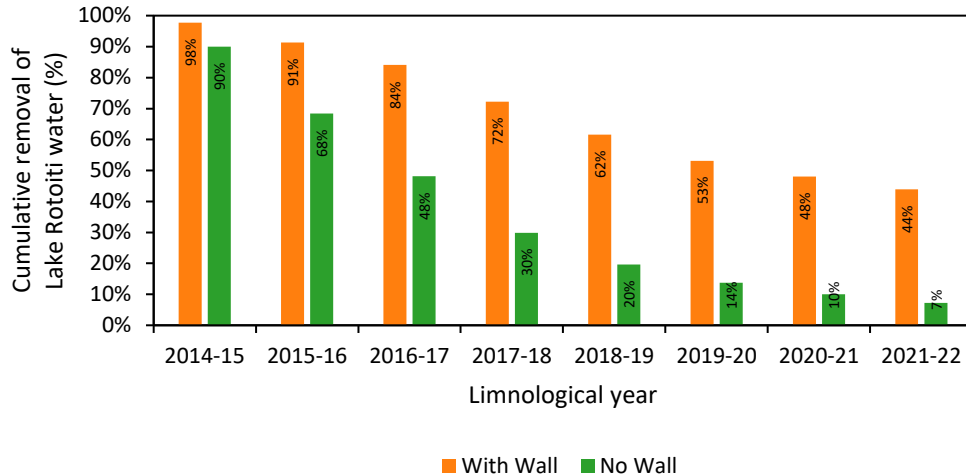


Figure 30: Simulated cumulative removal of Lake Rotoiti water 1) with and 2) without the wall in place over each limnological year during the hydrodynamic-ecological simulation period. Date represents mid-point of each simulation year. Mid-point for 2014-15 year (1-10-2014 through 30-6-2015) was 15-02-2015; Mid-point for all other years was 31-12 of the given year.

In contrast to TP, simulations demonstrated TN (Figure 31b; Figure 32b) and chlorophyll *a* (Figure 31c; Figure 32c) concentrations to increase under the wall-out scenario with the Ōhau Channel at baseline TLI, and under the wall-out scenario with Ōhau Channel flow adjusted to a maximum TLI of 4.2, yet decrease under the wall-out scenario with the Ōhau Channel flow adjusted to a maximum TLI <3.8. By the eighth year, TN was simulated to have increased (relative to the wall-in scenario) by 0.010 mg L⁻¹ (or 5.6%) under the wall-out scenario with Ōhau Channel inflow at baseline TLI, and 0.003 mg L⁻¹ (or 1.6%) under the wall-out scenario with Ōhau Channel inflow adjusted to a maximum TLI of 4.2, however decreased by 0.009 mg L⁻¹ (or 5.4%) under the wall-out scenario with Ōhau Channel inflow adjusted to a maximum TLI of 3.8. Similarly, By the eighth year, chlorophyll *a* was simulated to have increased (relative to the wall-in scenario) by 0.47 µg L⁻¹ (or 6.9%) under the wall-out scenario with Ōhau Channel inflow at baseline TLI, and 0.23 µg L⁻¹ (or 3.4%) under the wall-out scenario with Ōhau Channel inflow adjusted to a maximum TLI of 4.2, however decreased by 0.15 µg L⁻¹ (or 2.1%) under the wall-out scenario with Ōhau Channel inflow adjusted to a maximum TLI of 3.8.

Simulated changes in TP, TN, and chlorophyll *a* concentrations seemingly reached a new equilibrium in the third or fourth year following the removal of the wall (Figure 32). This new equilibrium, correlated with between 52% (i.e., third year) and 70% (i.e., fourth year) of the water existing at the beginning of the simulation period (i.e., with properties of wall in water) having been removed from the lake. Consequently, simulations demonstrated changes in TN, TP, and chlorophyll *a* following the removal of Ōhau Channel diversion wall will not stabilise for approximately 3-4 years under typical hydrological conditions.

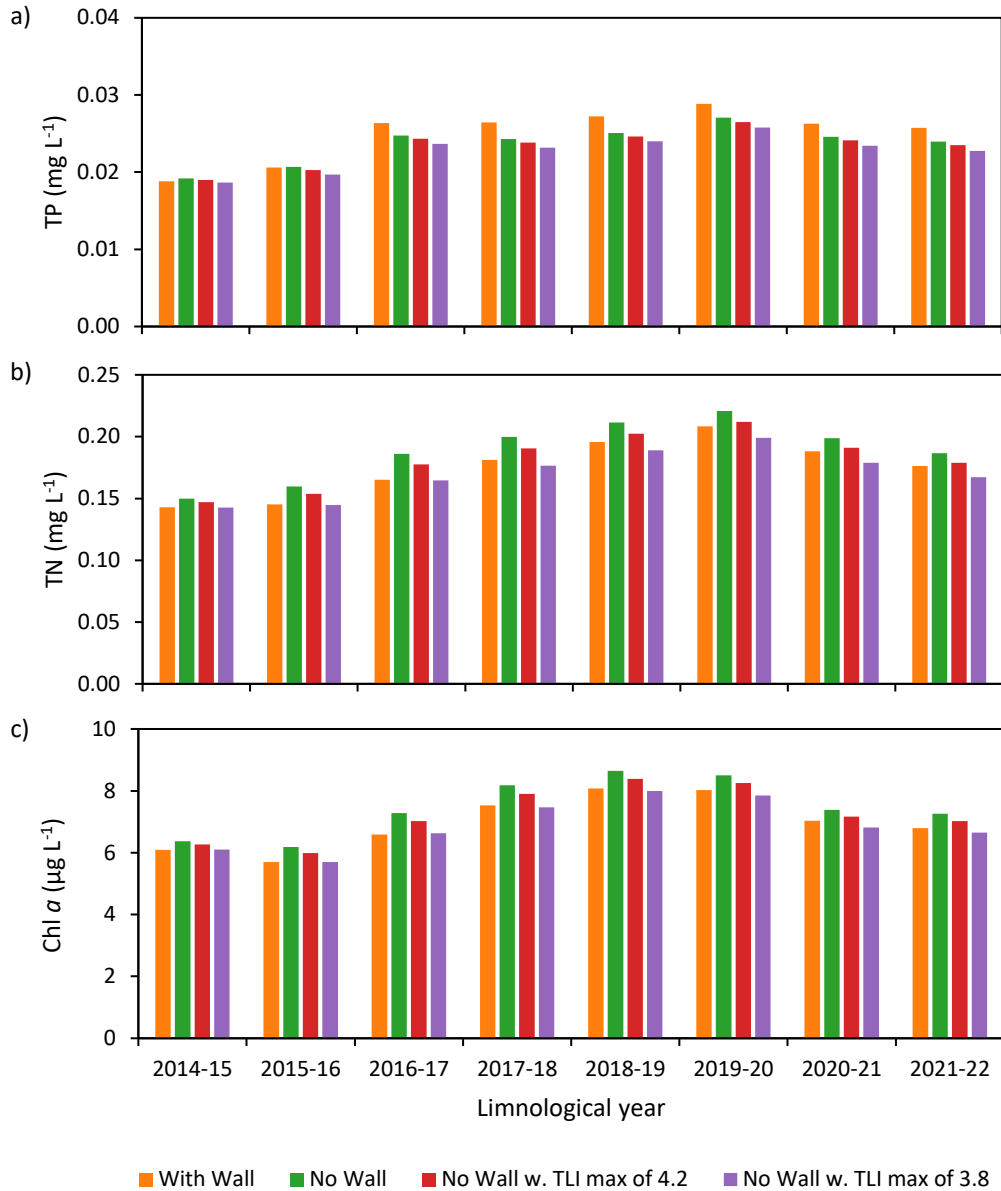


Figure 31: Simulated Surface total phosphorus (TP), total nitrogen (TN), and chlorophyll *a* at Site 4, as limnological year means, for the 1) wall-in, 2) wall-out, 3) wall-out with TLI max of 4.2, and 4) wall-out with TLI max of 3.8 configurations, across the 2014-15 through 2021-22 limnological years (i.e., 1-Jul through 30-Jun of the subsequent year). N.b. variable vertical scale.

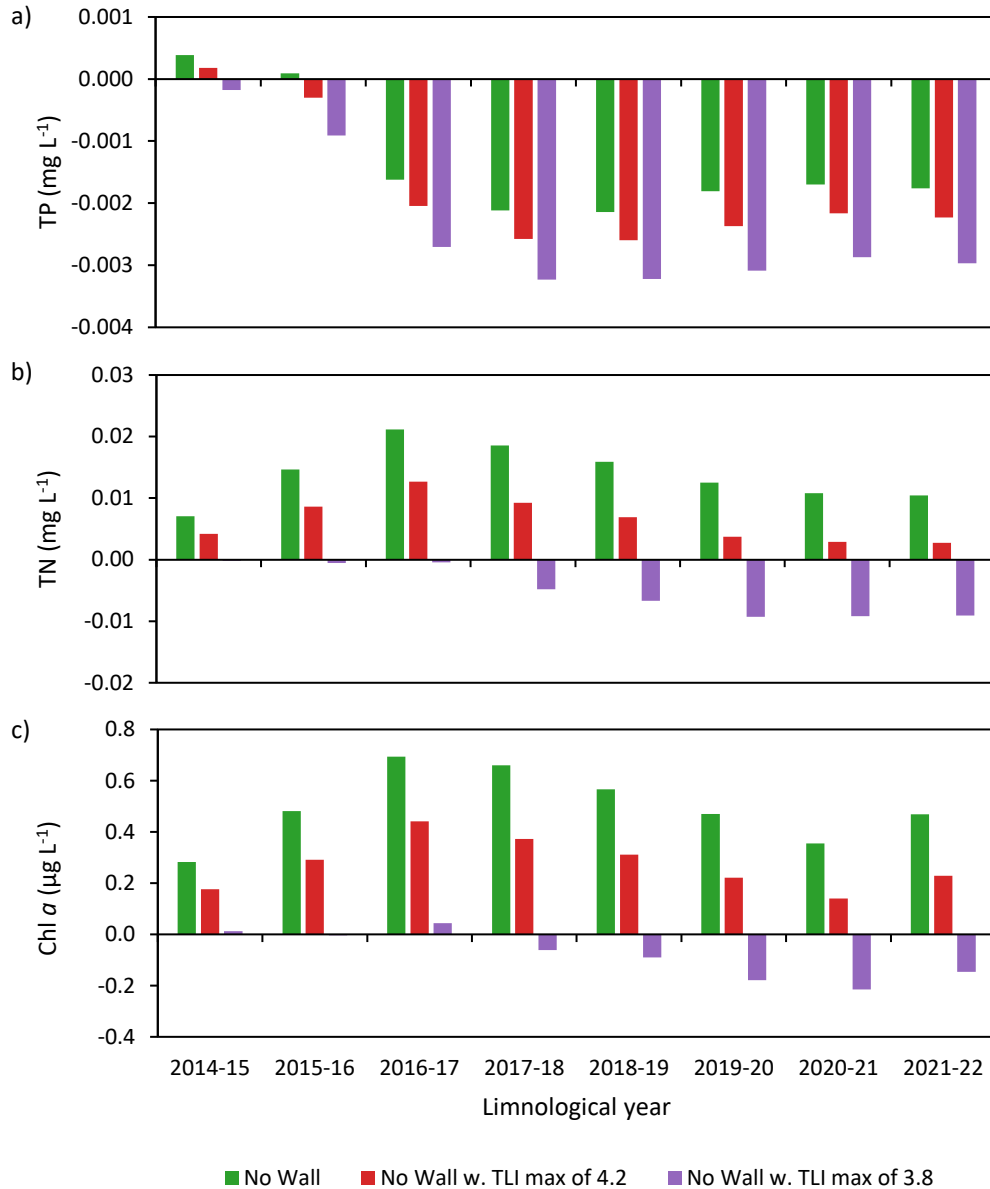


Figure 32: Simulated relative change—i.e., to the simulated ‘wall-in’ configuration—in Surface total phosphorus (TP), total nitrogen (TN), and chlorophyll *a* at Site 4, as limnological year means, for the 1) wall-out, 2) wall-out with TLI max of 4.2, and 3) wall-out with TLI max of 3.8 configurations, across the 2014-15 through 2021-22 Limnological years (i.e., 1-Jul through 30-Jun of the subsequent year). N.b. variable vertical scale.

As with TP concentrations, simulations demonstrated TLp to decrease in the surface waters under the wall-out scenario with the Ōhau Channel at baseline TLI (Figure 33a; Figure 34a), with the reduction most pronounced under the under the wall-out scenario with Ōhau Channel inflow adjusted to a maximum TLI of 3.8. Specifically, by the eighth year, when ~93% of water existing at the beginning of the simulation period is simulated to have been removed from the lake (Figure 30), TP was simulated to have reduced (relative to the wall-in scenario) by 0.09 TLI units (or 2.1%) under the wall-out scenario with the Ōhau Channel inflow at baseline TLI, 0.12 TLI units (or 2.7%) under the wall-out scenario with the Ōhau Channel inflow adjusted to a maximum TLI of 4.2, and 0.16 TLI units (or 3.6%) under the wall-out scenario with the Ōhau Channel inflow adjusted to a maximum TLI of 3.8.

As with TN and chlorophyll *a* concentrations, simulations demonstrated TL_n (Figure 33b; Figure 34b) and TL_c (Figure 33c; Figure 34c) to increase under the wall-out scenario with Ōhau Channel flow under baseline conditions and under the wall-out scenario with Ōhau Channel flow adjusted to a maximum TLI <4.2, but decrease under the wall-out scenario with the Ōhau Channel flow adjusted to a maximum TLI <3.8. By the eighth year, TL_n was simulated to have increased (relative to the wall-in scenario) by 0.08 TLI units (or 2.4%) under the wall-out scenario with Ōhau Channel inflow at baseline TLI, and 0.02 TLI units (or 0.6%) under the wall-out scenario with Ōhau Channel inflow max-TLI of 4.2, however decreased by and 0.07 TLI units (or 2.2%) under the wall-out scenario with Ōhau Channel inflow max-TLI of 3.8. Similarly, By the eighth year, TL_c was simulated to have increased (relative to the wall-in scenario) by 0.07 TLI units (or 1.7%) under the wall-out scenario with Ōhau Channel inflow at baseline TLI, and 0.04 TLI units (or 0.9%) under the wall-out scenario with the Ōhau Channel inflow adjusted to a maximum TLI of 4.2, however decreased by and 0.02 TLI units (or 0.6%) under the wall-out scenario with the Ōhau Channel inflow adjusted to a maximum TLI of 3.8.

Simulations demonstrated TLI (Figure 33d; Figure 34d) to increase under the scenarios in which the wall was removed with Ōhau Channel flow under baseline conditions, but decrease under scenarios where the wall was removed with Ōhau Channel flow adjusted to a maximum TLI 4.2 and 3.8. Specifically, by the eighth year, TLI was simulated to have increased (relative to the wall-in scenario) by 0.02 TLI units (or 0.5%) under the wall-out scenario with Ōhau Channel inflow at baseline TLI, but decreased and by 0.02 TLI units (or 0.5%) under the wall-out scenario with the Ōhau Channel inflow adjusted to a maximum TLI of 4.2, and decreased by and 0.08 TLI units (or 2.1%) under the wall-out scenario with the Ōhau Channel inflow adjusted to a maximum TLI of 3.8.

As with TP, TN, and chlorophyll *a* concentrations, simulated changes in TLI and its constituents seemingly reached a new equilibrium in the third or fourth year following the removal of the wall (Figure 34). Consequently, simulations demonstrated changes in TLI and its constituents following the removal of Ōhau Channel diversion wall will not stabilise for approximately 3-4 years under typical hydrological conditions.

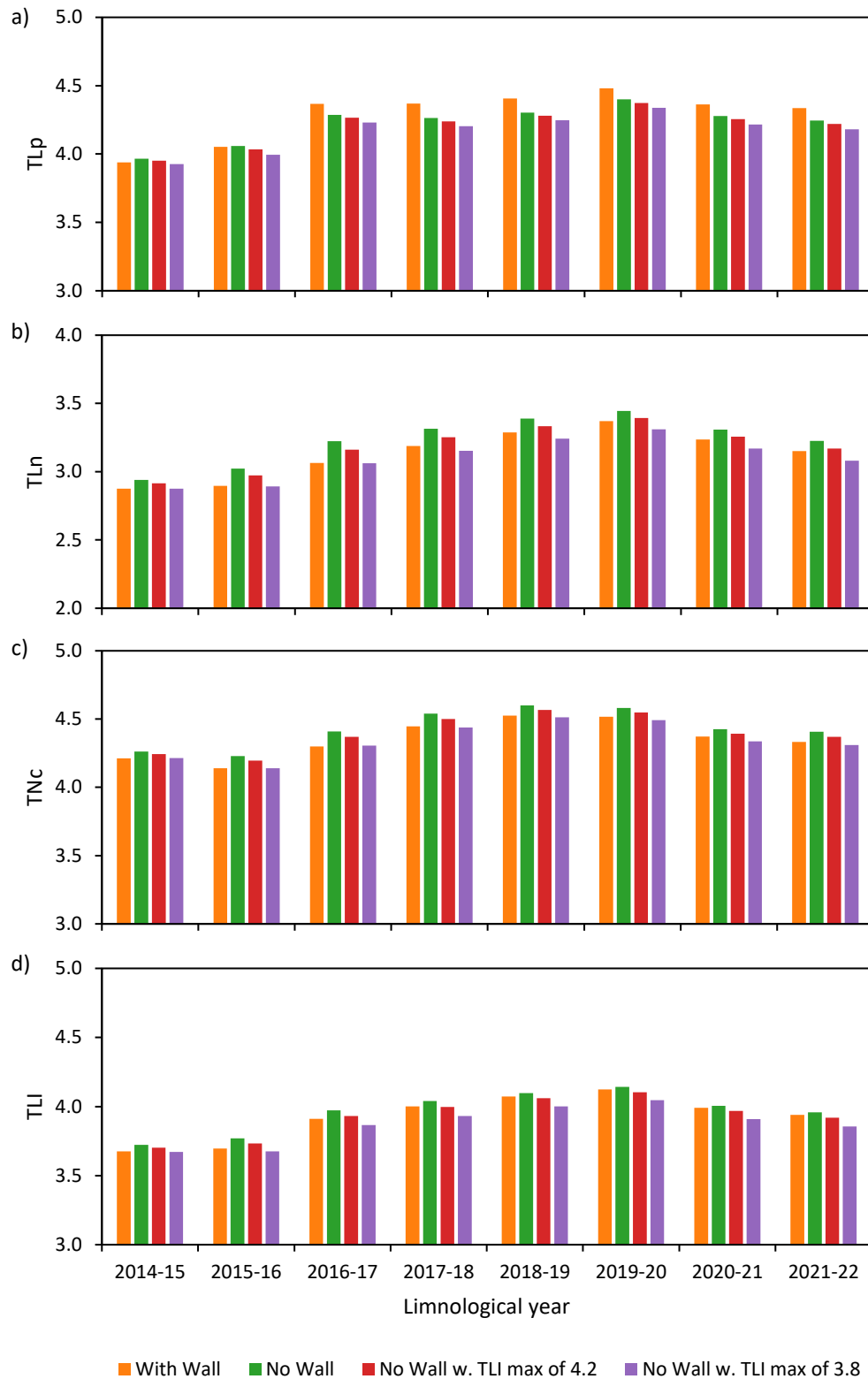


Figure 33: Simulated Trophic Level phosphorus (TLp), TL nitrogen (TLn), TL chlorophyll *a* (TLc), and TL Index (TLI) at Site 4, as limnological year means, for the 1) wall-in, 2) wall-out, 3) wall-out with TLI max of 4.2, and 4) wall-out with TLI max of 3.8 configurations, across the 2014-15 through 2021-22 Limnological years (i.e., 1-Jul through 30-Jun of the subsequent year). N.b. variable vertical scale.

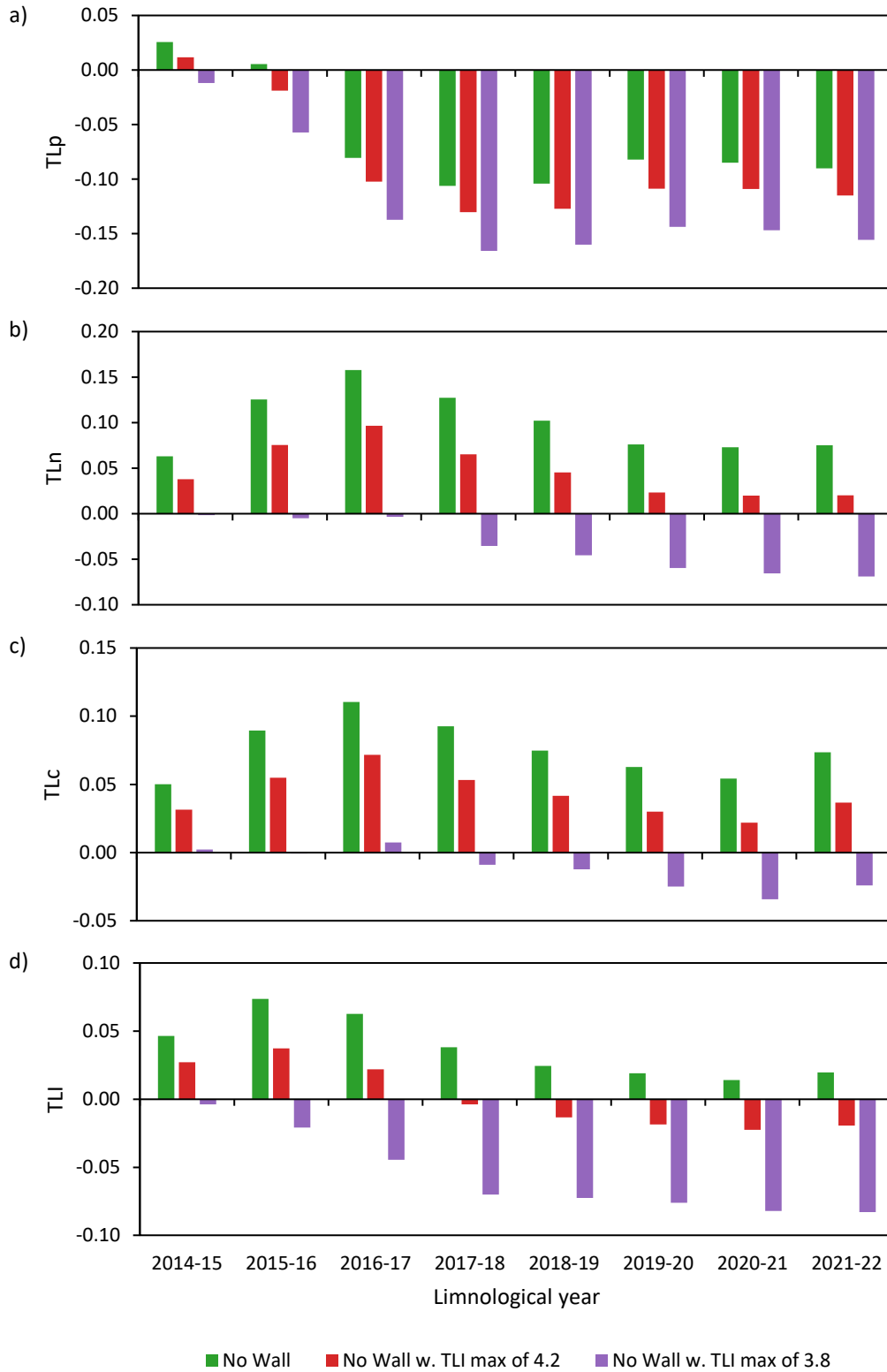


Figure 34: Simulated relative change—i.e., to the simulated ‘wall-in’ configuration—in Trophic Level phosphorus (TLp), TL nitrogen (TLn), TL chlorophyll *a* (Tlc), and TL Index (TLI) at Site 4, as limnological year means, for the 1) wall-out, 2) wall-out with TLI max of 4.2, and 3) wall-out with TLI max of 3.8 configurations, across the 2014-15 through 2021-22 Limnological years (i.e., 1-Jul through 30-Jun of the subsequent year). N.b. variable vertical scale.

4.3 Part 3: Assessment of holes in the diversion wall

4.3.1 Calculations

The estimation of discharge through the holes in the diversion wall was facilitated by conducting a series of hole size measurements and flow velocity measurements. The average hole size along the length of the wall was determined to be 0.035 m^2 , with a distance-weighted average flow of 0.156 m s^{-1} . Since the total number of holes in the diversion wall is currently unknown, it was necessary to estimate this number to enable discharge calculations through the holes. Assuming a total of 100 holes along the length of the diversion wall, approximately 3.3% of the Ōhau Channel water was estimated to leak through the holes into Lake Rotoiti (Figure 35). This percentage increased to 9.8% of the Ōhau Channel water when the total number of holes was assumed to be 300.

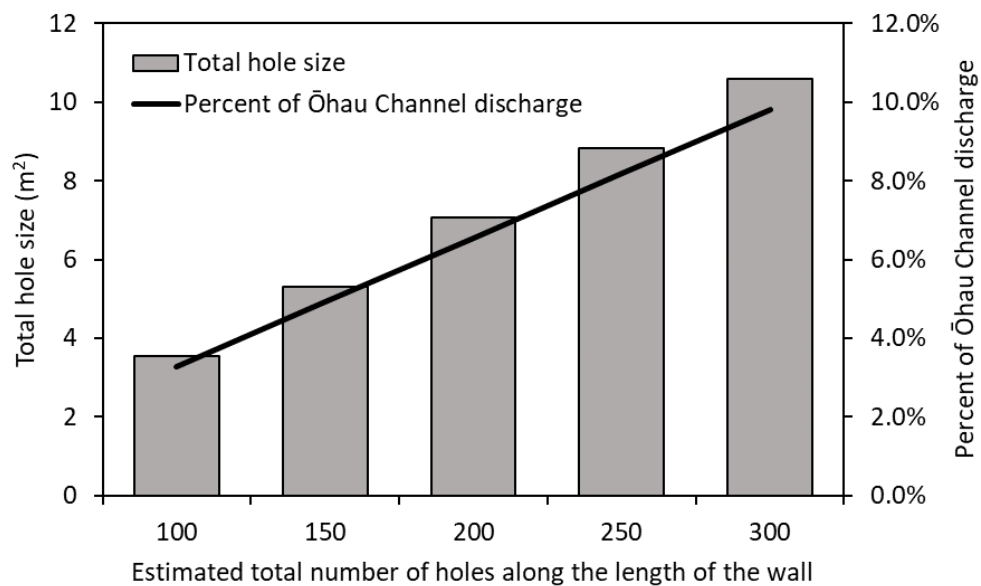


Figure 35: Summary of calculations of discharge through the holes in the Ōhau Channel diversion wall. Percent discharge of Ōhau Channel water was based on measurements of average hole size and flow velocities through the holes, using different estimated of the total number of holes (which is currently unknown).

4.3.2 Modelling

Model scenarios demonstrated an appreciable contribution of Ōhau-derived water to Lake Rotoiti under all six scenarios with holes in the wall. The six scenarios (which varied the placement of the hole in the wall) resulted in contribution rates (i.e., contribution of Ōhau-derived water to Lake Rotoiti as $\% \text{ yr}^{-1}$) of between 6.9-13.4% as compared to 0.8% in the wall-in (with no holes) scenario, and 22.6% in the wall-out scenario (Figure 36; Figure 37a). Further, the six scenarios resulted in retention rates, (i.e., retention of Ōhau-flow in Lake Rotoiti as $\% \text{ yr}^{-1}$) of between 14.9-28.9% as compared to 1.7% in the wall-in (with no holes) scenario, and 46.7% in the wall-out scenario (Figure 37b). Critically, this resulted in wall efficiency of 45.0-70.7%, and declines in wall efficiency of 29.3-55.0% as a result of a single 1×100 -meter hole in the wall (Figure 37c).

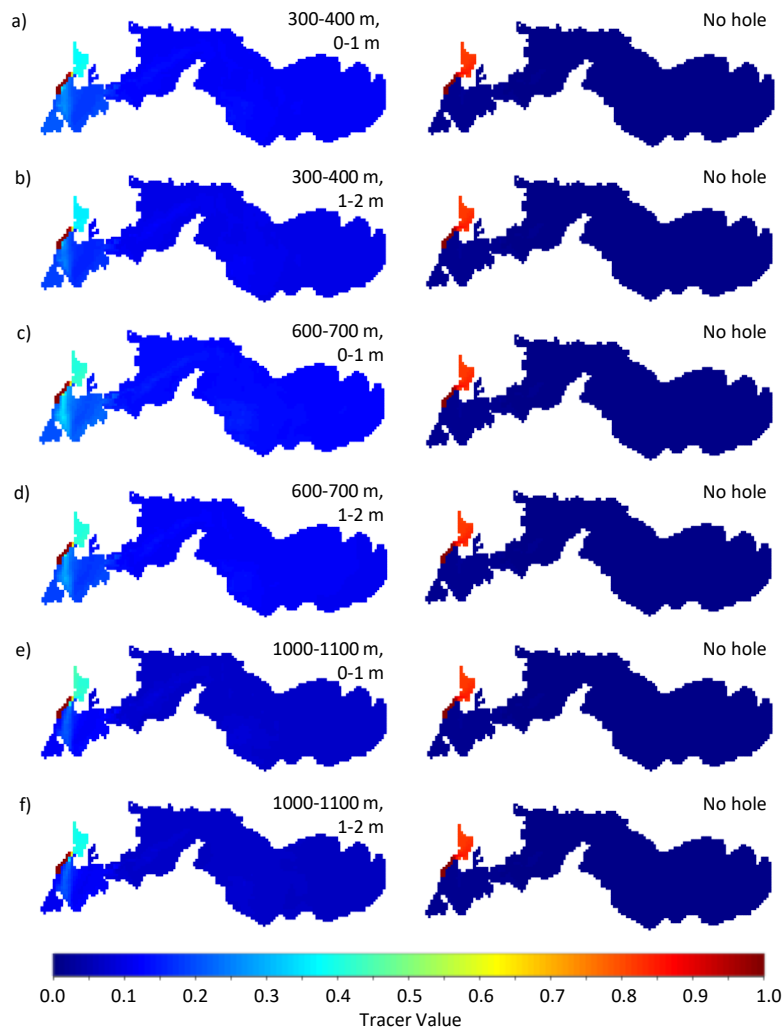


Figure 36: Simulated contribution of Ōhau Channel (tracer value = 1) derived water with the wall in place and a 1×100 -m hole in the wall; a) hole 300-400 m along the wall at ~ 0 -1 m depth, b) hole 300-400 m along the wall at ~ 1 -2 m depth, c) hole 600-700 m along the wall at ~ 0 -1 m depth, d) hole 600-700 m along the wall at ~ 1 -2 m depth, e) hole 1000-1100 m along the wall at ~ 0 -1 m depth, and f) hole 1000-1100 m along the wall at ~ 1 -2 m depth. Left column contains scenario, and right column contains control, as wall in with no hole in the wall.

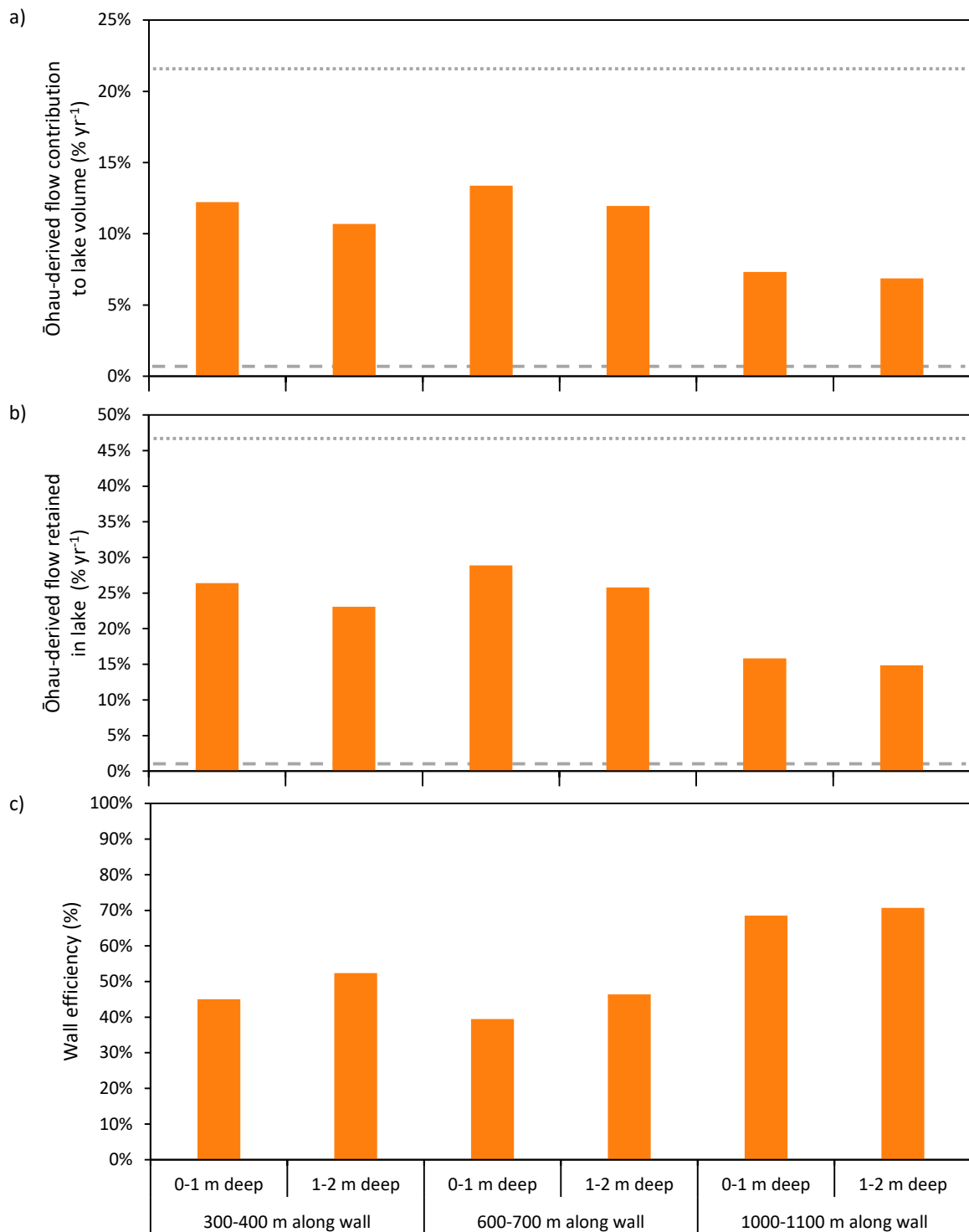


Figure 37: Simulated comparison of a) the contribution of Ōhau Channel-derived water, b) the retention of Ōhau Channel-derived water, and c) wall efficiency, with combinations of holes in the wall at 300-400 m, 600-700 m, or 1000-1100 m along the wall, and ~0-1 m depth or ~1-2 m depth. N.b. For reference, short-dashed line equals wall-out, and long dashed lines equals wall-in (with no holes).

5 DISCUSSION

The results from the analysis of the current water quality data for Lake Rotoiti and the modelling highlight the importance of the Ōhau Channel diversion wall preventing water quality degradation of Lake Rotoiti. Data analysis demonstrated improvements of water quality following installation of the wall in Lake Rotoiti, with TN, Secchi depth, and the TLI displaying a step change following the construction of the wall. Model simulations illustrated that removal of the wall would lead to water quality deterioration and a slight increase in the TLI in the lake. The removal of the wall with moderate reductions in the maximum TLI of the Ōhau Channel inflow (i.e., 4.2) would be insufficient to prevent an increase in TL_n and TL_c in Lake Rotoiti, yet be sufficient to prevent an increase in overall TLI in the lake. The removal of the wall with the most ambitious reductions in the maximum TLI of the Ōhau Channel inflow (i.e., 3.8) would only be sufficient to result in a TLI in Lake Rotoiti between 4.0 and 4.1. Finally, data analysis and hydrodynamic modelling suggest that holes in the Ōhau Channel diversion wall resulted in an appreciable amount of Ōhau Channel water leaking into Lake Rotoiti.

5.1 *Water quality data analysis*

Utilising a three-step approach to analyse existing water quality data for Lake Rotoiti has yielded multiple lines of evidence regarding the impacts of the Ōhau Channel diversion wall on the lake. Proceeding in ascending order of confidence in the inference drawn from the statistical analysis employed, it becomes apparent that nutrient concentrations and chlorophyll *a* concentration generally exhibited improvement during the post-wall study period (i.e., 2008-2023). While the visual interpretation of data support this conclusion, the formal analyses (correlation and intervention analysis) reveal a more complicated pattern.

The results of the correlation analysis suggest that many of the observed differences are not statistically significant. For Secchi depth, the construction of the wall has altered the underlying connection between Lake Rotorua and Lake Rotoiti. Two explanations may account for why the correlation analysis did not reveal strong evidence for the effects of the wall on water quality in Lake Rotoiti. Firstly, correlation analysis may not be effective in detecting changes. The analysis presented in this study builds upon the previous review of the Ōhau Channel diversion wall and aimed to maintain consistency across different review periods. However, it relies on assumptions that remain largely unconfirmed. The primary assumption is that hydrological connectivity between Lake Rotorua and Rotoiti via the Ōhau Channel would result in similar water quality patterns and characteristics in both lakes. Although the Ōhau Channel is the primary inflow to Lake Rotoiti and water quality changes in Lake Rotorua will to some extent be reflected in Lake Rotoiti, it is worth noting that Lake Rotorua is comparatively shallow and polymictic, while Lake Rotoiti is deep and monomictic. Therefore, the differences in lake functioning and seasonality of water quality may significantly differ between these lakes, leading to a muted response of water quality in Lake Rotoiti to changes in Lake Rotorua. Secondly, Lake Rotorua has undergone substantial management interventions before, during, and after the construction of the diversion wall (including improved catchment management and alum applications), resulting in water quality improvements in the lake independent of any potential improvements observed in Lake Rotoiti. Hence, it is plausible that these improvements in Lake Rotorua could have influenced the detection of changes in correlations between these lakes.

The intervention analysis arguably constitutes the most robust analysis in this study for detecting any changes in water quality in Lake Rotoiti due to the construction of the diversion wall. This analysis, based on interrupted time series analysis, commonly employed in medical clinical trials and conservation work of terrestrial ecosystems, enables a formal test of changes in a response variable

following some intervention, using the concept of a counterfactual and comparison of changes to a control site. It was found that TN, Secchi depth, and TLI exhibited a step change following the construction of the wall, although no shifts in long-term trend slopes were observed. This suggests that the overall trajectory of water quality in Lake Rotoiti remained unaffected by the wall, and the step changes that occurred immediately following the wall construction persisted for the remainder of the study period. It is important to note that no control site was included in the analysis presented in this study. While Lake Rotorua was identified as the only reasonable candidate lake as a control site due to the direct hydrological connection between the lakes, the active management and resulting water quality improvement would have impacted the ability to draw strong inferences regarding any changes in Lake Rotoiti.

Additionally, the construction of the diversion wall coincided with an upgrade to more advanced lab analytical equipment (flow injection analysis) used for water quality sample analysis. This upgrade may have reduced data variability after the change, potentially leading to an incorrect assumption that the diversion wall had a positive impact (James Dare, personal communication, April 2024). It is possible that the change in analytical equipment contributed to the observed patterns in the data. Therefore, interpreting the results of observational data analysis should be done with caution and in conjunction with modelling results, which can account for confounding factors that might otherwise influence the findings.

5.2 Lake system modelling: hydrodynamics scenario testing

As expected, that accumulation and propagation of Ōhau Channel-derived water through Lake Rotoiti was substantially reduced with the Ōhau Channel diversion wall in place as compared to the lake without a wall. Firstly, model scenarios demonstrated that the Ōhau Channel diversion wall increases the fraction of the Ōhau Channel-derived flow short-circuited through the lake down the Kaituna River from 55.2% (i.e., without the wall in place) to 99.3%. Consequently, the Ōhau Channel diversion wall decreased the contribution of Ōhau Channel-derived water to the lake (defined as the lake less the area inside the wall and in the Okere arm) over the course of a year from 22% (i.e., without the wall in place) to 0.3%. Secondly, model scenarios without the wall in place clearly demonstrated a propagation of the Ōhau Channel flow through the lake as an overflow during spring and summer, before transitioning into an interflow during autumn, and finally and underflow during winter. This agreed well with that reported by Vincent et al. (1986) and Hamilton et al. (2005) who inferred flow depth based on the relative difference in temperature between the Ōhau Channel inflow and vertical temperature profiles in Lake Rotoiti. Vincent et al. (1986) noted overflow to predominate during spring and summer, and inter- and under-flow (pooled together in this instance) to predominate during autumn and winter. Similarly, Hamilton et al. (2005) noted underflow to predominate during winter, and an overflow to predominate during spring before transitioning to an interflow during summer. The simulations reported in the current study, however, provide higher resolution information to the behaviour of the Ōhau Channel flow without the wall in place, owing to our data applying a 3-D model of the lake, over an extended period (19 years), and at two sites: The Narrows, Site 3, and in the main basin, Site 4. Further, this study demonstrated the depth at which the Ōhau-derived flow propagated through the lake was largely conserved through the Narrows and into the main basin, albeit with a signature decreasing by approximately an order of magnitude.

Residence time in Lake Rotoiti was shown to increase 3.3-fold with the Ōhau Channel diversion wall in place as compared to the lake in its natural state without a wall. Defining residence time in the study as the time in which 95% of the lakes water was cleared, we calculated residence times of 26.9 years with the wall in place and 8.2 years with no wall in place. These residence times represent an average residence time, based on the mean annual clearance rate from 19 limnological years from 2003-04 through 2021-22. Consequently, the method (i.e., a 3-D hydrodynamic model) and the

simulation period (i.e., 19-year annual mean) used in this study, enable a relatively high degree of certainty can be placed on the estimated residence times. Critically, these residence times have direct implications for runtimes of model scenarios, and more importantly expectations with regards to timeframes in the success of the intervention. As an example, assuming the Ōhau Channel diversion wall has been in effect for 16-17 years (i.e., current year, as 2024; installation year, as 2007-2008), and without holes, residence times calculated in this study indicate ~15-17% of the water present in Lake Rotoiti as of 2024 would have existed in the lake prior to the wall's completion. Therefore, the full extent of the wall's effect in protecting water quality in the lake would still not yet be fully realised. As a second example, the increased residence time with the wall in place would slow the clearance of inflow entering the eastern basin, including the geothermal flux emanating from the area in and around the crater. This hydraulic flux has been estimated as (350 L s^{-1}) (McBride et al., 2021), and assuming N concentrations observed in Tikitere Geothermal Field (up to 24.5 mg N L^{-1} ; Wairau Bay Stream), thus an unintended side-effect of the wall might be reducing the rate at which a potentially substantial flux of N is being removed from the system.

5.3 Lake system modelling: water quality scenario testing

TLI in Lake Rotoiti was shown to increase with the removal of the wall. Removal of the wall without any adjustment to water quality in the Ōhau Channel flow resulted an increase of 0.010 mg L^{-1} (or 5.6%) for TL_n, an increase of $0.47 \text{ } \mu\text{g L}^{-1}$ (or 6.9%) for TL_c, and a decrease of 0.0018 mg L^{-1} (or 6.9%) for TL_p. These changes in concentration resulted in an increase to the overall TLI (0.02 units, in the eighth and final simulation year), TL_n (0.08 units), and TL_c (0.07 units) in Lake Rotoiti. Interestingly, however, removal of the wall without any adjustment to TLI in the Ōhau Channel flow resulted in a minor reduction of TL_p in the of 0.09. The decrease in TL_p in Lake Rotoiti following the removal of the wall is likely attributed to P management strategies (e.g., alum dosing; Smith et al., 2016) taking place in Lake Rotorua prior to and during the 2014-15 through 2021-22 study period, driving a decline of TP in Lake Rotorua and indirectly Lake Rotoiti as the Lake Rotorua-derived water slowly accumulates in Lake Rotoiti. Simulated differences between wall-in and wall-out scenarios in this present study were comparable to, and overall less than, those initially modelled and simulated in Lake Rotoiti by Hamilton et al. (2005), who also predicted small improvements in water quality under wall-in (c.f., wall-out) scenarios. The smaller difference between the wall-in and wall-out scenarios quantified in this present study, c.f., that of Hamilton et al. (2005), likely reflect a smaller disparity between Lake Rotorua and Rotoiti water quality in this study and most likely the improving water quality in Lake Rotorua from July-2001 through Jan-2004 period as modelled in the study by Hamilton et al. (2005), through the October-2014 though Jun-2022 period as modelled in this current study.

An increasing TLI in Lake Rotoiti with removal of the wall could be mitigated when implemented concurrently with a reduction of the TLI in the Ōhau Channel inflow. Specifically, scenario simulations demonstrated that a maximum TLI of 4.2 (corresponding to the TLI target for Lake Rotorua) was insufficient to prevent an increase in TL_n and TL_c in Lake Rotoiti, but was sufficient to prevent an increase in overall TLI in the lake. This is explained by the reduction in TL_p simulated under the wall out scenario with baseline TLI (TL_p of 4.34 with wall in, cf. 4.25 with wall out), being reduced further under the wall out scenario with maximum TLI of 4.2 (TL_p of 4.22 with wall out and Ōhau Channel inflow max TLI of 4.2). Despite this, the scenario with a maximum TLI of 3.8 was sufficient to prevent an increase in TLI and its constituents. Consequently, a maximum TLI of ~4.3 in the Ōhau Channel inflow would be sufficient maintain current TLI in Lake Rotoiti, however a maximum TLI of ~4.0 would be required to not cause any further degradation of any of the three TLI constituents. Such reductions, however, would not be trivial and would require ~8% reduction in P, N,

and chlorophyll *a* in Lake Rotorua in the first instance (i.e., max TLI of 4.3), and ~28% reduction in the second instance (i.e., max TLI of 4.0).

Water quality improvements in Lake Rotoiti expected from improved the Ōhau Channel inflow water quality appear to be buffered against by internal processes. This was demonstrated by a reduction to TL_n, TL_p, and TL_c, as well as N, P, and chlorophyll *a* concentrations in the Ōhau Channel inflow, not directly correlating with changes in Lake Rotoiti. For example, reducing the TLI of the Ōhau Channel inflow from a maximum TLI of 4.41 (i.e., baseline scenario) to 4.2 (i.e., a 15.5% reduction to N, P, and chlorophyll *a* concentrations) only resulted in reducing the TLI in Lake Rotoiti (in the 8th simulation year) from 3.96 (i.e., baseline scenario) to 3.92 (i.e., 4.1% reductions to N, 1.9% reductions to P, and 3.4% reductions chlorophyll *a* concentrations). Even accounting for the Ōhau-derived contribution of water in the lake (~62%), realised improvements in water quality were less than what would be expected based on concentration of the Ōhau Channel inflow and dilution and dispersion of the Ōhau Channel inflow within Lake Rotoiti. This buffering capacity is further emphasised by the additional reduction of the TLI to the Ōhau Channel inflow from a maximum TLI of 4.2 (i.e., a 15.5% reduction to N, P, and chlorophyll *a* concentrations) to 3.8 (i.e., a 28% reduction to N, P, and chlorophyll *a* concentrations) only resulted in reducing the TLI in Lake Rotoiti from 3.92 (i.e., 4.1% reductions to N, 1.9% reductions to P, and 3.4% reductions chlorophyll *a* concentrations) to 3.86 (i.e., 6.6% reduction to N, 3.1% reductions to P, and 5.4% reductions chlorophyll *a* concentrations). It is likely that this is attributed to N and P legacies in the system released from the sediments during anoxia (Jeppesen et al., 2024; Sharpley et al., 2013), and/or N and P derived from a substantive unquantified groundwater-based geothermal flux (McBride et al., 2021). Consequently, future improvement to the water quality in Lake Rotoiti may require additional water quality management measures in Lake Rotorua, and within Lake Rotoiti itself.

5.4 Assessment of holes in the diversion wall

The estimation of discharge through the holes in the diversion wall suggests that even with a relatively small total number of estimated holes, the leakage of Ōhau Channel water into Lake Rotoiti is appreciable. These discharge rates compare well with the hydrodynamic modelled output, where a single 1 × 100-meter hole in the Ōhau Channel diversion wall was shown to reduce the effectiveness of the wall in preventing the accumulation of Ōhau-derived water within the lake by 29.3-55.0%. These estimates, however, represent a highly conservative estimate only, as the finest scale hole in the wall that could be simulated was 1 × 100 meters, per the 3-D cartesian mesh applied in this study, with uniform cell spacing of 100 m in each of the horizontal directions (*x* and *y*) and a 1 m resolution on the vertical dimension (*z*). It is understood that this method is an oversimplification, and the process is far more complex in reality, and as such analysis focused on aspects less sensitive to the model resolution. For example, we did not consider extracting fine-scale and localised metrics such as velocities entering or exiting the holes in the levee (i.e., wall), and instead focused on a broad-scale metrics in that of the movement of tracers over long periods of time (i.e., a year). Nevertheless, the corroboration of the measured and modelled data provides sufficient evidence that all holes in the wall collectively, although small individually, can result in a substantial flux of Ōhau Channel-derived water and ultimately accumulation within the lake. Due to remaining uncertainties regarding the total number of holes in the diversion wall, the assessment in this study prioritised estimating the discharge of water through the holes rather than calculating, for instance, nutrient load through the wall. Additionally, an examination of the effects of the holes on water quality in Lake Rotoiti was not undertaken due to these same uncertainties.

5.5 Lake system modelling: calibration

Developing a lake water quality model, with confidence in its ability to capture and represent specific lake, requires considerable time and effort spent on model calibration. The time and effort involved in model calibrations is typically related to; data availability, the state of knowledge, and summarising complex biogeochemical or ecological aspects in more general terms. The model in this study was able to well represent temperature and DO dynamics in the lake. Specifically, the current model was able to better capture bottom water temperatures and the decline in DO during early stages of stratification (October to December) than a previously produced 1-D model of Lake Rotoiti (Hamilton et al., 2005). Model calibration in this present study, demonstrated accurate representation of bottom water temperatures and the resultant decline in DO during early stages of stratification was driven by the ground water geothermal flux, and thus assumptions relating to the representation of the ground water geothermal flux in the model. It is also likely that improved representation of temperature and DO in this current study, may be attributed to the application of 3-D model in this study and a 1-D model in the study Hamilton et al. (2005), and the improved ability of a 3-D model to capture such localised processes. Critically, however, the calibration process confirmed the model in this present study was able to well capture the geothermally driven hypolimnetic mixing in Lake Rotoiti, and its ability to destabilise the water column and thus disrupt early stratification (Gibbs, 1992). More generally, the model in this current study compared well with the temperature and DO calibrations across a suite of other studies in the Bay of Plenty, New Zealand (e.g., Me et al., 2018; Özkundakci et al., 2011).

The model in this study was able to well represent P dynamics, as evidenced by a strong model fit (i.e., R) and adequate model accuracy (i.e., RMSE and MAE; Table 9). Reasons for not achieving an even better fit for P dynamics are likely attributed to model 1) the model over-representing bottom-water mixing, and 2) the model not being able to explicitly model atmospheric deposition.

1. In the bottom waters, not achieving a better fit appears to be driven by the model underrepresenting TP and PO₄ in the hypolimnion. This was confirmed during the calibration process, whereby accurate bottom water TP and PO₄ concentrations resulted in substantial overrepresentations of TP and PO₄ at surface and depth upon turnover; while less accurate bottom water TP and PO₄ concentrations resulted in accurate representations of TP and PO₄ at surface and depth upon turnover. Consequently, the reduced model accuracy was a necessary trade-off to not have TP and PO₄ accumulate in the system from year to year. This issue appears to be attributed to the model overrepresenting mixing processes in the bottom waters throughout the hypolimnion rather than with intensity decreasing from the sediments towards the metalimnion (Gibbs, 1992). This very issue was also noted in the study of Hamilton et al. (2005).
2. In the surface waters, not achieving a better fit may be influenced by the inability to model atmospheric deposition explicitly. Due to atmospheric deposition not being able to be modelled explicitly, we instead applied some 39 small surface inflows around the periphery of the lake, of which delivered small volumes of water hyper-concentrated N and P to best mimic the process. Although this method was considerably more effective than ignoring the process of atmospheric deposition of N and P, an explicit means to incorporate the atmospheric flux would have no doubt resulted in improved model accuracy.

The model in this study was able to adequately represent N dynamics, as evidenced by adequate model fit (i.e., R) and model accuracy (i.e., RMSE and MAE; Table 9). Reasons for not achieving a better model fit for N dynamics are likely related to the same processes outlined for P (i.e., the model over-representing bottom-water mixing, and the model not being able to explicitly model atmospheric deposition), and other processes unique to or more heavily implicated with N, including 1) the

contribution and composition of the groundwater geothermal flux, 2) driver(s) of N succession in the hypolimnion, and 3) simulating N fixation:

1. The contribution and composition of the groundwater geothermal flux remains largely unknown. Consequently, in this study we chose to implement a conservative approach to simulate the accumulation of N and P in the hypolimnion based on a dynamic sediment flux, rather than introducing the uncertainty of a static geothermal groundwater flux as done in other modelling studies. Despite this, surface water geothermal inputs entering the lake from the Tikitere Geothermal Field are known for the high concentrations (up to 24.5 mg N L⁻¹; Wairau Bay Stream), and thus in scaling up such concentrations alongside estimates of geothermal groundwater discharge (350 L s⁻¹) the groundwater-derived geothermal flux could be significant (McBride et al., 2021).
2. The underlying mechanisms governing the interactions between NH₄ and NO₃ in the hypolimnion of Lake Rotoiti remain unresolved. Despite a considerable calibration effort, the model was able to capture the later NH₄ peak but unable to reproduce the initial NH₄ peak and the magnitude of the NO₃ peak, similar to what was found in Hamilton et al. (2005). Although nitrification is necessary to occur for the observed succession in the monitoring data, it cannot sufficiently explain the unique succession of NH₄-NO₃-NH₄ observed in Lake Rotoiti. It has been speculated in previous work that the initial NH₄ peak might be related to regeneration of NH₄ from the winter diatom ‘bloom’ (Hamilton et al., 2005). Nevertheless, phytoplankton crashes are common occurrences in lakes (e.g., Tiselius & Kuylenstierna, 1996; Yamamoto & Nakahara, 2005), and the observed succession of N in the hypolimnion appears to be unique to Lake Rotoiti. As such, we posit that the observed succession might be related to pH and/or a groundwater geothermal flux at the Crater. There may be two mechanisms to support this hypothesis. Firstly, low pH is known to reduce ammonification and nitrification processes (e.g., Leoni et al., 2018). We suggest that a declining pH in the hypolimnion as stratification progresses might reduce the rates of ammonification and nitrification overtime. If true, then this would have enabled capturing of the succession through configuring higher NH₄ sediment release and nitrification rates which would have reduced in scale as pH reduced over time. Unfortunately, such a process is not easily captured in the model in its current configuration. Secondly, with groundwater geothermal unknown we suggest that an unknown seasonality of N or pH of the flux contribute to the observed N seasonality.
3. N-fixation was not modelled explicitly as modelling N-fixation is not trivial, requires relevant observational data for model verification, and often results in adding more uncertainty than it solves. Moreover, the N flux derived for N-fixation is likely to be small owing to measurements of N-fixation in Lake Rotoiti in the 2002-3 summer (in the midst of a substantial bloom of the known N-fixer *Anabaena* sp.) indicating that rates of N fixation were considerably low with respect to the total mass of N present in the lake (Hamilton et al., 2005).

Despite the above gaps in knowledge, we are confident in the calibration of this model, and its ability to scenario test within the context of the aims of this study.

5.6 Implications and future work

This research echoes the observations and conclusions of previous studies (e.g., Hamilton et al., 2005; Priscu et al., 1986) indicating that nutrient dynamics in Lake Rotoiti are complex and not well understood. These complexities add to the difficulty of capturing and understanding the processes with respect to model calibration and confidence in scenario outcomes. Nutrient-related dynamics in Lake Rotoiti that would benefit from a further understanding are primarily related to: 1) processes driving the NH₄-NO₃-NH₄ succession in the hypolimnion of Lake Rotoiti; 2) geothermal fluxes relating to temperature, pH, and most notably P and N, and their constituents; and 3) atmospheric

deposition of P and N, and their constituents. Although, developing and understanding of ‘1)’ and ‘2)’ is not trivial, they are identified as the key processes, with ‘1)’ possibly driven by the pH- and N-component of ‘2)’, of which would enable a better understanding of nutrient dynamics and related processes in the lake. In contrast, developing an understanding of ‘3’ is understood to be a relatively simple undertaking and necessary to ensure that the overall nutrient budget becomes more accurate. Furthermore, recent findings (e.g., McBride et al., 2021; Verburg et al., 2018) have identified atmospheric deposition as a significant flux of N and P as bioavailable NH_4 , NO_3 , and PO_4 , critically of which enters directly at the lake surface for uptake by primary producers. Of note, developing and understanding of the groundwater derived N flux not only has implications with respect to capturing and understanding the processes for modelling purposes, but also has implications with respect to understanding the impact of management interventions and feasibility of meeting the TLI target in the lake.

This present study was an ambitious undertaking whereby 3-D water quality scenarios were run across an 8 year simulation period. The coming years, however, will see continued advancement in computational power and lake model capabilities, and breakthrough and advancement of critical scientific processes which will enable more ambitious scenario testing. First, advancements in computational power will, for example, enable longer model runs times, a greater number of scenarios tested, and finer model grids enabling added resolution in and around the Ōhau Channel diversion wall. Second, advancements in lake modelling capabilities, for example, might enable the use of dynamic (flexible) grid (mesh), enabling finer scale resolution in and around the Ōhau Channel diversion wall. Although use of dynamic grids was not an option for this current study, use of dynamic grids is an evolving field of research and will become a feasible option in the coming years. Such an approach might also enable an explicit means to incorporate an atmospheric deposition flux in the model. Although this was not an option in this study, recent work emphasising the scale of the flux in some systems, might incentivise model developers to include the capacity to stipulate atmospheric deposition in the future. Third, breakthrough and advancement of critical scientific processes might, for example, lead to a better understanding of the unique N succession in the hypolimnion of Lake Rotoiti, thus providing improved model performance, and confidence in model simulations.

This present study provided a concise set of scenarios best designed, per time and resource constraints, to investigate the implications of removing the in-lake Ōhau Channel diversion wall for water quality measures and targets in Lake Rotoiti. Despite this, future work might endeavour to explore the impact of a greater variety of Ōhau Channel inflow scenarios, the impact of future climate scenarios, and the interplay of these two factors. In the instance of investigating a greater variety of Ōhau Channel inflow scenarios, future work might adjust TLI parameters in isolation of one another to best reflect proposed in-lake management strategies in Lake Rotorua and/or the Ōhau Channel. This would build on the work done in the present study, which applied adjustments to TLI parameters equally. In the instance of investigating the impact of future climate scenarios, future work might apply downscaled GCMs (coupled models, comprising an atmosphere-ocean general circulation model [AOGCM] and Earth system model [ESM]) of Coupled Model Intercomparison Project Phase 6 (CMIP6; see Eyring et al., 2016) to force the meteorological conditions in the model. CMIP6 data of which is available at an hourly resolution (unlike its previous incarnation; CMIP5), when dynamically downscaled (i.e., as high-resolution, regionally specific data; Chapman et al., 2023), would provide the ideal input to investigate the influence of future climate scenarios in Lake Rotoiti, with and without the Ōhau Channel diversion wall in place.

5.7 Conclusions

5.7.1 Overview

A thorough evaluation of water quality in Lake Rotoiti involved a systematic analysis of long-term datasets and detailed 3-D hydrodynamic and hydrodynamic-ecological modelling to better understand the impacts of the Ōhau Channel diversion wall and the potential effects of its removal on the lake. Data analysis demonstrated improvements in water quality in Lake Rotoiti were evident, with TN, Secchi depth, and the TLI displaying a step change following the construction of the wall. This underscores the critical role of the Ōhau Channel diversion wall in preventing degradation in Lake Rotoiti. It is worth noting that drawing strong inference on the effects of an intervention on a large ecosystem such as Lake Rotoiti from non-experimental routine monitoring data is not trivial and uncertainties exist in this study's assessment due to a lack of an appropriate control site (i.e., a similar lake that has not been affected by the diversion wall). In lieu of a control site, model simulations were used to illustrate that removal of the wall would lead to water quality deterioration and a slight increase in the TLI in the lake. Even with the most ambitious reduction in the maximum TLI of the Ōhau Channel inflow (i.e., 3.8), removal of the wall would only marginally lower Lake Rotoiti's TLI to between 4.0 and 4.1. Consequently, removal of the wall alongside the most ambitious reduction in maximum TLI in Lake Rotorua would likely necessitate additional water quality management in Lake Rotoiti to achieve its TLI target of 3.5. An assessment of the effects of the holes in the diversion wall using the best available data and hydrodynamic modelling suggests that there is an appreciable amount of Ōhau Channel water leaking into Lake Rotoiti. A considerable amount of uncertainty remains in this assessment as the total number of holes remains unknown.

5.7.2 Answers to research questions

5.7.2.1 Water quality review

Has the wall achieved its objective of improving water quality?

Evidence suggests that the diversion wall has led to enhanced water quality in Lake Rotoiti. Total nitrogen, Secchi depth, and TLI showed a step change after the wall's construction, although there were no shifts in long-term trend slopes.

Has the wall resulted in the lake reaching its TLI target in advance of improvements to Lake Rotorua water quality impacting Lake Rotoiti?

There is some evidence suggesting that water quality in Lake Rotoiti improved before the construction of the wall. Total nitrogen and chlorophyll *a* concentrations, as well as Secchi depth, showed improvement prior to the wall's construction. However, drawing strong conclusions from the data is challenging as the observed patterns in the long-term dataset may or may not be fluctuating cyclically.

Does current monitoring support the continued placement of the wall, diverting Ōhau Channel water?

The TLI in Lake Rotoiti is still above its target. There is also no clear evidence that water quality in the lake is still improving. However, there is some evidence that the TN and TP concentrations are going through a period of increase. This suggests that (together with conclusions drawn from the modelling work; see below), the continued placement of the wall is still warranted.

What impact has the diversion wall had on the quality of the Kaituna River.

There is no evidence to suggest that the diversion wall had an impact on the water quality dynamics in the Kaituna River.

5.7.2.2 Water quality modelling

What is the modelled impact of the diversion wall on water quality and ecology?

Modelling showed that the implementation of the diversion wall has resulted in small reductions to TN and chlorophyll *a*, but increases in TP concentrations (Figure 32). Taken together, the wall has resulted in a reduction in TLI in Lake Rotoiti (Figure 34d).

Does this align with the water quality and ecological monitoring of Lake Rotoiti?

Simulated TLI and its constituents over longer-term periods (i.e., 8 years), agree well with the data analysis of even longer-term data sets carried out in part 1 of this current study. Further, the effects of the observed reduction in TLP in Lake Rotorua (because of catchment management practices and alum dosing in Lake Rotorua), and thus the Ōhau Channel inflow entering Lake Rotoiti, were well captured by model simulations through simulating a decrease in TLP in Lake Rotoiti as the Lake Rotorua-derived water accumulated within the lake.

The diversion wall is expected to be in place for 50 to 100 years. Once it has been removed what is the likely water quality expectation for Lake Rotoiti if Lake Rotorua meets the TLI of 4.2 +, when Lake Rotoiti is expected to meet a TLI of 3.5?

Simulations run from 2014-2022 in which the Ōhau diversion wall was removed in conjunction with water quality in Lake Rotorua equivalent to a maximum annual TLI of 4.2, resulted in a TLI in Lake Rotoiti after eight years of 4.2. Although eight years is ample time for the lake to reach a new equilibrium, this assumes all other inputs are at baseline, and thus no concomitant in-lake or catchment management practices implemented in Lake Rotoiti. Therefore, removal of the wall alongside a maximum annual TLI in Lake Rotorua of 4.2, without additional measures, will be insufficient to have Lake Rotoiti meet its a TLI target of 3.5.

The diversion wall has effectively changed the water residence time in Lake Rotoiti from about 1.5 years to 5+ years. How does this impact Lake Rotoiti water quality, potentially having an impact on bottom water dissolved oxygen levels and especially the western arm of the lake?

Simulations suggest residence times (determined as the time to clear 95% of existing water) substantially longer than 1.5 and 5+ years for wall-out and wall-in scenarios. Simulations instead indicated residence times of 8.2 and 26.9 years for wall out and wall in scenarios, respectively. Nevertheless, model simulations in the eastern (i.e., Narrows) and western (i.e., Crater) basins demonstrated the wall-in scenario compared to the wall-out scenario to maintain a small increase of <0.1-0.2 mg DO L⁻¹ in the bottom waters during the stratified period., which is well within the range of uncertainty of the model simulations. There was no clear evidence of any changes in bottom water DO levels in the monitoring data at sites 3 and 4 (see data analysis in part 1)

6 ACKNOWLEDGEMENTS

We thank Andy Bruere for initiating the study, and the Bay of Plenty Regional Council for funding. We thank all members of the Ōhau Channel diversion wall review working group for constructive feedback on the results of this study during an earlier presentation of our findings. We thank Mathew Allan and Christopher McBride for modelling advice. We thank David Hamilton, Hannah Jones, Moritz Lehmann, Christopher McBride, Kohji Muraoka, Nina von Westernhagen for their previous modelling work in Lake Rotoiti. Andy Bruere, James Dare, and Whitney Woelmer provided a thorough and insightful manuscript review. Bay of Plenty Regional Council provided bathymetric data, and flow and water quality data, and would like to thank the environmental data team for assistance with quality control of the data. MetService provided meteorological data.

7 REFERENCES

- Abell, J., McBride, C., & Hamilton, D. (2015). *Lake Rotorua Treated Wastewater Discharge: Environmental Effects Study*. ERI Report 80. Environmental Research Institute, University of Waikato, Hamilton, New Zealand. 99 pp.
- Antenucci, J. P., Ghadouani, A., Burford, M. A., & Romero, J. R. (2005). The long-term effect of artificial destratification on phytoplankton species composition in a subtropical reservoir. *Freshwater Biology*, 50(6), 1081-1093. <https://doi.org/10.1111/j.1365-2427.2005.01374.x>
- Bird, R. E., & Hulstrom, R. L. (1981). *A Simplified Clear Sky Model for Direct and Diffuse Insolation on Horizontal Surfaces*. SERI/TR-642-761. Solar Energy Research Institute.
- Bruce, L. C., Hamilton, D., Imberger, J., Gal, G., Gophen, M., Zohary, T., & Hambright, K. D. (2006). A numerical simulation of the role of zooplankton in C, N and P cycling in Lake Kinneret, Israel [Article]. *Ecological Modelling*, 193(3-4), 412-436. <https://doi.org/10.1016/j.ecolmodel.2005.09.008>
- Carmichael, W. W., & Boyer, G. L. (2016). Health impacts from cyanobacteria harmful algae blooms: Implications for the North American Great Lakes. *Harmful Algae*, 54, 194–212. <https://doi.org/http://dx.doi.org/10.1016/j.hal.2016.02.002>
- Carpenter, S. R., Stanley, E. H., & Vander Zanden, M. J. (2011). State of the world's freshwater ecosystems: Physical, chemical, and biological Changes. *Annual Review of Environment and Resources*, 36(1), 75–99. <https://doi.org/10.1146/annurev-environ-021810-094524>
- Chan, T. U., & Hamilton, D. P. (2001). Effect of freshwater flow on the succession and biomass of phytoplankton in a seasonal estuary. *Marine and Freshwater Research*, 52(6), 869–884. <https://doi.org/10.1071/MF00088>
- Chapman, S., Syktus, J., Trancoso, R., Thatcher, M., Toombs, N., Wong, K. K.-H., & Takbash, A. (2023). Evaluation of Dynamically Downscaled CMIP6-CCAM Models Over Australia. *Earth's Future*, 11(11), e2023EF003548. <https://doi.org/https://doi.org/10.1029/2023EF003548>
- Chung, S. W., Hipsey, M. R., & Imberger, J. (2009). Modelling the propagation of turbid density inflows into a stratified lake: Daecheong Reservoir, Korea [Article]. *Environmental Modelling and Software*, 24(12), 1467-1482. <https://doi.org/10.1016/j.envsoft.2009.05.016>
- Conley, D. J., Paerl, H. W., Howarth, R. W., Boesch, D. F., Seitzinger, S. P., Havens, K. E., Lancelot, C., & Likens, G. E. (2009). Controlling eutrophication: Nitrogen and phosphorus. *Science*, 323(5917), 1014–1015. <https://doi.org/10.1126/science.1167755>
- Dixit, S. S., Smol, J. P., Charles, D. F., Hughes, R. M., Paulsen, S. G., & Collins, G. B. (1999). Assessing water quality changes in the lakes of the northeastern United States using sediment diatoms. *Canadian Journal of Fisheries and Aquatic Sciences*, 56(1), 131–152. <https://doi.org/10.1139/f98-148>
- Eyring, V., Bony, S., Meehl, G. A., Senior, C. A., Stevens, B., Stouffer, R. J., & Taylor, K. E. (2016). Overview of the Coupled Model Intercomparison Project Phase 6 (CMIP6) experimental

- design and organization. *Geosci. Model Dev.*, 9(5), 1937-1958. <https://doi.org/10.5194/gmd-9-1937-2016>
- Fish, G. R., & Chapman, M. A. (1969). Synoptic surveys of lakes Rotorua and Rotoiti. *New Zealand Journal of Marine and Freshwater Research*, 3(4), 571-584. <https://doi.org/10.1080/00288330.1969.9515318>
- Gao, X., Xu, L., & Zhang, C. (2015). Modelling the effect of water diversion projects on renewal capacity in an urban artificial lake in China. *Journal of Hydroinformatics*, 17(6), 990-1002. <https://doi.org/10.2166/hydro.2015.004>
- Gibbs, M., Hawes, I., & Stephens, S. (2003). *Lake Rotoiti - Ohau Channel : assessment of effects of engineering options on water quality*. NIWA Client Report HAM2003-142. National Institute of Water & Atmospheric Research, New Zealand. 70 pp.
- Gibbs, M. M. (1992). Influence of hypolimnetic stirring and underflow on the limnology of Lake Rotoiti, New Zealand. *New Zealand Journal of Marine and Freshwater Research*, 26(3-4), 453-463. <https://doi.org/10.1080/00288330.1992.9516538>
- Gleick, P. H. (1996). Water resources. In S. H. Schneider (Ed.), *Encyclopedia of climate and weather* (Vol. 2, pp. 817–823). Oxford University Press.
- Hamill, K. (2022). *Trophic Level Index Review of targets and variability for Rotorua Lakes*. River Lake Ltd, Whakatane, New Zealand. 98 pp.
- Hamilton, D., McBride, C., & Uraoka, T. (2005). *Lake Rotoiti fieldwork and modelling to support considerations of Ohau Channel diversion from Lake Rotoiti*. Centre for Biodiversity and Ecology Research, University of Waikato, Hamilton, New Zealand. 109 pp.
- Hamilton, D. P., Paul, W. J., McBride, C., & Immenga, D. (2009). *Water flow between Ohau Channel and Lake Rotoiti following implementation of a diversion wall*. CBER Contract Report 96. Centre for Biodiversity and Ecology Research, University of Waikato, Hamilton, New Zealand. 34 pp.
- Hamilton, D. P., Salmaso, N., & Paerl, H. W. (2016). Mitigating harmful cyanobacterial blooms: Strategies for control of nitrogen and phosphorus loads [journal article]. *Aquatic Ecology*, 50(3), 351–366. <https://doi.org/10.1007/s10452-016-9594-z>
- Harke, M. J., Steffen, M. M., Gobler, C. J., Otten, T. G., Wilhelm, S. W., Wood, S. A., & Paerl, H. W. (2016). A review of the global ecology, genomics, and biogeography of the toxic cyanobacterium, *Microcystis* spp. *Harmful Algae*, 54, 4–20. <https://doi.org/10.1016/j.hal.2015.12.007>
- Hipsey, M. R., Bruce, L. C., Boon, C., Busch, B., Carey, C. C., Hamilton, D. P., Hanson, P. C., Read, J. S., de Sousa, E., Weber, M., & Winslow, L. A. (2019). A General Lake Model (GLM 3.0) for linking with high-frequency sensor data from the Global Lake Ecological Observatory Network (GLEON). *Geoscientific Model Development*, 12(1), 473-523. <https://doi.org/10.5194/gmd-12-473-2019>
- Hodges, B., & Dallimore, C. (2018). *Aquatic Ecosystem Model: AEM3D. v1.0 User manual*. In Hydronumerics.

- Hodges, B. R., Imberger, J., Saggio, A., & Winters, K. B. (2000). Modeling basin-scale internal waves in a stratified lake. *Limnology and Oceanography*, 45(7), 1603–1620. <https://doi.org/10.4319/lo.2000.45.7.1603>
- Jeppesen, E., Sørensen, P. B., Johansson, L. S., Søndergaard, M., Lauridsen, T. L., Nielsen, A., & Mejlhede, P. (2024). Recovery of lakes from eutrophication: changes in nitrogen retention capacity and the role of nitrogen legacy in 10 Danish lakes studied over 30 years. *Hydrobiologia*. <https://doi.org/10.1007/s10750-024-05478-6>
- Lakes Rotorua and Rotoiti Action Plan Action Plan*. (2009). Environmental Publication 2009/03. Environment Bay of Plenty, Rotorua District Council, Te Arawa Lakes Trust, New Zealand. 29 pp.
- León, L. F., Imberger, J., Smith, R. E. H., Hecky, R. E., Lam, D. C. L., & Schertzer, W. M. (2005). Modeling as a tool for nutrient management in Lake Erie: A hydrodynamics study. *Journal of Great Lakes Research*, 31, 309–318. [https://doi.org/https://doi.org/10.1016/S0380-1330\(05\)70323-3](https://doi.org/https://doi.org/10.1016/S0380-1330(05)70323-3)
- Leonard, B. P. (1991). The ULTIMATE conservative difference scheme applied to unsteady one-dimensional advection. *Computer Methods in Applied Mechanics and Engineering*, 88(1), 17-74. [https://doi.org/https://doi.org/10.1016/0045-7825\(91\)90232-U](https://doi.org/https://doi.org/10.1016/0045-7825(91)90232-U)
- Leoni, B., Patelli, M., Soler, V., & Nava, V. (2018). Ammonium Transformation in 14 Lakes along a Trophic Gradient. *Water*, 10(3).
- Liu, Y., Wang, Y., Sheng, H., Dong, F., Zou, R., Zhao, L., Guo, H., Zhu, X., & He, B. (2014). Quantitative evaluation of lake eutrophication responses under alternative water diversion scenarios: A water quality modeling based statistical analysis approach. *Science of The Total Environment*, 468-469, 219-227. <https://doi.org/https://doi.org/10.1016/j.scitotenv.2013.08.054>
- Luo, L., Hamilton, D., & Han, B. (2010). Estimation of total cloud cover from solar radiation observations at Lake Rotorua, New Zealand. *Solar Energy*, 84(3), 501-506. <https://doi.org/https://doi.org/10.1016/j.solener.2010.01.012>
- McBride, C. G. (2022). *Long-term nutrient loads and water quality for Lake Rotorua: 1965 to 2022*. Limnotrack, Hamilton, New Zealand. 21 pp.
- McBride, C. G., MacCormick, A., & Verburg, P. (2021). *Estimated catchment loads of nitrogen and phosphorus to the Rotorua Te Arawa Lakes*. ERI Report 143. Environmental Research Institute, University of Waikato, Hamilton, New Zealand. 93 pp.
- Me, W., Hamilton, D. P., McBride, C. G., Abell, J. M., & Hicks, B. J. (2018). Modelling hydrology and water quality in a mixed land use catchment and eutrophic lake: Effects of nutrient load reductions and climate change. *Environmental Modelling & Software*, 109, 114-133. <https://doi.org/https://doi.org/10.1016/j.envsoft.2018.08.001>
- Muraoka, K., Paul, W., Hamilton, D. P., & Von Westernhagen, N. (2010). *Effect of different operational regimes of Okere Gates on the effectiveness of the Ohau Channel diversion wall in Lake Rotoiti*. ERI Report 119. Environmental Research Institute, University of Waikato, Hamilton, New Zealand. 29 pp.

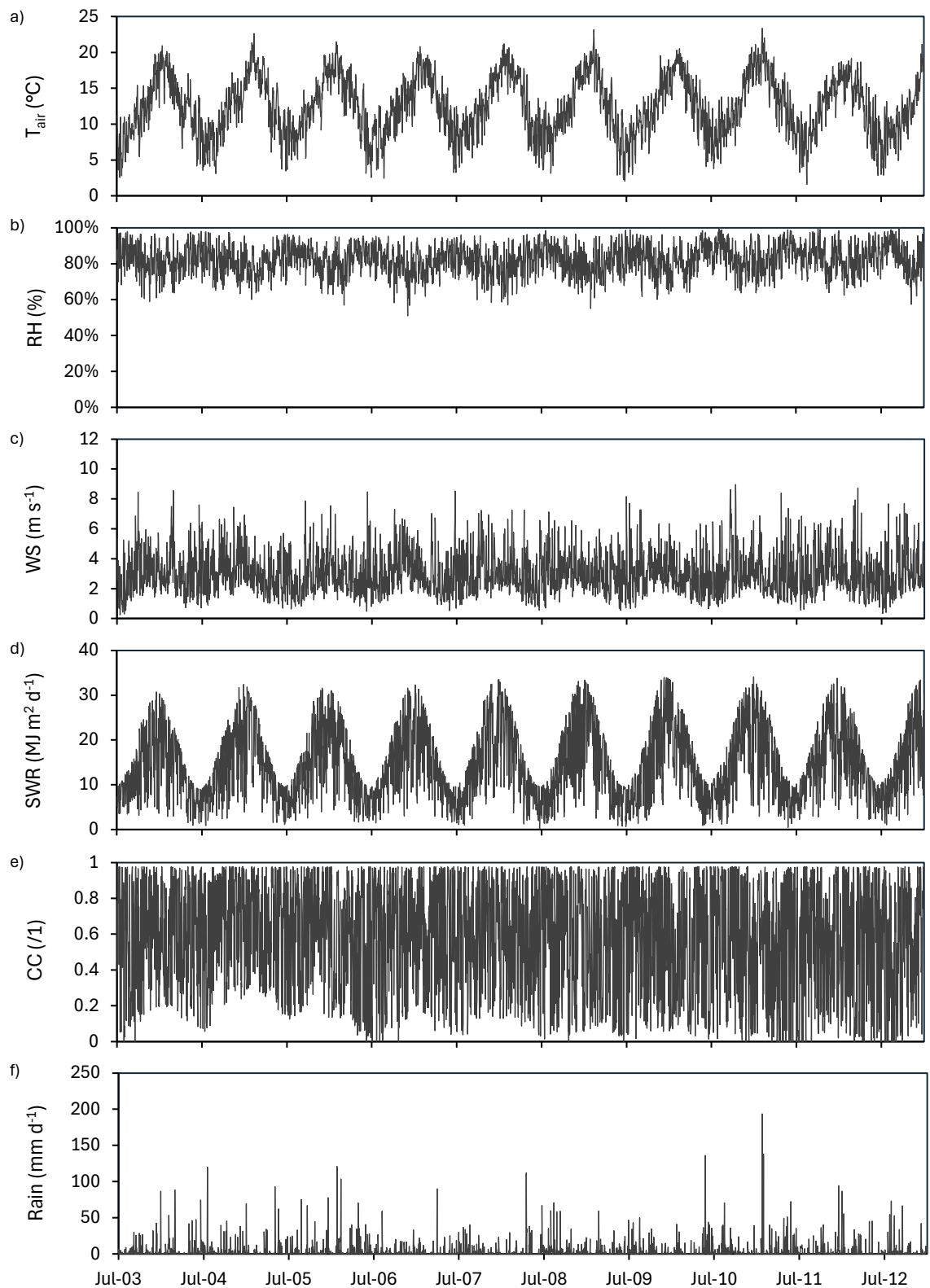
- Myers, D. R. *Bird Clear Sky Model*. <https://www.nrel.gov/grid/solar-resource/clear-sky.html>
- Özkundakci, D., Hamilton, D. P., & Trolle, D. (2011). Modelling the response of a highly eutrophic lake to reductions in external and internal nutrient loading. *New Zealand Journal of Marine and Freshwater Research*, 45(2), 165-185. <https://doi.org/10.1080/00288330.2010.548072>
- Paerl, H. W., Fulton, R. S., Moisander, P. H., & Dyble, J. (2001). Harmful freshwater algal blooms with an emphasis on cyanobacteria. *The Scientific World*, 1, 76–113.
- Priscu, J. C., Spigel, R. H., Gibbs, M. M., & Downes, M. T. (1986). A numerical analysis of hypolimnetic nitrogen and phosphorus transformations in Lake Rotoiti, New Zealand: A geothermally influenced lake. *Limnology and Oceanography*, 31(4), 812-831. <https://doi.org/https://doi.org/10.4319/lo.1986.31.4.0812>
- QGIS.org. (2023). *QGIS Geographic Information System*. In QGIS Association. <http://www.qgis.org>
- Romero, J. R., Antenucci, J. P., & Imberger, J. (2004). One- and three-dimensional biogeochemical simulations of two differing reservoirs [Article]. *Ecological Modelling*, 174(1-2), 143-160. <https://doi.org/10.1016/j.ecolmodel.2004.01.005>
- Schallenberg, M., de Winton, M. D., Verburg, P., Kelly, D. J., Hamill, K. D., & Hamilton, D. P. (2013). Ecosystem services of lakes. In J. R. Dymond (Ed.), *Ecosystem services in New Zealand – conditions and trends* (pp. 203–225). Manaaki Whenua Press.
- Sharpley, A., Jarvie, H. P., Buda, A., May, L., Spears, B., & Kleinman, P. (2013). Phosphorus Legacy: Overcoming the Effects of Past Management Practices to Mitigate Future Water Quality Impairment. *Journal of Environmental Quality*, 42(5), 1308-1326. <https://doi.org/https://doi.org/10.2134/jeq2013.03.0098>
- Smith, V. H., Wood, S. A., McBride, C. G., Atalah, J., Hamilton, D. P., & Abell, J. (2016). Phosphorus and nitrogen loading restraints are essential for successful eutrophication control of Lake Rotorua, New Zealand. *Inland Waters*, 6(2), 273-283. <https://doi.org/10.5268/IW-6.2.998>
- Tiselius, P., & Kuylenstierna, M. (1996). Growth and decline of a diatom spring bloom phytoplankton species composition, formation of marine snow and the role of heterotrophic dinoflagellates. *Journal of Plankton Research*, 18(2), 133-155. <https://doi.org/10.1093/plankt/18.2.133>
- Van Rossum, G., & Drake, F. L. (2009). *Python 3 Reference Manual*. In CreateSpace.
- Vant, B., & Gibbs, M. (2006). *Nitrogen and Phosphorus in Taupō Rainfall*. Waikato Regional Council.
- Verburg, P., Schallenberg, M., Elliott, S., & McBride, C. G. (2018). Lake Nutrient budgets. In D. P. Hamilton, K. J. Collier, J. M. Quinn, & C. Howard-Williams (Eds.), *Lake restoration handbook: A New Zealand perspective*. Springer.
- Vincent, W. F., Gibbs, M. M., & Dryden, S. J. (1984). Accelerated eutrophication in a New Zealand lake: Lake Rotoiti, central North Island. *New Zealand Journal of Marine and Freshwater Research*, 18(4), 431-440. <https://doi.org/10.1080/00288330.1984.9516064>

- Vincent, W. F., Gibbs, M. M., & Spigel, R. H. (1991). Eutrophication processes regulated by a plunging river inflow. *Hydrobiologia*, 226(1), 51-63. <https://doi.org/10.1007/BF00007779>
- Vincent, W. F., Spigel, W. F., Gibbs, M. M., Payne, G. W., Dryden, S. J., May, L. M., Woods, P., Pickmere, S., Davies, J., & Shakespeare, B. (1986). *The impact of the Ohau Channel outflow from Lake Rotorua on Lake Rotoiti*. Taupo Research Laboratory.
- Von Westernhagen, N. (2010). *Measurements and modelling of eutrophication processes in Lake Rotoiti, New Zealand* [Doctoral Thesis, University of Waikato].
- von Westernhagen, N., Hamilton, D. P., & Pilditch, C. A. (2010). Temporal and spatial variations in phytoplankton productivity in surface waters of a warm-temperate, monomictic lake in New Zealand. *Hydrobiologia*, 652(1), 57-70. <https://doi.org/10.1007/s10750-010-0318-4>
- Williams, W. (1986). Conductivity and salinity of Australian salt lakes. *Marine and Freshwater Research*, 37(2), 177-182. <https://doi.org/https://doi.org/10.1071/MF9860177>
- Woodhouse, J. N., Rapadas, M., & Neilan, B. A. (2014). Cyanotoxins. In N. K. Sharma, A. K. Rai, & L. J. Stal (Eds.), *Cyanobacteria : An Economic Perspective* (pp. 257–268). John Wiley & Sons, Incorporated.
- Yamamoto, Y., & Nakahara, H. (2005). The formation and degradation of cyanobacterium *Aphanizomenon flos-aquae* blooms: the importance of pH, water temperature, and day length. *Limnology*, 6(1), 1-6. <https://doi.org/10.1007/s10201-004-0138-1>
- Yang, H., Wang, J., Li, J., Zhou, H., & Liu, Z. (2021). Modelling impacts of water diversion on water quality in an urban artificial lake. *Environmental Pollution*, 276, 116694. <https://doi.org/https://doi.org/10.1016/j.envpol.2021.116694>
- Zhang, X., Zou, R., Wang, Y., Liu, Y., Zhao, L., Zhu, X., & Guo, H. (2016). Is water age a reliable indicator for evaluating water quality effectiveness of water diversion projects in eutrophic lakes? *Journal of Hydrology*, 542, 281-291. <https://doi.org/https://doi.org/10.1016/j.jhydrol.2016.09.002>
- Zhang, Y., Luo, P., Zhao, S., Kang, S., Wang, P., Zhou, M., & Lyu, J. (2020). Control and remediation methods for eutrophic lakes in the past 30 years. *Water Science and Technology*, 81(6), 1099-1113. <https://doi.org/10.2166/wst.2020.218>

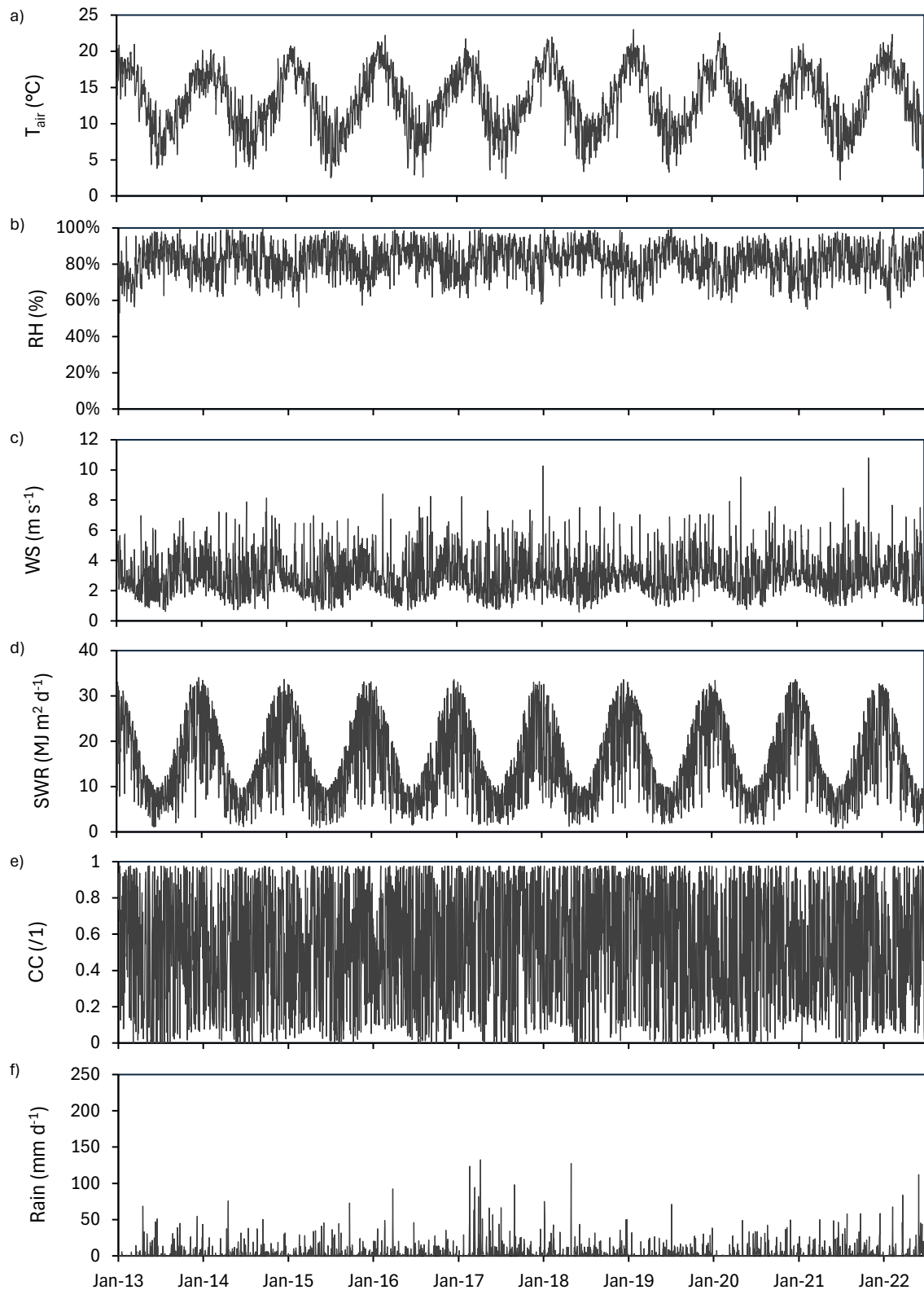
8 APPENDICES

Appendix 1 Inventory of minor inflow sites and data sets used to calculate flow (as residual flow in water budget), and water quality (WQ) parameters (as generalised seasonal models).

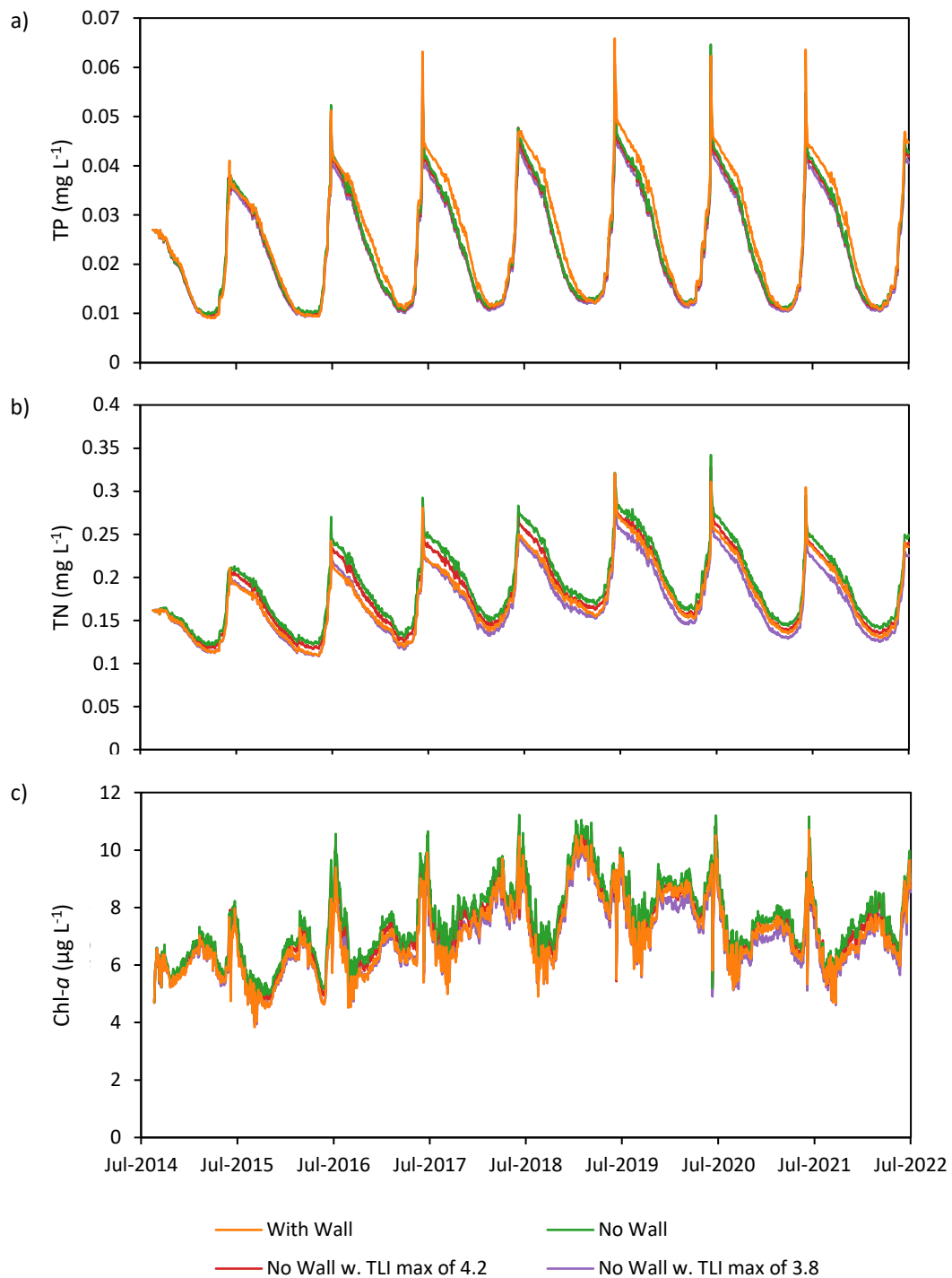
Name	Description	Reference	Location		Flow data years			WQ data years	
			Easting	Northing	93-94	05-06	09-10	05-06	09-10
Waiiti Stream	SH 30 Bridge	BOP120009	176 28 35.781 E	38 03 10.394 S	✓	✓	✓	✓	✓
Te Toroa Stream	20m u/s of Lake Rotoiti	BOP120007	176 24 39.935 E	38 02 32.130 S	✓	✓	✓		✓
Ruato Stream	Inflow into Lake Rotoiti	BOP120043	176 25 58.025 E	38 03 24.951 S	✓	✓	✓	✓	✓
Ruato Stream West	SH 30 Culvert	BOP120256	176 25 53.973 E	38 03 26.048 S			✓		✓
Hauparu Stream	5m d/s of culvert under SH 30	BOP120008	176 24 49.542 E	38 03 01.055 S	✓	✓	✓	✓	✓
Tumoana Stream	Outlet to Rotoiti	BOP120257	176 21 56.343 E	38 02 27.296 S			✓		✓
Te arero Stream	Outlet to Rotoiti	BOP120261	176 23 22.118 E	38 00 44.427 S			✓		✓
Hinehopu	Hinehopu, drain at lake edge	BOP130058	176 29 16.184 E	38 02 15.587 S			✓		✓
Tawhakarere Stream	Lakefront at SH 30	BOP120015	176 28 47.600 E	38 03 00.292 S	✓	✓	✓	✓	✓
Tapuaeharuru Stream	d/s SH 30 culvert (93-94 & 05-06); Inflow into Lake Rotoiti (09-10)	BOP120042	176 29 12.725 E	38 02 28.679 S	✓	✓	✓	✓	✓
Ruahine Stream	At bridge crossing Stream	BOP120016	176 21 56.450 E	38 02 46.770 S			✓		✓
Taupo Stream	Inflow into Lake Rotoiti	BOP120041	176 29 13.778 E	38 02 25.075 S	✓	✓	✓	✓	✓
Parengarenga Springs	Stream entering Lake Rotoiti	BOP120012	176 21 31.548 E	38 02 41.018 S	✓		✓		✓
Tokerau Stream	Outlet to Rotoiti	BOP120260	176 24 49.143 E	38 00 53.818 S			✓		✓
Wharetata West Stream	Pool near outlet	BOP120265	176 22 30.192 E	38 02 39.920 S			✓		✓
Wairau Bay Stream	Outlet to Rotoiti	BOP120263	176 20 45.972 E	38 03 06.716 S			✓		✓
Te Arero West Stream	Outlet to Rotoiti	BOP120264	175 59 15.592 E	38 01 24.686 S			✓		✓



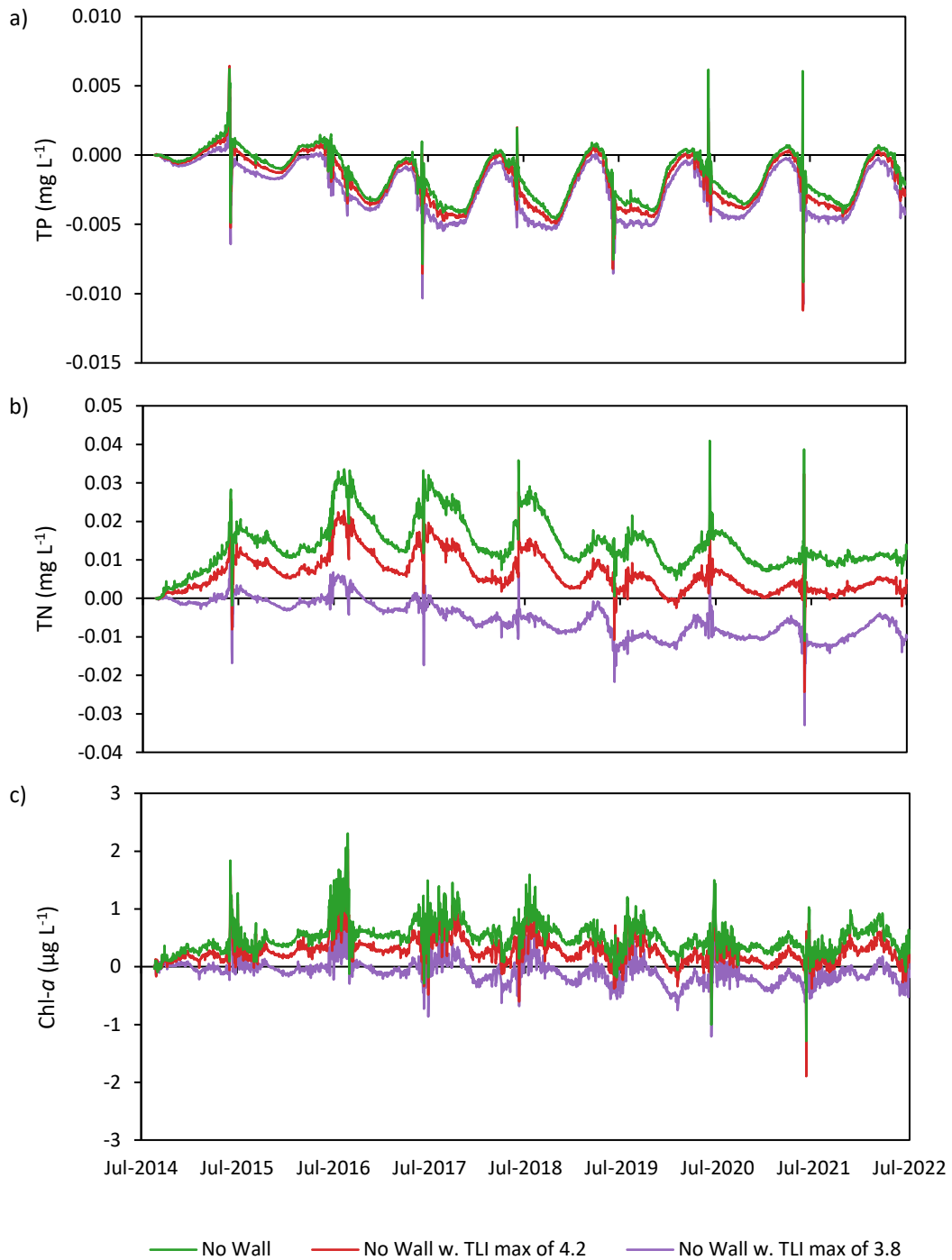
Appendix 2: Meteorological input (as daily values) from 1-Jul-2003 through 30-Jun-2012, for a) air temperature (T_{air}), b) relative humidity (RH), c) wind speed (WS), d) shortwave radiation (SWR), e) cloud cover (CC), and f) rainfall (Rain) N.b. variable vertical scale.



Appendix 3: Meteorological input (as daily values) from 1-Jul-2012 through 30-Jun-2023, for a) air temperature (T_{air}), b) relative humidity (RH), c) wind speed (WS), d) shortwave radiation (SWR), e) cloud cover (CC), and f) rainfall (Rain) N.b. variable vertical scale.



Appendix 4: Simulated Surface Total P, Total N, and chlorophyll a as daily values for the 1) with wall, 2) no wall, 3) no wall with TLI max of 4.2, and 4) no wall with TLI max of 3.8 configurations, across the 2014-15 through 2021-22 Limnological years (i.e., 1-Jul through 30-Jun of the subsequent year). N.b. variable vertical scale.



Appendix 5: Simulated relative change—i.e., to the simulated ‘wall-in’ configuration—in Surface Total P, Total N, and chlorophyll a as daily values for the 1) no wall, 2) no wall with TLI max of 4.2, and 3) no wall with TLI max of 3.8 configurations, across the 2014-15 through 2021-22 Limnological years (i.e., 1-Jul through 30-Jun of the subsequent year). N.b. variable vertical scale.